2026

COP
Circular Ocean-bound Plastic

Mechanical tests & material analysis on recycled samples

Report

March 2026

Report on Mechanical tests and material analysis on recycled Ocean-Bound Plastic samples

Publisher
Interreg South Baltic project
Circular Ocean-bound Plastic

www.circularoceanplastic.eu

Authors
Geraldo Mihut, The Foundation Plast Center Danmark

Plast Center Danmark

Partners in the COP project and contributors
Clean - The Danish Water and Environmental Cluster (DK) - leadpartner
Ocean Plastic Forum (DK)
Danish Materials Network (DK)
Sustainable Business Hub (SE)
Leibniz Institute for Baltic Sea Research (DE)
University of Rostock (DE)
University of Gdansk (PL)
Gdansk Water Foundation (PL)
Gdansk Sport Center (PL)

Layout
Kasper Gregersen, Clean - The Danish Water and Enviornmental Cluster

ISBN 978-87-975281-5-0 (digital)

For more information
To receive information about the project and other related publications, please visit www.circularoceanplastic.eu

Interreg South Baltic

Co-funded by the European Union

OPERATION OF STRATEGIC IMPORTANCE

Content

1. Introduction

Plastic pollution in aquatic environments represents a significant environmental challenge, with rivers acting as major transport pathways for plastic waste from land-based sources to the marine environment. Within the framework of the Interreg project Circular Ocean-bound Plastic (COP), urban rivers have been identified as key contributors to the transfer of plastic litter to coastal waters. Previous studies conducted as part of the COP project have provided detailed insights into the quantities, composition, and temporal dynamics of floating macro-litter collected at the river–sea interface in Aarhus, Denmark. These investigations demonstrated that plastics constitute the dominant fraction of recovered material and highlighted the relevance of this material stream as a potential secondary resource.

While the identification and quantification of ocean-bound plastic have been essential first steps, the possibility of reusing recovered material depends largely on its material properties. Plastics collected from aquatic environments are typically exposed to prolonged stressors such as ultraviolet radiation, oxygen, moisture, and mechanical abrasion. These factors could lead to polymer chain scission, oxidation, and depletion of stabilizing additives, which may significantly affect mechanical performance, thermal stability, and processing behaviour. As a result, a comprehensive material characterization was required to assess whether recovered plastic could be reintroduced into value-retaining material applications.

In this study, recycled polypropylene (PP) recovered from the Aarhus River was investigated and compared with virgin polypropylene. Polypropylene is widely used in consumer and industrial applications due to its low density, favourable mechanical properties, and good processability, making it a relevant material for evaluating reuse potential within a circular economy framework. To assess the influence of environmental exposure and blending strategies on material performance, three material scenarios were considered: 100% recycled polypropylene recovered from the Aarhus River, a blend consisting of 50% recycled Aarhus polypropylene and 50% virgin polypropylene, and 100% virgin polypropylene. The blended material was included to evaluate whether dilution of degraded recycled material with virgin polymer can improve performance while maintaining a substantial recycled content.

The objective of this work was to determine and compare the physical, mechanical, chemical, and thermal properties of the three material scenarios to support an evaluation of their suitability for reuse in new plastic products. The materials were characterized using a combination of standardized mechanical tests and analytical techniques, including density measurement, Shore hardness testing, tensile testing, three-point bending testing, and impact testing, as well as Fourier Transform

Infrared Spectroscopy (FTIR), Oxidative Induction Time (OIT) determination, and Thermogravimetric Analysis (TGA). Together, these methods provided insight into the degree of material degradation, oxidative and thermal stability, and performance differences between recycled, blended, and virgin polypropylene.

By linking material recovery with detailed material characterization, this study contributes to the development of circular solutions for ocean-bound plastic and supports informed decision-making regarding potential reuse pathways for plastics recovered from riverine environments.

2. Samples

The material investigated in this study consisted of polypropylene (PP) recovered from the Aarhus River, Denmark, and virgin polypropylene used as reference material. The recycled material originated from plastic items collected at the river–sea interface as part of ongoing monitoring and collection activities within the Circular Ocean-bound Plastic (COP) project. Following collection, the plastic material was sorted to isolate polypropylene-based fractions suitable for further processing and material characterization.

To enable a systematic comparison of material performance, three material scenarios were investigated: (i) 100% recycled polypropylene recovered from the Aarhus River, (ii) a 50/50 blend of recycled and virgin polypropylene, and (iii) 100% virgin polypropylene. For the blended and virgin scenarios, two virgin grades (EP 400 and EP 500) were included, resulting in five tested sample variants (Samples A–E).

The samples are referred to throughout this report as follows:

- **Sample A:** 100% recycled polypropylene recovered from the Aarhus River
- **Sample B:** Blend containing 50% recycled Aarhus River polypropylene and 50% virgin polypropylene (EP 400)
- **Sample C:** Blend containing 50% recycled Aarhus River polypropylene and 50% virgin polypropylene (EP 500)
- **Sample D:** 100% virgin polypropylene (EP 400)
- **Sample E:** 100% virgin polypropylene (EP 500)

Samples B and C are both 50/50 blends of recycled Aarhus River PP and virgin PP and were produced and tested under the same conditions; the only difference is the virgin grade (EP 400 vs EP 500). Likewise, Samples D and E are both 100% virgin PP references, differing only by grade (EP 400 vs EP 500).

The virgin polypropylene grades EP 400 and EP 500 were selected to provide reference materials with known and consistent properties and to allow comparison with blended materials produced using the same grades. The inclusion of two virgin reference materials further enabled assessment of whether observed differences were related to recycled content or to differences between virgin material grades.

The virgin reference materials (Samples D and E) were injection moulded to reflect the expected processing history of the recovered Aarhus River PP stream, which largely consists of injection-moulded consumer products (e.g., cups and similar items). This was done to ensure that comparisons to the recycled material are made using a relevant processing route and specimen production method.

Interpretation note: The virgin grades EP 400 and EP 500 were selected as practical reference materials with well-defined properties; however, the recovered Aarhus River PP (Sample A) may originate from a different PP grade/type than these references. Therefore, observed differences between Sample A and Samples D/E may reflect grade-related effects in addition to any potential degradation effects from environmental exposure.

Figure 1: Recovered Aarhus River polypropylene fraction (Sample A) prior to cleaning and mechanical processing, showing visible dirt and adhered residues.

A representative photo of the recovered Aarhus River PP fraction (Sample A) prior to cleaning and mechanical processing is shown in Figure 1. Visible residues and adhered contaminants are present on the collected items, illustrating the need for cleaning and sorting prior to reprocessing.

Prior to specimen production, the recycled polypropylene was cleaned and mechanically processed to obtain a homogeneous feedstock suitable for further processing. Visible contaminants, foreign materials, and non-polypropylene fractions were removed to the extent possible. For the blended materials (Sample B and Sample C), recycled and virgin polypropylene were combined at a mass ratio of 50:50 and mixed thoroughly prior to processing to ensure uniform material composition.

Test specimens for mechanical and thermal characterization were produced in accordance with the relevant testing standards. Specimens for Sample A were manufactured according to ISO 527-1B, while specimens for Samples B–E were manufactured according to ISO 527-1A. Following production, the specimens were conditioned under controlled laboratory conditions prior to testing to ensure thermal and moisture equilibrium.

The prepared samples were subsequently used for density measurements, Shore hardness testing, tensile testing, three-point bending testing, E-modulus determination, and impact testing, as well as for Fourier Transform Infrared Spectroscopy (FTIR), Differential Scanning Calorimetry (DSC), Oxidative Induction Time (OIT) determination, Thermogravimetric Analysis (TGA), Vicat, HDT, and CTE.

Representative dogbone-shaped test specimens for the different material variants are shown in Figure 2.

Sample A

Sample B (left) and Sample C (right)

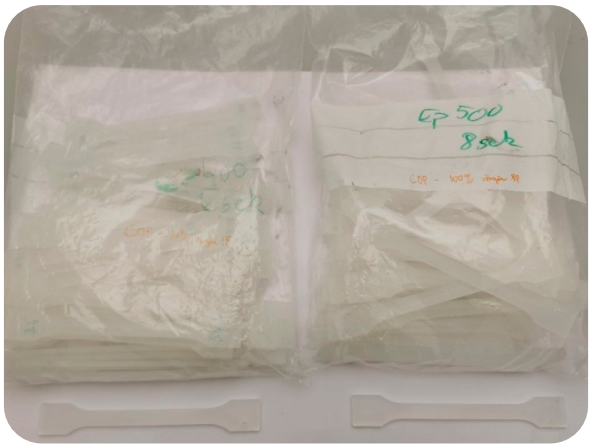

Sample D (left) and Sample E (right)

Figure 1: Dogbone-shaped test specimens of the investigated material variants: Sample A (100% recycled Aarhus River PP), Sample B (50% recycled Aarhus River PP + 50% virgin PP, EP 400), Sample C (50% recycled Aarhus River PP + 50% virgin PP, EP 500), Sample D (100% virgin PP, EP 400), and Sample E (100% virgin PP, EP 500)

Impact test specimens were prepared in accordance with ISO 179-1 (Charpy). The wide ends of the injection-moulded tensile specimens were removed, and the remaining bars were notched according to ISO 179-1/1eA prior to testing.

Specimens were injection moulded using process settings based on supplier/reference recommendations and adjusted to the capabilities of the injection moulding machine. The applied process parameters are summarized in Table 1.

Table 1: Injection moulding process parameters used for specimen production

Parameter	Unit	Reference value	Set value
Mass temperature	°C	200-250	245
Mould temperature	°C	15-50	40
Back pressure	bar	5-15	25
Injection pressure	bar	70-1200	1200
Injection speed	cm^3/s	30-120	69
Injection time	s	0,2-2,0	0,2
Post pressure	bar	400-800	500
Post pressure time	s	4-12	8
Dosing time	s	2-6	3,5
Dosing speed	mm/s	100-400	300
Dosing time	s	10-30	13

3. Melt Flow Index

Melt Flow Index (MFI), also referred to as melt mass-flow rate (MFR), was determined in accordance with ISO 1133 to evaluate the melt flow behaviour (processability) of the investigated polypropylene materials. Measurements were carried out at 230 °C under a load of 2.16 kg. Extrudate was collected using a constant cut interval of 20 s, and each cut was weighed. The MFI was calculated from the cut mass using:

$$MFR\left(\frac{g}{10min}\right) = \frac{600}{t}m$$

where t is the cut time (20 s) and m is the mass extruded during that interval in grams (g). For t=20 s , this simplifies to:

$$\mathrm{MFR} = 30\mathrm{m}$$

MFI results are relevant for assessing whether the recycled Aarhus River PP (Sample A) differs in melt viscosity compared with virgin PP and whether blending with virgin material shifts the melt flow behaviour toward the reference grades.

The calculated MFI results for the five materials are summarized in Table 2. Values are reported as average MFI with standard deviation and 95% confidence interval where repeat measurements were available.

Table 2: Melt flow rate (MFR) at 230°C / 2.16 kg for Samples A–E.

Samples	Mean mass per 20 s (g)	Mean MFR (g/10min)	Std. dev.	95% CI (g/10min)
A	0.1974	5.9	1.0	[5.4, 6.5]
B	0.3552	10.7	0.5	[10.4, 11.0]
C	0.4515	13.5	1.1	[12.8, 14,3]
D	1.1832	35.5	-	-
E	0.9359	28.1	10.9	[17.4, 38.7]

The MFI results show a clear difference in melt flow behaviour between the recycled Aarhus River PP and the virgin reference materials. Sample A (100% Aarhus PP) has the lowest MFI (5.9 g/10 min), indicating the highest melt viscosity / lowest flowability among the tested materials. In contrast, the virgin reference materials exhibit substantially higher MFI values (28.1–35.5 g/10 min), reflecting easier melt flow and higher processability under the applied conditions.

Both blended materials show intermediate behaviour compared with the recycled and virgin materials. Sample B (EP400 blend) has an average MFI of 10.7 g/10 min, and Sample C (EP500 blend) has an average MFI of 13.5 g/10 min. These values are higher than Sample A but still far below the virgin reference materials, showing that adding 50% virgin PP improves melt flow relative to 100% recycled material but does not restore the high flowability of the virgin grades.

With respect to degradation interpretation, it is important to note that oxidation-driven chain scission often leads to increased MFI (lower viscosity). The lower MFI observed for Sample A is not consistent with chain-scission-dominated oxidation (which typically increases MFI) and is more consistent with grade/molecular-weight differences and stream heterogeneity. Instead, the large difference between the recycled material and the virgin references may also reflect differences in PP grade and intended processing route. It is possible that the recovered Aarhus River PP represents a material stream closer to an extrusion-grade PP (typically lower MFI), while the virgin reference materials (EP400/EP500) are injection-moulding grades (typically higher MFI). In this case, the melt flow behaviour is influenced by grade/molecular-weight differences and material heterogeneity, in addition to any potential ageing effects. The blend results further demonstrate that melt flow is strongly affected by the recycled fraction and remains substantially different from the virgin reference grades even at 50% virgin content.

Summary MFI

MFI measurements at 230 ^{O}C/ 2.16 kg show that Sample A (100% Aarhus PP) has markedly lower melt flow (5.9 g/10 min) than the virgin reference materials (28.1–35.5 g/10 min), indicating reduced flowability and potentially more demanding processing conditions. The blends (Samples B and C) provide intermediate flow behaviour (10.7–13.5 g/10 min), showing that blending improves processability compared with 100% recycled material but remains substantially different from virgin PP. Overall, MFI results support that the recycled fraction strongly influences melt viscosity and should be considered when evaluating feasible reuse and processing pathways. From a practical processing perspective, these results suggest that the recovered Aarhus River PP may consist of a mixed PP grade distribution (e.g., lower-flow material closer to extrusion-type PP combined with higher-flow fractions). This heterogeneity can strongly influence melt flow and thereby processing stability. Therefore, for consistent reuse and process settings, it may be beneficial to separate or classify the recovered material into distinct flow/grade fractions (e.g., low-MFI vs high-MFI streams) prior to compounding or product manufacturing.

4. Fourier Transform Infrared Spectroscopy (FTIR)

Fourier Transform Infrared Spectroscopy (FTIR) was used to confirm polymer identity and to evaluate potential chemical changes related to environmental exposure of the recycled Aarhus River material. FTIR measures the absorption of infrared radiation as a function of wavenumber, where characteristic absorption bands correspond to molecular vibrations in the polymer. Differences in peak positions or relative intensities can indicate changes in chemical structure, oxidation products, or the presence of contaminants/additives.

FTIR spectra were recorded for Samples A–E under identical conditions and compared to assess similarities and differences between the recycled, blended, and virgin materials.

Figure 3 shows the overlay FTIR spectra for Samples A–E.

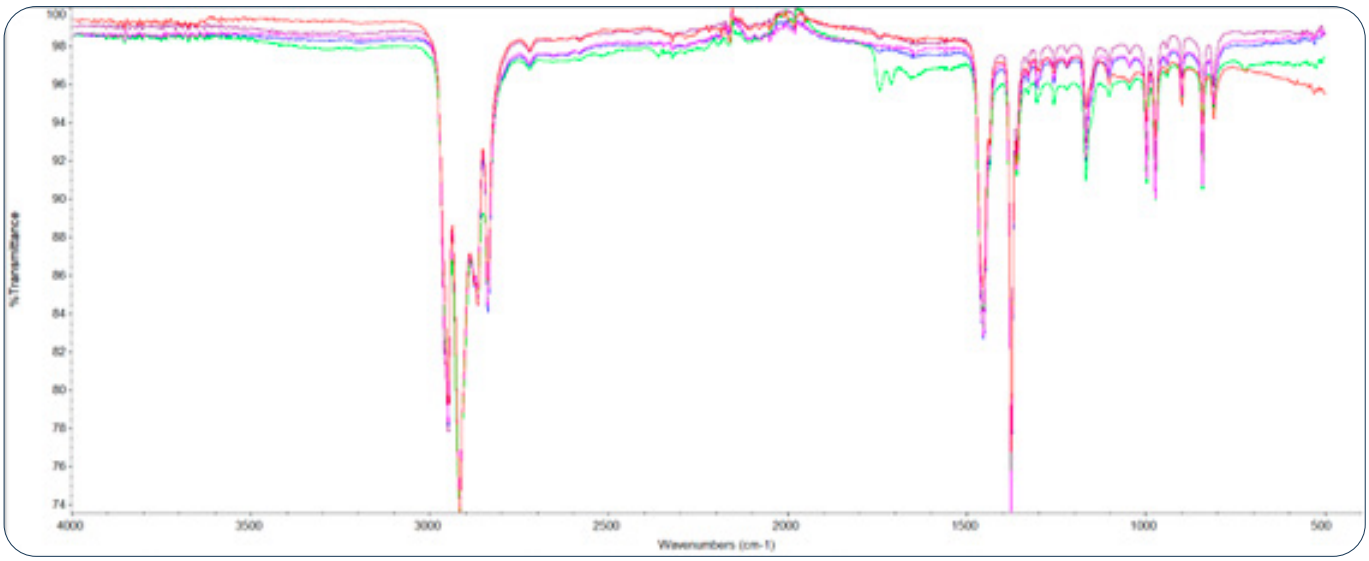

Figure 3: FTIR spectra for Samples A–E (recycled, blended, and virgin polypropylene). Sample A (Red), Sample B (Black), Sample C (Green), Sample D (Purple), Sample E (Blue).

The spectra of all samples show the characteristic absorption bands of polypropylene, confirming PP as the dominant polymer in Samples A–E. Only minor differences are observed between spectra, mainly small baseline offsets and slight intensity variations in the fingerprint region (~1200–800 cm^{-1}), which can be influenced by measurement conditions (e.g., surface contact/roughness) and/or microstructural differences such as crystallinity rather than major chemical changes. No distinct additional absorption bands were observed in the recycled or blended materials compared with the virgin references, indicating no strong FTIR-detectable contamination or polymer change.

To assess potential oxidation, the carbonyl region (~1850–1650 cm^{-1}) was examined. Weak features in the ~1710–1740 cm^{-1} range are also present in the virgin reference materials (Samples D and E), meaning that the presence of bands in this region in the recycled/blended materials is not, by itself, a unique indicator of environmental oxidation. Overall, the FTIR results do not show a pronounced oxidation signal unique to Sample A relative to the virgin references. It should be noted that FTIR may not detect low levels of oxidation products if the carbonyl concentration remains below the detection limit of the technique.

The spectra were also inspected for possible Si–O–Si bands associated with silicate/sand contamination (typically ~1100–1000 cm^{-1} and ~800 cm^{-1}). No clear additional silicate bands were observed for the recycled material relative to the virgin references within the sensitivity of FTIR in this region.

The spectra of the 5 samples are shown in Appendix A.

Summary FTIR

FTIR confirms polypropylene as the dominant polymer in all investigated samples (A–E). Differences between recycled, blended, and virgin materials are minor and mainly related to intensity/baseline variation rather than new chemical functional groups. No distinct FTIR-detectable oxidation peak unique to Sample A was observed, and no clear silicate (Si–O) signature was identified relative to the virgin references. Therefore, any differences in mechanical performance are more likely linked to factors not strongly resolved by FTIR alone (e.g., molecular weight changes, morphology, additive depletion) and should be interpreted together with OIT and TGA results.

5. Differential Scanning Calorimetry (DSC)

Differential Scanning Calorimetry (DSC) was used to evaluate the thermal transitions of the investigated polypropylene materials and to assess potential differences in melting behaviour and crystallinity between the recycled Aarhus River PP (Sample A), the blended materials (Samples B and C), and the virgin reference materials (Samples D and E). Differences in melting peak temperature and melting enthalpy can reflect differences in polymer grade, melting and crystallization behaviour, and microstructure, and may also be influenced by degradation mechanisms that affect crystallization behaviour.

An overlay of the DSC thermograms for Samples A–E is shown in Figure 4 to enable direct comparison. The individual DSC thermograms for each sample are provided in Appendix B.

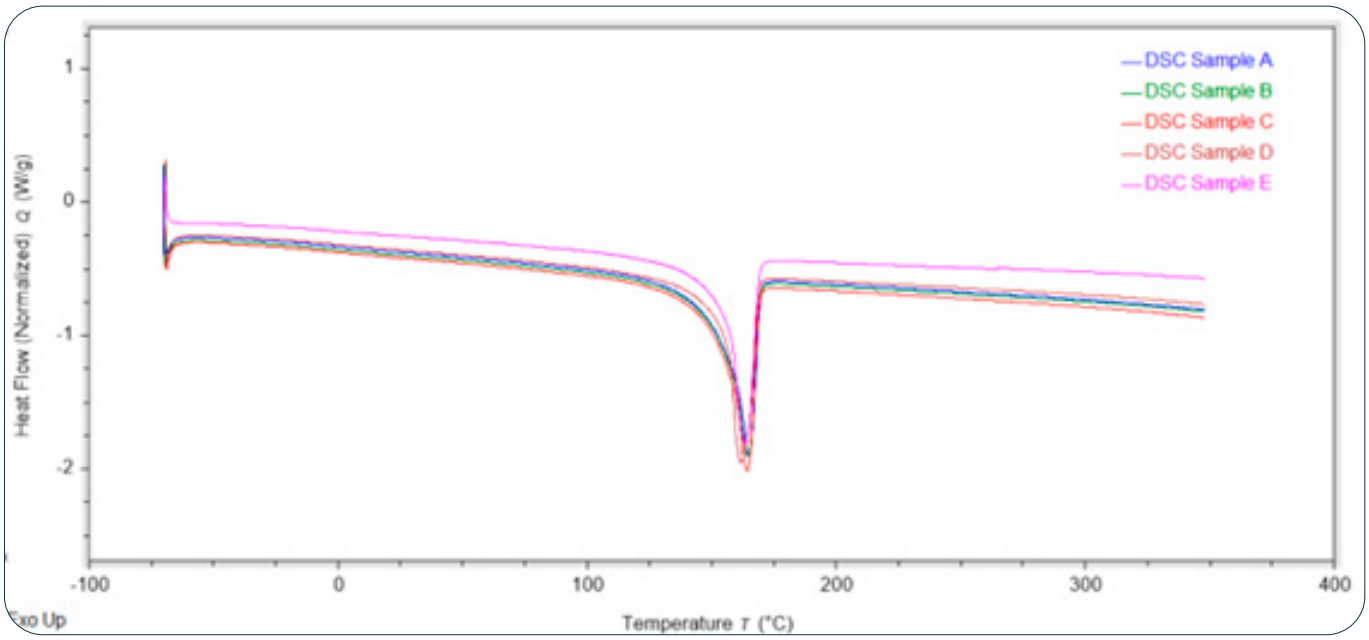

Figure 4: DSC thermograms for Samples A–E (overlay). Sample A (Blue), Sample B (Green), Sample C (Red), Sample D (Brown), Sample E (Purple).

The key DSC results extracted from the thermograms are summarized in Table 3. For each sample, the melting peak temperature (Tm) and the normalized melting enthalpy (ΔH_m) were obtained by peak integration. The degree of crystallinity (X_c) was estimated using 209 J/g as the reference enthalpy of fusion for 100% crystalline polypropylene:

$$X_C(\%) = \frac{\Delta H_m}{209 J/g} x100$$

Table 3: DSC melting peak temperature (Tm), normalized melting enthalpy (ΔHm), and estimated crystallinity for Samples A–E.

Samples	T_m (°C)	ΔH_m(J/g)	Estimated crystallinity X_c (%)
A	164.72	105.05	50.3
B	164.55	106.70	51.1
C	164.21	99.97	47.8
D	161.58	97.69	46.7
E	163.45	104.61	50.1

All samples exhibit melting behaviour typical of polypropylene, confirming that the investigated materials are PP-dominated and remain semi-crystalline after recovery, blending, and processing. No additional melting transitions characteristic of other common polymers were observed in the DSC thermograms, indicating no clear DSC-detectable contamination by other polymer types. The melting peak temperatures for Samples A–C are very similar (164.2–164.7 °C), indicating no substantial shift in melting behaviour for the recycled material or the blends. The melting peak temperatures for Samples A–C are very similar (164.2–164.7 °C), indicating no substantial shift in melting behaviour for the recycled material or the blends. The two virgin reference grades (Samples D and E) also show PP-typical melting behaviour and are broadly comparable. Sample D (EP400) exhibits a slightly lower melting peak temperature (161.6 °C) than Sample E (EP500, 163.5 °C), but the difference is modest and may be related to normal grade-to-grade variation (e.g., formulation and morphology) rather than indicating a degradation effect.

The melting enthalpy (ΔH_m) and estimated crystallinity (Xc) show modest variation between samples. Sample A exhibits an estimated crystallinity of approximately 50%, which is comparable to Sample E and slightly higher than Sample D. The blends show intermediate behaviour: Sample B has the highest $\Delta H_m/X_c$, while Sample C is lower and closer to Sample D.

Overall, DSC does not indicate a strong degradation signal for Sample A in terms of reduced melting temperature or reduced crystallinity compared with the virgin reference materials. Any degradation of the recovered material is therefore more likely to be reflected in properties that are more sensitive to oxidation, chain scission, and defects (e.g., OIT, impact behaviour, tensile fracture performance) rather than in melting behaviour alone.

Summary DSC

DSC confirms similar polypropylene melting behaviour across Samples A–E. The recycled Aarhus River PP (Sample A) shows a melting peak temperature and crystallinity comparable to the virgin EP500 reference (Sample E) and does not exhibit a clear reduction in thermal behaviour relative to the virgin materials. Differences observed in DSC parameters appear mainly related to virgin grade effects and crystallinity variation rather than strong thermal signatures of degradation.

6. Oxidation Induction Time (OIT)

Oxidation Induction Time (OIT) was determined using DSC to evaluate the oxidative stability of the investigated polypropylene materials. OIT represents the time elapsed until the onset of an oxidation exotherm under oxidative conditions and is commonly used as an indicator of remaining antioxidant protection and susceptibility to oxidative degradation. This parameter is particularly relevant for assessing whether the recovered Aarhus River polypropylene (Sample A) shows signs of aging and additive depletion compared with virgin polypropylene, and whether blending with virgin material improves oxidative stability.

An overlay of the OIT curves for Samples A–E is shown in Figure 5. The individual OIT thermograms for each sample are provided in Appendix C.

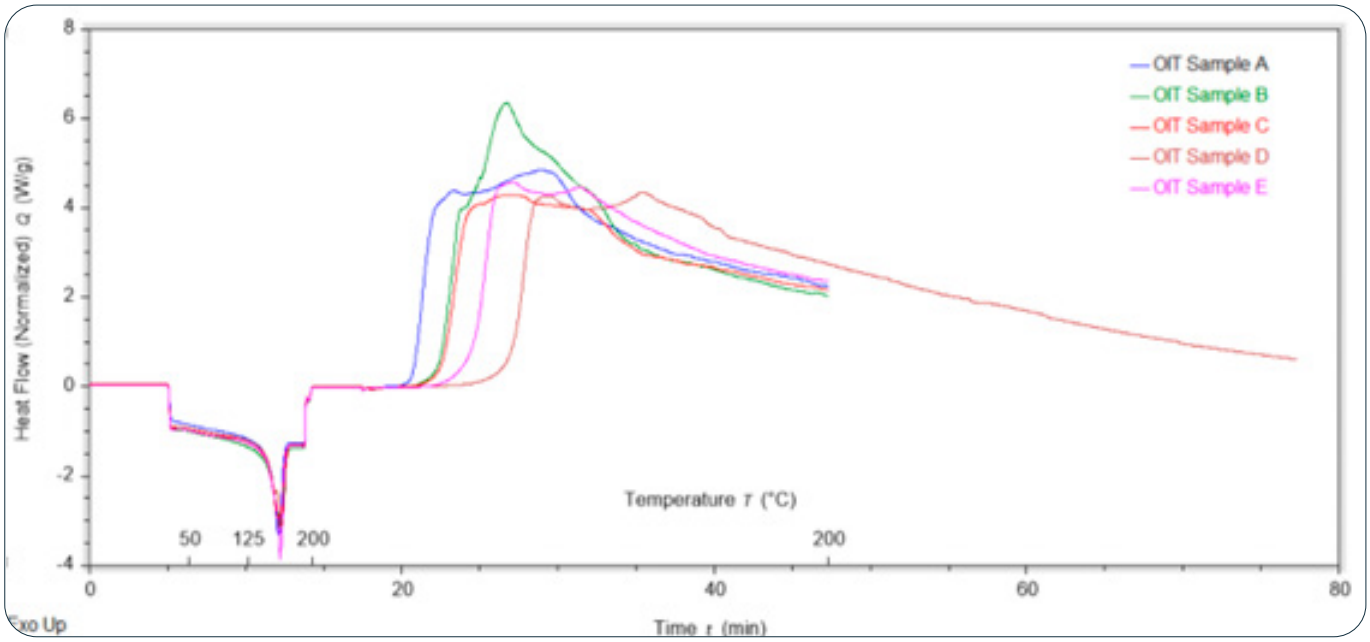

Figure 5: OIT thermograms for Samples A–E (overlay). Sample A (Blue), Sample B (Green), Sample C (Red), Sample D (Brown), Sample E (Purple).

The OIT values were determined as the onset time of the oxidation exotherm. The measured OIT values for Samples A–E are summarized in Table 4.

Table 4: Oxidation Induction Time (OIT) onset for Samples A–E.

Samples	OIT onset (min)
A	20.73
B	22.43
C	22.54
D	26.68
E	24.47

The OIT results show a clear reduction in oxidative stability for the recycled Aarhus River material compared with the virgin references. Sample A has the lowest OIT (~21 min) and is approximately 3–6 minutes lower than the virgin reference materials (Sample D ~27 min and Sample E ~24 min). This indicates that the recovered Aarhus River PP has reduced resistance to oxidation, which is consistent with antioxidant depletion and/or prior oxidative ageing due to environmental exposure and reprocessing. The difference in OIT between the two virgin reference grades (Sample D vs Sample E) is expected and likely reflects normal grade-to-grade variation in stabilization/additive package, rather than an ageing effect.

Both blended materials (Samples B and C, ~22–23 min) show slightly higher OIT values than Sample A, indicating that blending with virgin PP improves oxidative stability compared with the fully recycled material. However, the blends remain below the virgin reference materials, showing that a 50% virgin content only partially restores oxidative stability. Overall, OIT provides strong evidence that the recycled fraction has lower oxidative stability than virgin PP, and the results support the hypothesis that environmental exposure affects the ageing state of the recovered material.

Summary (OIT)

OIT measurements show that the recycled Aarhus River PP (Sample A) has the lowest oxidative stability among the investigated materials. The blends (Samples B and C) show moderate improvement compared with Sample A but do not reach the oxidative stability of the virgin reference materials. These findings support that the recovered material is more oxidation-prone than virgin PP and that blending provides only partial compensation.

7. Thermogravimetric Analysis (TGA)

Thermogravimetric Analysis (TGA) was used to compare the thermal decomposition behaviour and the non-volatile residue content of the investigated polypropylene materials. TGA records sample mass as a function of temperature/time under controlled conditions and is useful for detecting differences in thermal stability and estimating the amount of inorganic residue (ash) remaining after polymer decomposition. These parameters are relevant when evaluating whether the recovered Aarhus River material contains residual contamination and whether blending with virgin PP reduces this fraction.

An overlay of the TGA thermograms for Samples A–E is shown in Figure 6 to enable direct comparison. The individual TGA thermograms for each sample are provided in Appendix D.

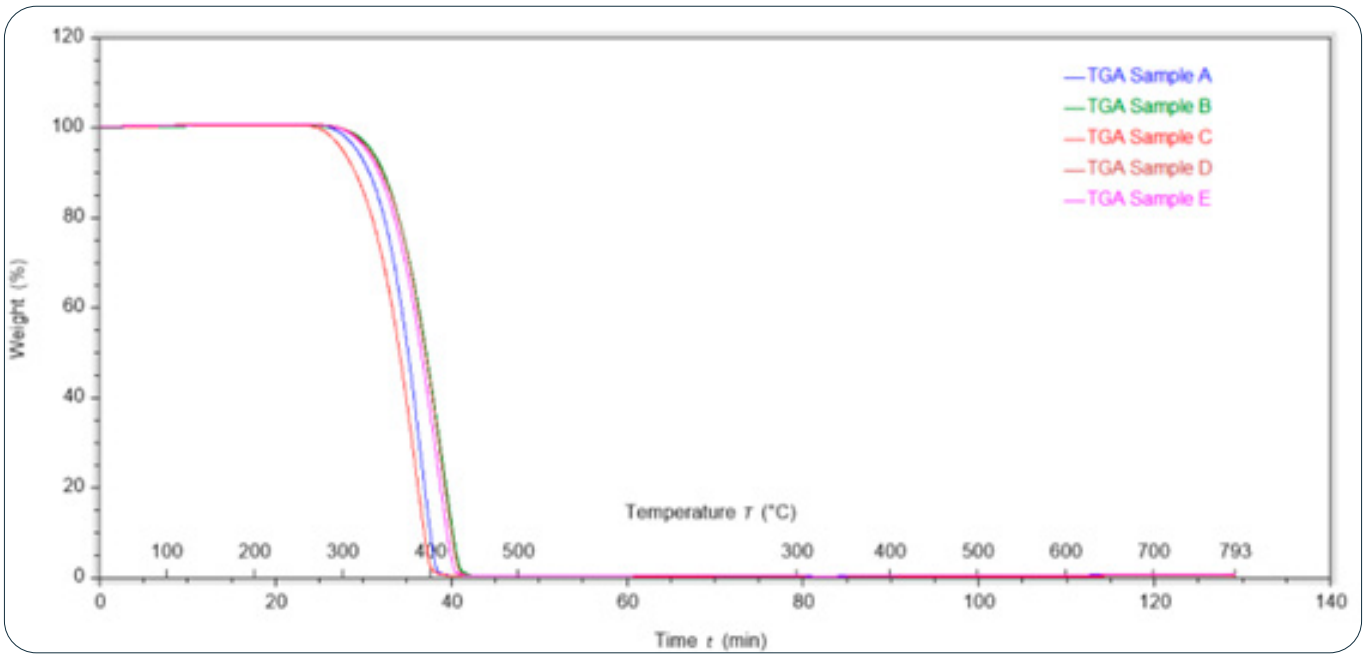

Figure 6: TGA thermograms for Samples A–E (overlay). Sample A (Blue), Sample B (Green), Sample C (Red), Sample D (Brown), Sample E (Purple).

The final residual mass (non-volatile residue) extracted from the thermograms is summarized in Table 5 for Samples A–E.

Table 5: Final residual mass (ash) from TGA for Samples A–E.

Samples	Residual mass (%)
A	0.748
B	0.589
C	0.442
D	0.663
E	0.744

All samples show a dominant single-step mass loss typical of polypropylene, indicating broadly similar thermal decomposition behaviour across recycled, blended, and virgin materials. The final residual mass values are all below 1%, indicating that the non-volatile fraction is small for all materials.

In addition to the residual mass, the overlay in Figure 6 indicates small differences in the onset of mass loss. Samples A and C show a slightly earlier onset of mass loss compared with the other samples, suggesting marginally lower thermal stability under the applied conditions. This behaviour may be influenced by the heterogeneous nature of these materials (mixed PP grades and additive packages and/or minor secondary components at low levels), rather than representing a systematic effect of recycled content alone.

With respect to potential residues/contamination in the recovered material, the residual mass values are very similar across all samples and remain below 1% (approximately 0.4–0.7%). Sample A shows a residual mass of 0.748%, which is in the same low range as the virgin reference materials (Sample D 0.663%, Sample E 0.744%). Given the small absolute differences (on the order of a few tenths of a percent), it is not meaningful to draw strong conclusions from ranking these values. Overall, the results indicate that the non-volatile (ash) fraction is low for all materials after cleaning and processing. It should also be noted that Sample A represents a heterogeneous recovered material stream, potentially consisting of polypropylene items with different grades and additive packages (and minor residual non-PP components at low levels). Such variability can influence both thermal stability behaviour and the final residue level. Consequently, the TGA residue results should be interpreted primarily as confirmation that the ash fraction is low (<1%), rather than as a definitive basis for comparing contamination differences between materials.

The blends (Samples B and C) show lower residue values than both the recycled material and the virgin references; given the low absolute residue levels, this difference may reflect grade/additive effects and/or experimental variability rather than a direct “dirt dilution” effect. Overall, TGA supports that all investigated materials are PP-like and that differences in mechanical performance are unlikely to be driven by large differences in inorganic residue.

Summary TGA

TGA shows similar polypropylene decomposition behaviour for Samples A–E, with low residual mass (<1%) for all materials. The residual mass of the recycled Aarhus River PP is comparable to the virgin references, indicating no strong TGA evidence of elevated inorganic contamination after processing. However, Sample A represents a heterogeneous recovered material stream, and the residue values should therefore be interpreted primarily as confirmation of a low ash fraction rather than as a definitive basis for ranking contamination differences between materials.

8. VICAT softening temperature

To further compare the thermal performance of the investigated polypropylene materials, the Vicat softening temperature was determined for Samples A–E. Vicat softening temperature was measured as the temperature at which an indenter penetrates 1 mm into the specimen under a load of 10 N (Vicat method according to ISO terminology).

For each sample, three replicate measurements were performed, and the mean value was calculated. The individual Vicat replicates and mean values are summarized in Table 6.

Table 6: Vicat softening temperature for Samples A–E (10 N load, 1 mm penetration). Values are reported as three replicates and the mean (gns).

Samples	Rep 1 (°C)	Rep 2 (°C)	Rep 3 (°C)	Mean, gns. (°C)
A	155.4	150.5	150.1	152.0
B	152.8	152.1	152.2	152.4
C	148.6	151.4	152.5	150.8
D	145.8	144.9	152.8	152.2
E	158.8	144.9	152.8	152.2

Overall, the investigated materials show comparable Vicat softening behaviour, with mean values in the range of approximately 148–152 °C. The recycled Aarhus River PP (Sample A) shows a mean Vicat value within the same range as the blended materials (Samples B and C) and the virgin reference materials (Samples D and E). This indicates that the softening behaviour measured by Vicat is not strongly reduced for the recycled material under the applied test conditions.

Summary Vicat

Vicat softening temperature results are broadly comparable across Samples A–E. Sample A shows a Vicat value within the same range as both blended and virgin materials, and Vicat does not indicate strong degradation-related deterioration for the recycled material.

9. Heat deflection temperature (HDT/DUL)

The heat deflection temperature is used to evaluate resistance to deformation under load at elevated temperature. HDT was determined as the temperature at which a specified deflection of 0.126 mm was reached under a load of 0.97 N.

For each sample, three replicate measurements were performed, and the mean value was calculated. The individual HDT replicates, and mean values are summarized in Table 7.

Table 7: Heat deflection temperature (HDT/DUL) for Samples A–E (0.97 N load, 0.126 mm deflection; adapted from ISO 75). Values are reported as three replicates and the mean (gns).

Samples	Rep 1 (°C)	Rep 2 (°C)	Rep 3 (°C)	Mean, gns. (°C)
A	52.6	56.7	59.0	56.1
B	50.1	57.5	58.0	55.2
C	52.8	55.4	58.6	55.6
D	50.7	53.6	49.1	51.1
E	52.3	52.4	52.6	52.4

The mean HDT values are in the range of approximately 51–56 °C across Samples A–E, indicating broadly similar resistance to deflection under the applied conditions. The recycled Aarhus River PP (Sample A) shows HDT values within the same range as the blended materials (Samples B and C) and the virgin reference materials (Samples D and E). Therefore, based on HDT, no clear reduction in thermal deformation resistance is observed for the recycled material compared with the other materials in this study.

Summary (HDT/DUL)

HDT results are comparable for Samples A–E. Sample A falls within the same range as the blended and virgin materials, suggesting no strong degradation-related deterioration in HDT behaviour under the applied test conditions.

10. Coefficent of thermal expansion (CTE)

The coefficient of thermal expansion (CTE) was determined to compare dimensional stability of the investigated materials with temperature. CTE was measured as the linear coefficient of thermal expansion over the temperature interval −30 to 50 ^{O}C, reported in µm/m·K.

For each sample, three replicate measurements were performed, and the mean value was calculated. The individual CTE replicates and mean values are summarized in Table 8.

Table 8: Coefficient of thermal expansion (CTE) for Samples A–E measured from −30 to 50 °C. Values are reported as three replicates and the mean (gns).

Samples	Rep 1 (µm/m·K)	Rep 2 (µm/m·K)	Rep 3 (µm/m·K)	Mean, gns. (µm/m·K)
A	62.7	72.2	73.0	69.3
B	62.4	79.6	76.3	72.7
C	67.9	77.0	74.0	73.0
D	90.7	85.7	80.1	85.5
E	87.9	87.5	61.2	78.9

The CTE results show more variation between samples than Vicat and HDT. In this dataset, the recycled and blended materials (Samples A–C) show similar mean CTE values (approximately 69–73 µm/m·K), while the virgin reference materials show higher mean values (~79–86 µm/m·K). CTE is sensitive to polymer grade, crystallinity, and morphology, and differences are therefore not necessarily direct indicators of degradation. In the context of this project, the CTE results indicate that the recycled material does not exhibit an abnormally high expansion coefficient compared with the investigated virgin references, and blending results in CTE values within a similar range to the recycled material.

Summary CTE

CTE shows some variation across Samples A–E, likely influenced by grade and morphology. The recycled Aarhus River PP has CTE values comparable to the blended materials and does not show an unusually high CTE relative to the virgin references in this dataset.

11. Density

The density of the specimens was determined in accordance with ISO 1183-1, Method A (immersion method). In this method, each specimen was weighed in air and subsequently weighed while immersed in a liquid of known density. Absolute ethanol was used as the immersion liquid and the measurements were carried out at 23 ^{O}C. Water was not suitable for this determination because the polypropylene specimens tended to float and could not be fully submerged in a stable and repeatable manner. During immersion weighing, the specimen was suspended on a thin wire attached to the balance apparatus.The density was calculated using:

$$\rho_S = \frac{m_{S,A} \cdot \rho_{IL}}{m_{S,A} - m_{S,IL}}$$

Where ρ_{IL} is the density of ethanol (0.79g/cm^3), $m_{s,a}$ is the mass of the specimen measured in air, and $m_{s,il}$ is the apparent mass measured while immersed in ethanol.
The calculated densities for Sample A–E are summarized in Table 9.

Table 9: The calculated, average density, standard deviation and confidence interval of the specimens.

Samples	Avg density g/cm^3	Std. deviation g/cm^3	95% confidence interval
A	0.91	0.00	[0.91, 0.91]
B	0.91	0.00	[0.91, 0.91]
C	0.91	0.00	[0.91, 0.91]
D	0.91	0.00	[0.91, 0.91]
E	0.91	0.00	[0.91, 0.91]

The density results (Table 9) showed an average value of 0.91 g/cm^3 for all investigated materials (Samples A–E). No measurable differences were observed between the recycled Aarhus River PP (Sample A), the blended materials (Samples B and C), and the virgin reference materials (Samples D and E) within the resolution of the ISO 1183-1 immersion method. This indicates that environmental exposure and potential residues associated with the recovered material did not result in a detectable change in bulk density after cleaning and processing.

The measured values were consistent with typical densities for polypropylene, suggesting that the materials are dominated by PP and did not contain substantial amounts of higher-density fillers or contaminants that would significantly increase density. Consequently, any differences observed in subsequent mechanical or thermal testing were expected to be related primarily to polymer degradation (e.g., chain scission/oxidation) or microstructural changes rather than differences in bulk material density. The reported scatter was very low and might also reflect rounding to the measurement resolution.

Summary Density

Density measurements (ISO 1183-1, Method A) showed an average density of 0.91 g/cm³ for all investigated materials (Samples A–E), with no measurable differences between the recycled material, blends, and virgin references within the resolution of the method. The results indicate that bulk density is not affected after processing and that performance differences observed in other tests are likely linked to degradation and microstructural effects rather than density differences.

12. Shore hardness

Shore hardness measurements were performed using a digital durometer (Durotech M202) in accordance with ISO 868. The method determines the resistance of a material to indentation. During the measurement, a standardized indenter was pressed into the specimen surface under defined conditions while ensuring that the pressure foot remains parallel to the surface. The measured hardness value was related to the penetration depth and was influenced by the material's elastic and viscoelastic response.

Two Shore scales are commonly used: Shore A for softer materials such as elastomers and Shore D for medium-hard to very hard materials, including most thermoplastics. Since polypropylene was a rigid thermoplastic, hardness was determined using the Shore D scale, which was the appropriate scale for this material according to ISO 868.

The Shore A and Shore D scales have an overlapping range, and their typical application areas are illustrated in Figure 7.

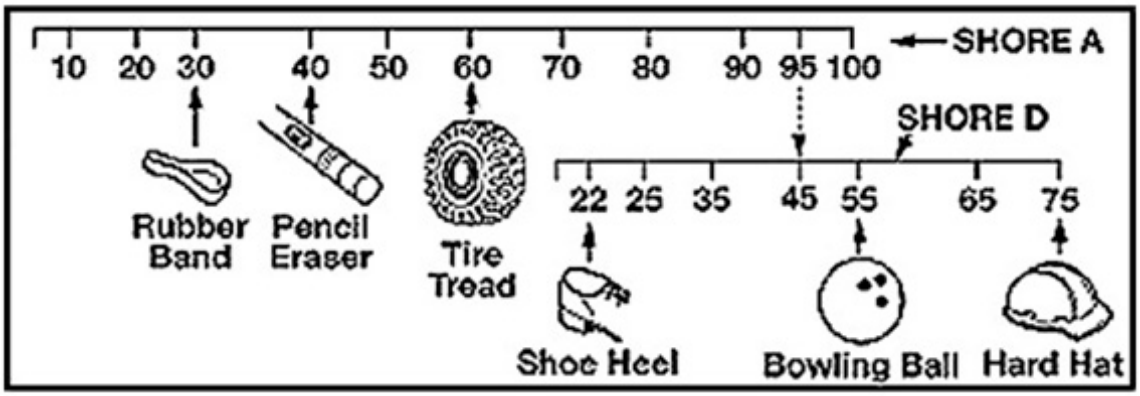

Figure 7: Comparison of Shore A and Shore D scales (modified from https://www.rocketseals.com).

Hardness was measured directly on the surface of the specimens. For each material variant (Sample A–E), ten measurements were performed to improve repeatability and statistical reliability. The average hardness values, standard deviations, and 95% confidence intervals are summarized in Table 10.

Table 10: Shore D hardness results for the investigated samples.

Samples	Avg hardness	Std. deviation	95% confidence interval
A	73.0	0.8	[72.5, 73.5]
B	73.4	1.6	[72.4, 74.3]
C	73.0	1.8	[71.9, 74.1]
D	70.2	1.3	[69.4, 71.0]
E	72.1	0.7	[71.7, 72.5]

The Shore D hardness results show that the recycled Aarhus River PP (Sample A) has an average hardness of 73.0, which is comparable to the blended materials (Samples B and C) and within the range of the virgin references (Samples D and E). Overall, the differences are modest (approximately 2–3 Shore D points) and the confidence intervals partially overlap, indicating broadly similar hardness across the materials. Importantly, no clear reduction in hardness is observed for the recycled material compared with virgin PP, suggesting that surface indentation resistance is not significantly decreased by environmental exposure, residues, or dirt within the sensitivity of the Shore D method. Because Shore hardness mainly reflects near-surface indentation behaviour, it may be less sensitive to degradation mechanisms such as chain scission and oxidative embrittlement, which are expected to be better captured by tensile, impact, FTIR, and OIT results; therefore, hardness is treated as a supporting indicator and interpreted together with the remaining results.

Summary Shore Hardness

Shore D hardness measurements (ISO 868) showed broadly similar hardness values for all investigated materials. The recycled Aarhus River PP (Sample A) and the blended materials (Samples B and C) had average hardness values around 73 Shore D, while the virgin reference materials (Samples D and E) showed slightly lower values (70.2–72.1 Shore D). Overall, the differences were modest (≈2–3 Shore D points) with partially overlapping confidence intervals, indicating that hardness is not strongly affected by recycled content or environmental exposure within the sensitivity of the method. Therefore, Shore D hardness is treated as a supporting indicator and should be interpreted together with tensile, bending, impact, and aging-related results when assessing degradation of the recovered material.

13. Tensile test

Tensile testing was performed using a universal testing machine (Lloyd LR50KPlus) in accordance with ISO 527. Specimens for Sample A were tested using ISO 527-1B geometry, while specimens for Samples B–E were tested using ISO 527-1A geometry. The tests were carried out to compare the tensile behaviour of the recycled Aarhus River polypropylene (Sample A), the blended materials (Samples B and C), and the virgin reference materials (Samples D and E). Two test speeds were applied: a low crosshead speed to determine E-modulus in the initial linear region and a higher crosshead speed to determine stress and strain characteristics up to fracture.

Specimens after tensile testing to break are shown in Figure 8, and the raw data and stress–strain curves are provided in Appendix G.

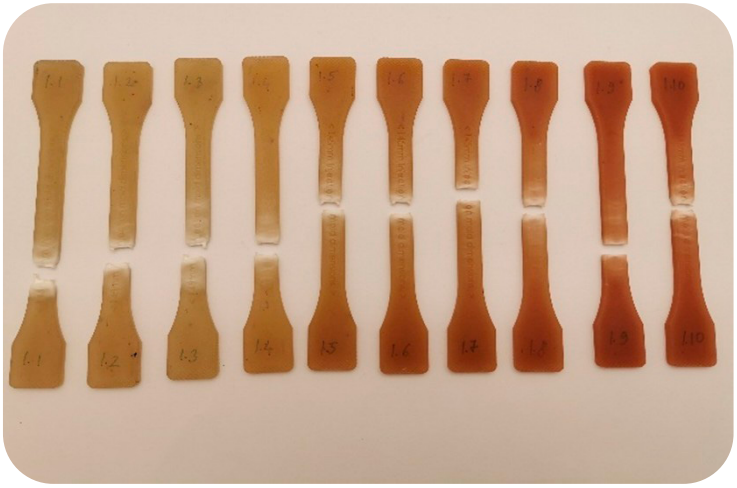

Sample A

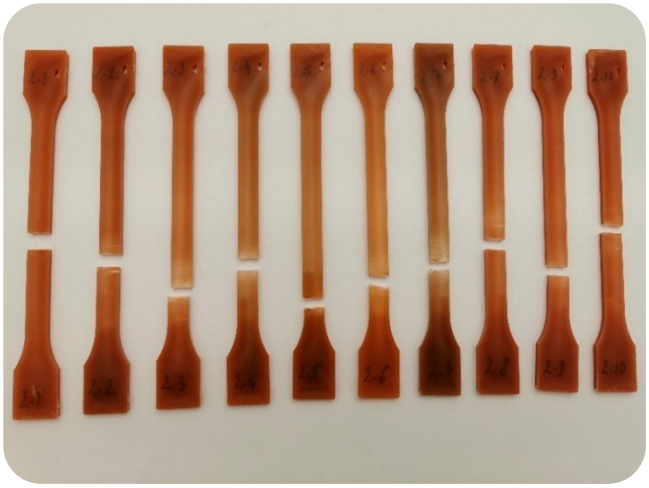

Sample B

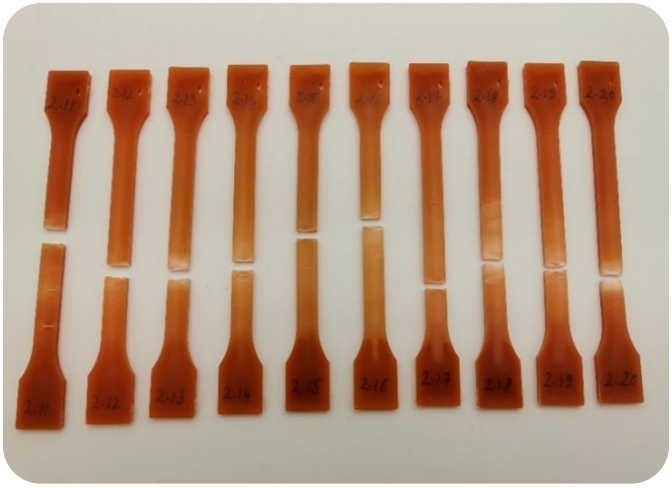

Sample C

Figure 8: Specimens of each material after tensile testing to fracture (continue on next page).

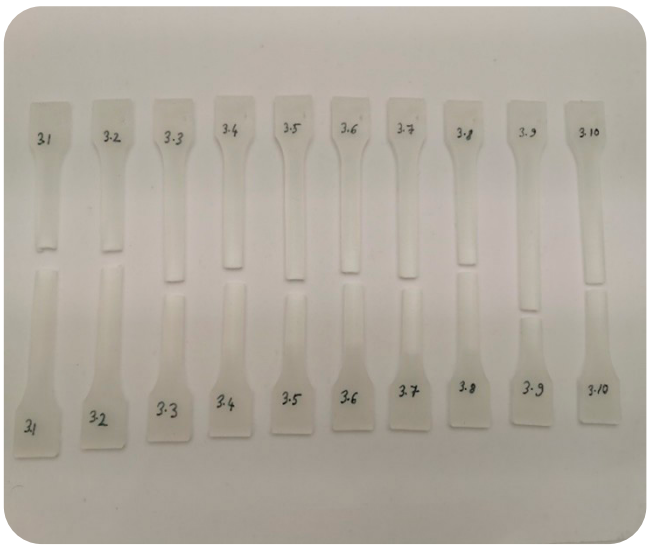

Sample D

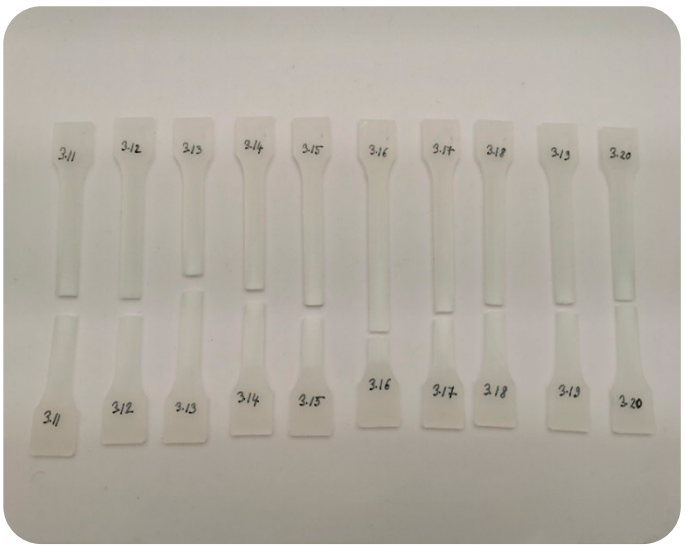

Sample E

Figure 8: Specimens of each material after tensile testing to fracture (continued).

Results for E-modulus, stress and percentage strain at yield/maximum load, and break of the sample are presented below.

Tensile modulus (E-modulus)

The E-modulus and Poisson's ratio (ν) were determined from tensile testing in the elastic region to compare the stiffness and elastic deformation behaviour of the investigated polypropylene materials. E-modulus represents the slope of the initial linear portion of the stress–strain curve, while Poisson's ratio describes the ratio between transverse contraction and axial extension during elastic loading. These parameters support the comparison of the recycled Aarhus River polypropylene (Sample A), the blended materials (Samples B and C), and the virgin reference materials (Samples D and E).

For each sample type, 10 specimens were evaluated. Results are reported as mean values with standard deviation and 95% confidence intervals.

The calculated Poisson's ratio values for Samples A–E are summarized in Table 11.

Table 11: Poisson's ratio for Samples A–E.

Samples	Repetition	Poisson's Ratio	Std. deviation	95% confidence interval
A	10	0.408	0.010	[0.402, 0.415]
B	10	0.438	0.021	[0.425, 0.457]
C	10	0.438	0.011	[0.432, 0.445]
D	10	0.436	0.034	[0.415, 0.457]
E	10	0.461	0.032	[0.441, 0.480]

All measured Poisson's ratios fall within the expected range for polypropylene. Differences between samples are modest and confidence intervals overlap, indicating broadly similar elastic lateral contraction behaviour across recycled, blended, and virgin materials. Poisson's ratio is therefore treated mainly as a supporting elastic parameter; degradation-related differences are expected to be more clearly reflected in oxidation stability (OIT) and fracture-sensitive mechanical properties (impact and tensile failure behaviour).
E-modulus modulus values calculated from the initial linear region are summarized in Table 12.

Table 12: E-modulus for Samples A–E.

Samples	Repetition	E-Modulus (MPa)	Std. deviation (MPa)	95% confidence interval (MPa)
A	10	1745.3	34.0	[1724.27, 1766.41]
B	10	1715.5	61.0	[1677.72, 1753.37]
C	10	1643.1	52.2	[1610.69, 1675.45]
D	10	1379.9	89.4	[1324.54, 1435.30]
E	10	1395.7	96.6	[1335.86, 1455.63]

The E-modulus results show clear differences in stiffness between the materials investigated. Sample A exhibits the highest modulus, followed by the blended materials (Samples B and C), while the virgin reference materials (Samples D and E) show lower modulus values in this dataset. An increased modulus does not necessarily indicate "better" material performance; in polypropylene, oxidative ageing can lead to stiffening (increased E-modulus) and may be associated with reduced ductility/ embrittlement.

At the same time, E-modulus is strongly influenced by polymer grade/type, crystallinity and morphology, and the recovered Aarhus River PP may represent a different grade mix than the EP400/EP500 references. Therefore, the stiffness differences cannot be attributed to oxidation alone. Consequently, E-modulus should be interpreted together with OIT (oxidative stability) and fracture-sensitive properties (impact behaviour and tensile break performance) when evaluating potential ageing effects in the recycled material.

It should be noted that in polypropylene, early-stage oxidative ageing can cause stiffening (increased E-modulus) before more advanced ageing leads to chain scission and loss of ductility. Therefore, the combination of high E-modulus for Sample A together with its low OIT may be consistent with the onset of ageing/oxidation, although grade/morphology effects and heterogeneity can also contribute and should be considered.

Stress at maximum load (tensile strength at maximum)

The maximum engineering stress reached during the test (stress at maximum load) was determined from the stress–strain curves recorded during tensile testing to break at 50 mm/min using a 5 kN load cell. The statistical results are presented in the table below.

Table 13: Stress at maximum load

Samples	Stress at max. load (MPa)	Std. deviation (MPa)	95% confidence interval (MPa)
A	37.0	0.2	[36.9, 37.2]
B	33.2	0.4	[33.0, 33.4]
C	33.9	0.2	[33.8, 34.1]
D	31.7	0.3	[31.5, 31.8]
E	32.1	0.4	[31.9, 32.3]

Stress at maximum load is highest for Sample A (37.0 MPa) and lowest for the virgin reference materials (31.7–32.1 MPa), while the blends fall in between (33.2–33.9 MPa).

As noted in the Samples section, differences may also reflect grade effects.

For polypropylene, the maximum engineering stress typically occurs at, or close to, the yield point, and the reported “stress at maximum load” can therefore be interpreted as a tensile yield stress under the applied conditions. Yield stress is strongly dependent on polymer grade and intended processing route (e.g., injection-moulding vs extrusion grades) and should be interpreted in the context of the selected virgin grades (EP400 and EP500). Consequently, the higher value observed for Sample A does not by itself indicate improved performance or reduced degradation; it may reflect that the recovered Aarhus River PP represents a different PP grade/type (e.g., different molecular weight distribution and morphology/crystallinity) compared with EP400/EP500. A comparison to the technical data sheets (TDS) for EP400/EP500 would support interpretation of whether the measured levels align with the expected grade behaviour. Degradation assessment should therefore rely more strongly on ductility and fracture-related results (stress/strain at break), together with impact performance and OIT.

Strain at maximum load

The strain at maximum load represents the elongation at which the maximum tensile stress occurs. This parameter can provide insight into the onset of yielding and the deformation behaviour before necking and fracture. The statistical results are presented in the table below.

Table 14. Strain at maximum load.

Samples	Stress at max. load (%)	Std. deviation (%)	95% confidence interval (%)
A	13.8	0.4	[13.5, 14.0]
B	9.7	0.5	[9.4, 9.9]
C	10.3	1.7	[10.2, 10.4]
D	11.5	0.3	[11.4, 11.7]
E	11.7	0.3	[11.5, 11.9]

Sample A shows the highest strain at maximum load (13.8%), while the blends (9.7–10.3%) and the virgin references (11.5–11.7%) are lower. A higher strain at maximum load indicates that Sample A reaches its maximum stress at a larger deformation, which may reflect differences in deformation and necking behaviour. However, strain-based parameters should be interpreted with caution because the gauge length used for strain evaluation differed between sample sets (Sample A: 50 mm; Samples B–E: 75 mm). In addition, variability in the blend results may be influenced by the degree of homogeneity achieved during compounding/mixing prior to processing; incomplete mixing can lead to specimen-to-specimen differences in recycled/virgin distribution and therefore affect strain values. Consequently, strain at maximum load should be interpreted together with stress-based tensile metrics and fracture-related parameters (stress/strain at break), and supported by impact behaviour and OIT when assessing potential embrittlement of the recycled material.

Stress at break

Stress at break reflects the engineering stress at fracture and is influenced by both strength and failure behaviour. The statistical results for Samples A–E are shown in Table 15.

Table 15. Stress at break.

Samples	Stress at break (MPa)	Std. deviation (MPa)	95% confidence interval (MPa)
A	25.9	2.9	[24.1, 27.6]
B	29.4	1.4	[28.6, 30.3]
C	28.7	1.9	[27.5, 29.9]
D	28.4	0.6	[28.0, 28.7]
E	29.3	1.1	[28.6, 29.9]

Sample A shows the lowest stress at break (25.9 MPa) compared with the blended materials and virgin reference materials (28.4–29.4 MPa). This indicates that, although Sample A reaches a relatively high stress at maximum load, it loses load-carrying capacity earlier during the later stage of deformation and fractures at a lower stress. However, stress at break is strongly influenced by failure mode and material homogeneity.

For the blends in particular, incomplete mixing or local variations in recycled/virgin distribution can contribute to scatter and may affect the measured break behaviour. In addition, differences between Sample A and the virgin references may also reflect PP grade/type differences rather than degradation alone. Therefore, stress at break should be interpreted together with strain at break, impact performance, and OIT, which provide a more complete picture of potential embrittlement and oxidative ageing of the recycled material.

Strain at break (elongation at break)

Elongation at break is a key indicator of ductility and is often highly sensitive to environmental aging and polymer degradation. The statistical results for Samples A–E are presented in Table 16.

Table 16. Percentage Strain at Break.

Samples	Stress at break (%)	Std. deviation (%)	95% confidence interval (%)
A	33.0	2.9	[31.1, 34.8]
B	18.9	4.0	[16.4, 21.4]
C	21.5	3.1	[19.6, 23.5]
D	20.1	1.8	[19.0, 21.2]
E	18.4	2.0	[17.2, 19.7]

Sample A shows the highest strain at break (33.0%), while Samples B–E fall in a lower range (18.4–21.5%). Strain at break is often used as an indicator of ductility and potential embrittlement; however, the strain results should be interpreted with caution because the gauge length used for strain evaluation differed between sample sets (Sample A: 50 mm; Samples B–E: 75 mm). If strain is derived from crosshead displacement or affected by system compliance, a shorter gauge length can lead to higher reported strain values and may therefore partially explain the elevated strain at break for Sample A.

In addition, strain at break is sensitive to failure mode (necking vs. premature fracture), local defects, and material homogeneity. For the blended materials, incomplete mixing or local variations in recycled/virgin distribution can contribute to scatter and influence fracture behaviour. Finally, differences between Sample A and the virgin reference grades may also reflect PP grade/type differences rather than degradation alone.

Consequently, strain at break should be evaluated together with stress at break, impact performance, and oxidative stability (OIT) when assessing whether the recycled material shows signs of embrittlement.

Summary Tensile Test

Tensile testing (ISO 527) was used to compare elastic behaviour, strength and fracture behaviour of the recycled Aarhus River PP (Sample A), the blends (Samples B and C), and the virgin reference materials (Samples D and E). Overall, the elastic properties show only modest variation between materials: Poisson's ratio values are within the expected range for polypropylene and broadly comparable across samples. E-modulus results indicate that Sample A has stiffness comparable to or higher than the other investigated materials and does not show reduced elastic stiffness relative to the virgin references; therefore, elastic stiffness alone does not suggest significant deterioration of the recycled material.

For strength-related behaviour, stress at maximum load (often close to tensile yield stress for PP under these conditions) is highest for Sample A, while the blends are intermediate and the virgin grades show lower values. Because yield/maximum stress is strongly grade-dependent (and can differ between injection and extrusion-type PP grades), this ranking should not be interpreted as evidence of improved performance or reduced degradation of Sample A. The observed differences may reflect underlying PP grade/type differences and morphology (e.g., crystallinity), as well as potential heterogeneity in the recycled feedstock.

Fracture-related results show a different trend: Sample A has the lowest stress at break compared with the other samples, indicating earlier loss of load-carrying capacity in the later stage of deformation. Strain-based parameters (strain at maximum load and strain at break) show higher values for Sample A; however, these values must be interpreted with caution because the gauge length used for strain evaluation differed between sample sets (Sample A: 50 mm; Samples B–E: 75 mm). Additionally, strain at break and stress at break are sensitive to failure mode, defects and material homogeneity; for the blends, incomplete mixing or local variations in recycled/virgin distribution may contribute to scatter and influence fracture behaviour.

In summary, the tensile results do not indicate reduced stiffness of the recycled Aarhus River PP, but fracture-related behaviour suggests that failure characteristics may differ from the virgin references. For evaluation of potential degradation and embrittlement, tensile results should be interpreted together with notch-sensitive impact performance and oxidative stability (OIT), which provide the most direct evidence of ageing-related changes.

14. Three-point bending test

Three-point bending (flexural) testing was performed using a universal testing machine (Lloyd LR50KPlus) in accordance with ISO 178. Each specimen was supported on two supports and loaded at the midpoint by a loading nose (three-point configuration). The test was performed at a constant crosshead speed (Method A) until specimen failure or until a maximum deflection of 24 mm was reached. During the test, the applied load and the corresponding mid-span deflection were continuously recorded.

A suitable load cell was selected to ensure adequate measurement resolution within the expected force range of the specimens. All samples (A–E) were tested using the same test configuration and speed (10 mm/min) to ensure comparability. Representative specimens after testing are shown in Figure 9. The complete raw data and load–deflection curves are provided in Appendix H.

The specimens corresponding to each sample after testing are shown below.

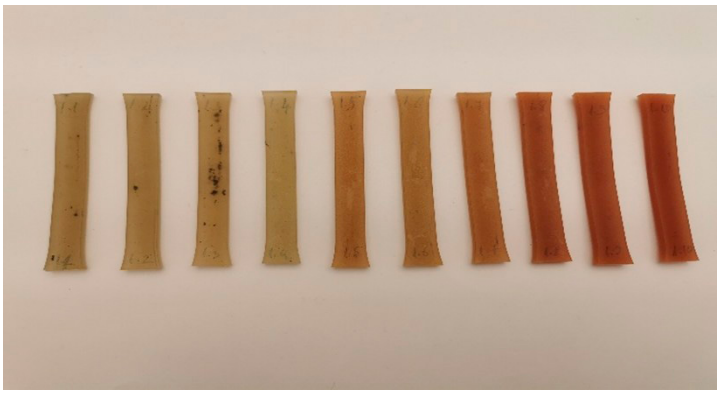

Sample A

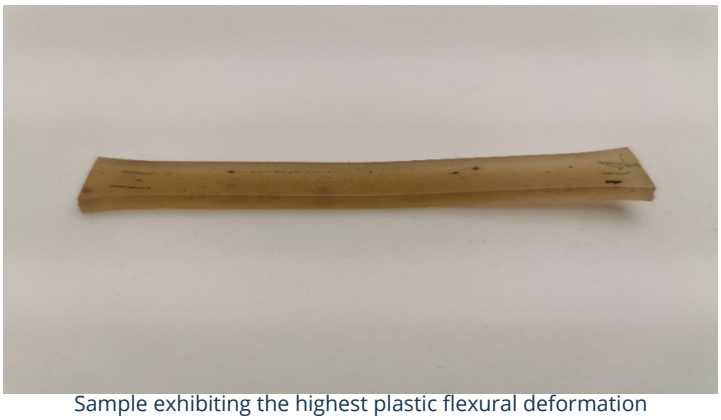

Sample exhibiting the highest plastic flexural deformation following three-point bending of Sample A specimens.

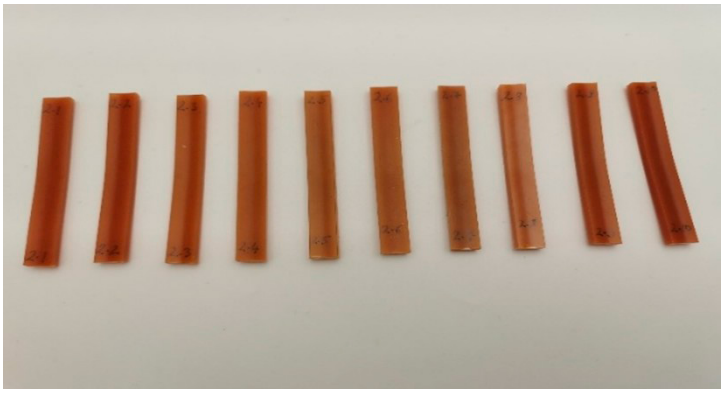

Sample B

Sample exhibiting the highest plastic flexural deformation following three-point bending of Sample B specimens.

Figure 9. Representative specimens after three-point bending for Samples A–E (continued on next page).

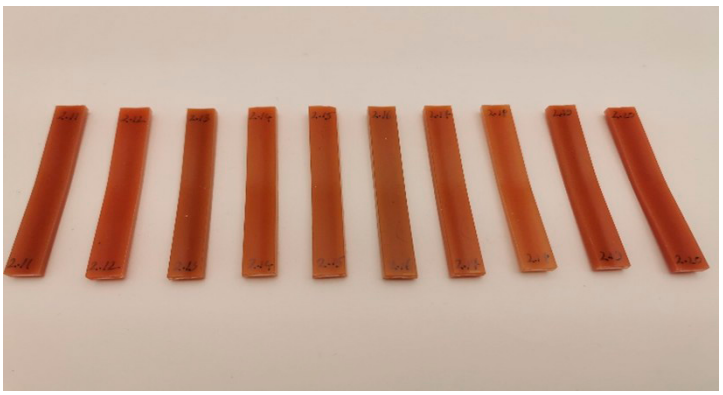

Sample C

Sample exhibiting the highest plastic flexural deformation following three-point bending of Sample C specimens.

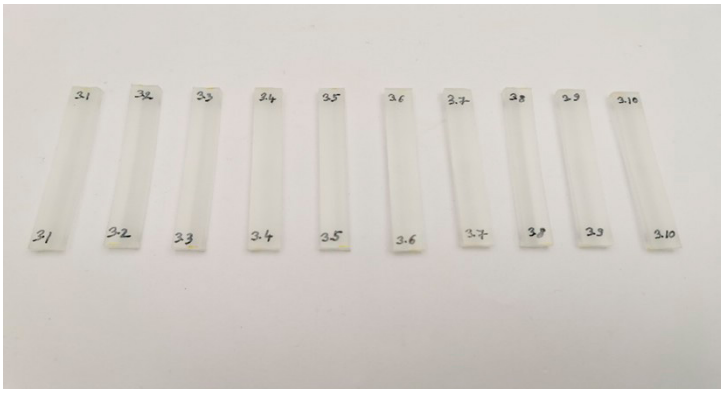

Sample D

Sample exhibiting the highest plastic flexural deformation following three-point bending of Sample D specimens.

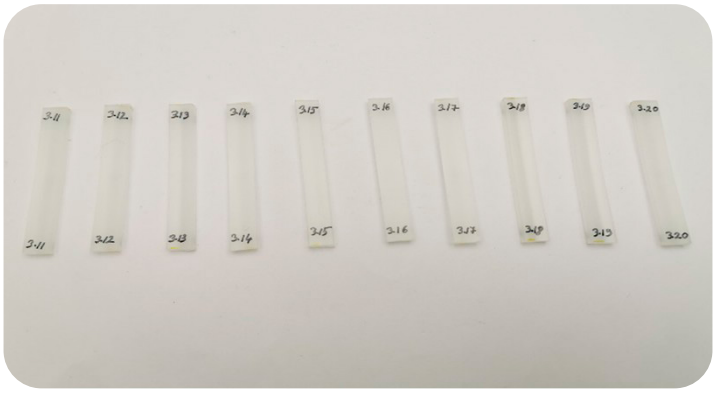

Sample E

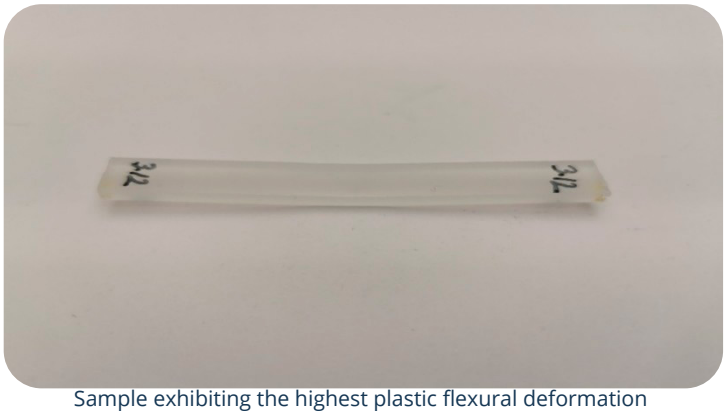

Sample exhibiting the highest plastic flexural deformation following three-point bending of Sample E specimens.

Flexural properties were calculated according to ISO 178, including flexural modulus, flexural stress at maximum load (flexural strength), and flexural strain at maximum load. The calculated results and associated statistics for Samples A–E are presented in Tables 17–19.

Results of flexural modulus

The statistical results of flexural modulus for the 5 samples are shown in Table 17.

Table 17: Statistical results of flexural modulus for the 5 samples.

Samples	Repetition	Flexural Modulus (MPa)	Std. deviation (MPa)	95% confidence interval (MPa)
A	10	1337.4	48.8	[1307.2, 1367.6]
B	10	1137.2	26.5	[1120.8, 1153.6]
C	10	1191.6	35.9	[1169.3, 1213.8]
D	10	974.4	56.8	[939.2, 1009.6]
E	10	1019.6	34.7	[998.1, 1041.1]

The flexural modulus results show clear differences between the materials investigated. The recycled Aarhus River PP (Sample A) exhibits the highest stiffness, while the virgin reference materials (Samples D and E) show lower modulus values. The blended materials (Samples B and C) fall between these two extremes. In the context of environmental exposure and potential degradation, an increased flexural modulus for Sample A may indicate a stiffer and potentially more brittle material state, which can be consistent with oxidative ageing and microstructural changes rather than improved mechanical performance. However, flexural stiffness is also strongly influenced by PP grade/type and intended processing route (e.g., extrusion-type vs injection-moulding grades), as well as crystallinity and morphology; therefore, differences in flexural modulus cannot be attributed to degradation alone. The intermediate modulus values of the blends suggest that blending with virgin PP can shift stiffness toward the virgin reference level in this dataset.

Results of flexural stress

The statistical results of flexural strength, which is the flexural stress at maximum, and the respective strain for the 5 samples 2 are shown in Table 18.

Table 18: Statistical results of flexural stress for the 5 Samples.

Samples	Repetition	Flexural stress (MPa)	Std. deviation (MPa)	95% confidence interval (MPa)
A	10	45.9	1.1	[45.2, 46.5]
B	10	40.9	0.6	[40.5, 41.2]
C	10	42.1	0.4	[41.9, 42.3]
D	10	36.4	0.4	[36.1, 36.6]
E	10	37.3	0.3	[37.1, 37.5]

The flexural stress results (Table 18) show that Sample A exhibits the highest stress at maximum load, while Samples D and E display lower values. Samples B and C fall between the recycled and virgin materials. Although environmental degradation is often associated with reduced mechanical performance, changes do not necessarily appear as an immediate reduction in strength. In the early stages of oxidative ageing, polypropylene can exhibit increased stiffness and strength due to changes

in microstructure and reduced chain mobility (often described as an initial crosslinking/stiffening phase), whereas more advanced ageing is typically dominated by chain scission and molecular weight reduction, which leads to loss of ductility and eventual embrittlement.

Therefore, the higher flexural strength observed for Sample A may reflect an early-stage ageing effect and/or differences in polymer grade and morphology (e.g., crystallinity), and it does not by itself confirm improved long-term performance. Consequently, the flexural strength results should be interpreted together with flexural strain and, in particular, impact and tensile ductility results (noting that tensile strain values are interpreted with caution due to differing gauge length) when evaluating potential embrittlement of the recycled material.

Results of flexural strain

Table 19: Statistical results of percentage of flexural strain for the 5 Samples.

Samples	Repetition	Flexural stress (%)	Std. deviation (%)	95% confidence interval (%)
A	10	7.6	0.6	[7.3, 8.0]
B	10	7.7	0.2	[7.6, 7.8]
C	10	7.6	0.1	[7.5, 7.7]
D	10	7.9	0.2	[7.8, 8.0]
E	10	7.9	0.1	[7.8, 8.0]

The flexural strain at maximum load (Table 19) is similar for all materials, with overlapping confidence intervals. This indicates that the strain level at which maximum flexural stress occurs is broadly comparable across Samples A–E. However, flexural strain at maximum load is not always highly sensitive to degradation effects, and embrittlement phenomena may instead become apparent in failure behaviour (e.g., crack initiation, stress whitening) and in more degradation-sensitive properties such as impact strength, elongation at break in tensile testing, and oxidative stability measurements (OIT).

Summary Three-point bending test

The three-point bending results show clear differences in flexural stiffness and strength between the materials. The recycled Aarhus River PP (Sample A) exhibited the highest flexural modulus (1337 MPa) and flexural stress at maximum (45.9 MPa), while the virgin reference materials (Samples D and E) showed lower values for both properties (modulus: 974–1020 MPa; stress at maximum: 36.4–37.3 MPa).

The blended materials (Samples B and C) fell between the recycled and virgin materials, indicating that blending shifts the flexural properties toward the virgin references.

In contrast, the flexural strain at maximum load was similar for all samples (~7.6–7.9%), with overlapping confidence intervals, suggesting that this parameter is less sensitive for distinguishing the material variants under the applied test conditions.

Overall, the bending results indicate that the recycled material is stiffer than the virgin references, while blending provides an intermediate response; the implications for degradation (e.g., possible embrittlement) should be evaluated together with tensile ductility, impact strength, oxidative stability results, and polymer grade differences.

15. Impact test

The Charpy impact test evaluates the resistance of a specimen to rapid fracture under impact loading. In the test, a rectangular bar supported at both ends was struck by a pendulum hammer at mid-span, resulting in bending at a high and approximately constant velocity. The energy absorbed during fracture was recorded and used to calculate the Charpy impact strength. In addition, the fracture mode was recorded in accordance with the standard classification.

Charpy impact testing was performed in accordance with ISO 179-1 (Charpy impact properties), using notched specimens prepared according to ISO 179-1/1eA and unnotched specimens for comparison. The test was performed using a CEAST Torino impact tester at 23□. For each material variant (Samples A–E), 10 unnotched and 10 notched specimens were tested to evaluate both the intrinsic impact resistance and the notch sensitivity of the materials.

In addition to the absorbed impact energy, the fracture mode was recorded for each specimen and classified according to the standard as:

- C – complete break, including hinge break (H)
- P – partial break
- N – non-break

This classification was used to support interpretation of the impact strength results and to describe differences in failure behaviour between the investigated materials.

A 2J pendulum was selected to provide adequate measurement resolution and ensure reliable comparability between the investigated materials within the expected absorbed energy range.

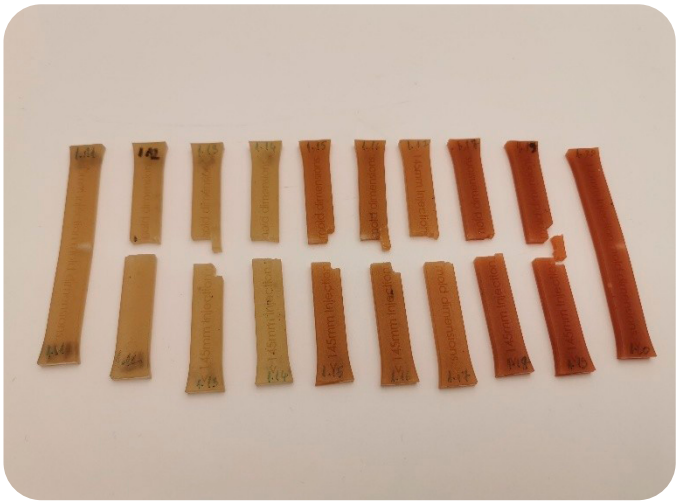

Sample A - Specimens without notch

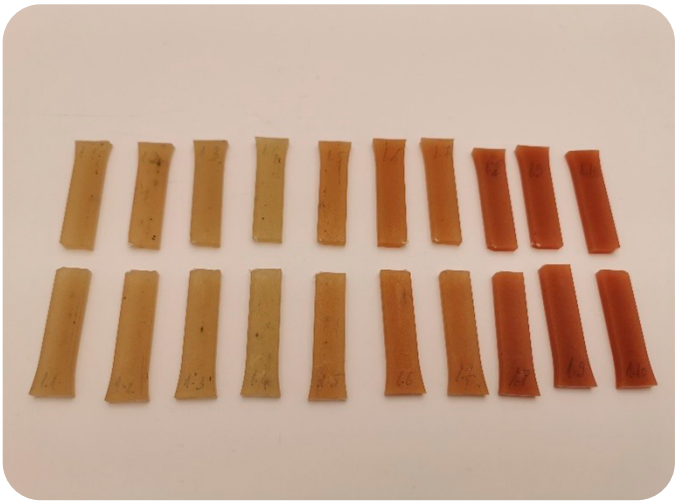

Sample A - Speciemens with notch

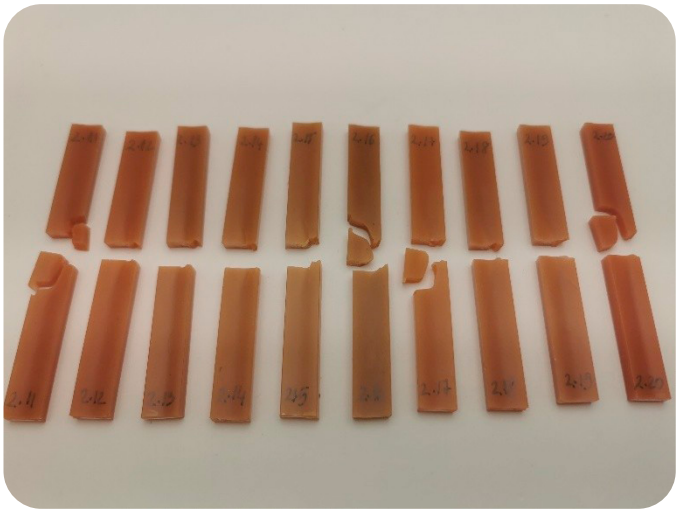

Sample B - Specimens without notch

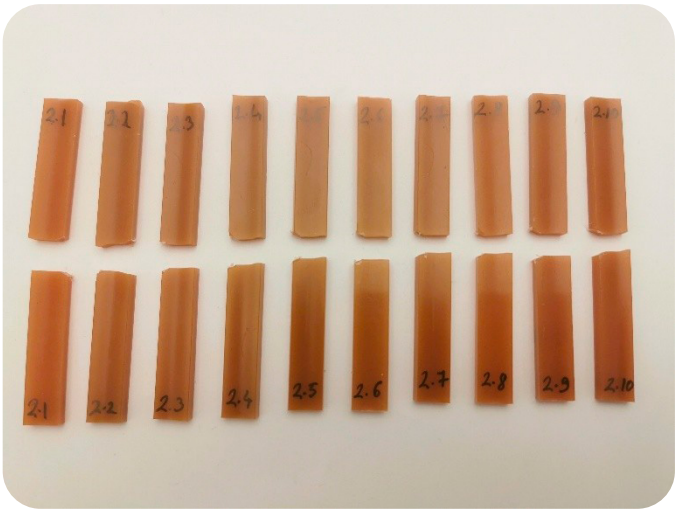

Sample B - Speciemens with notch

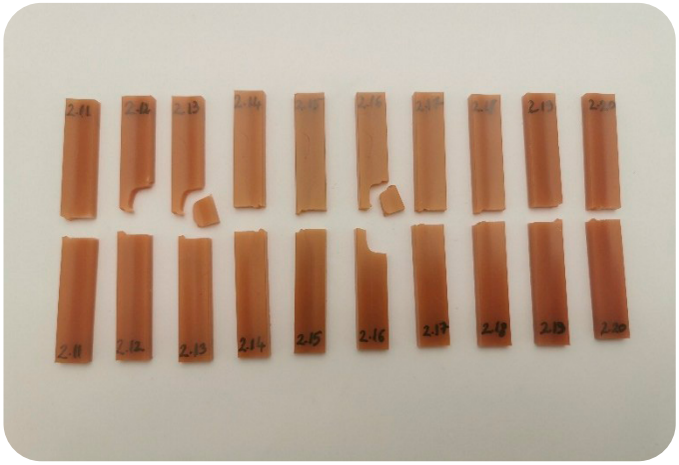

Sample C - Specimens without notch

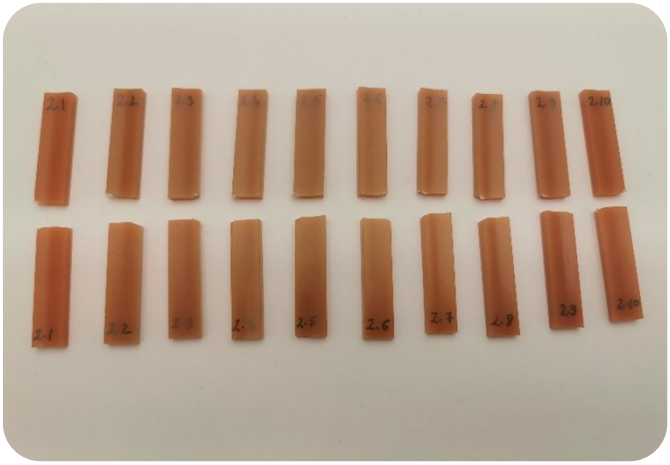

Sample C - Speciemens with notch

Figure 10: Charpy impact strength at 23 ^{O}C for unnotched and notched specimens of Samples A-E (continue on next page).

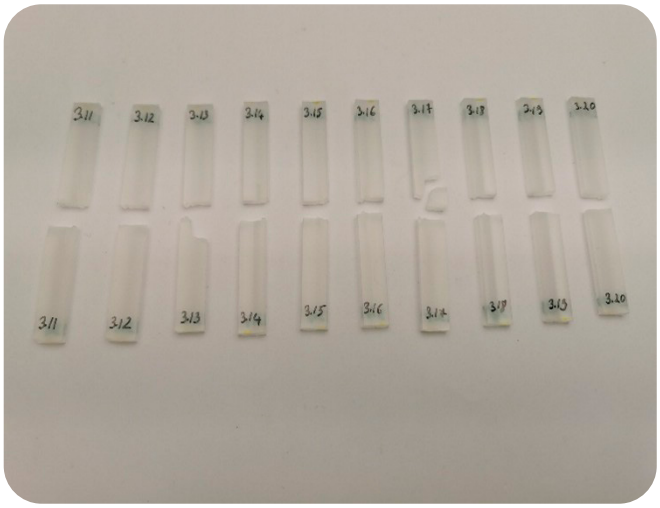

Sample D - Specimens without notch

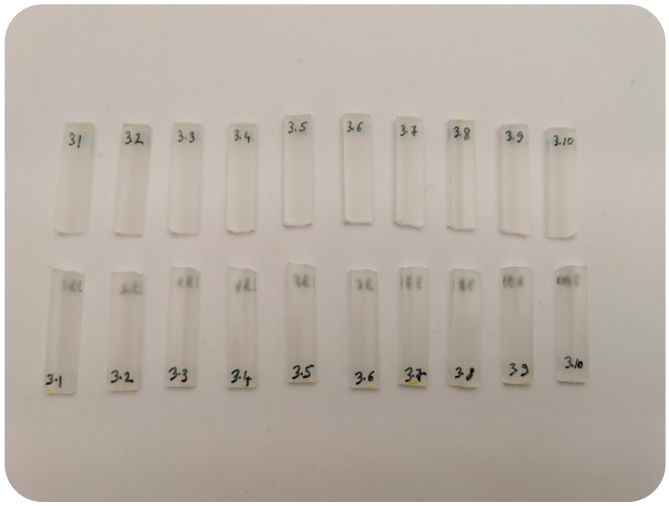

Sample D - Speciemens with notch

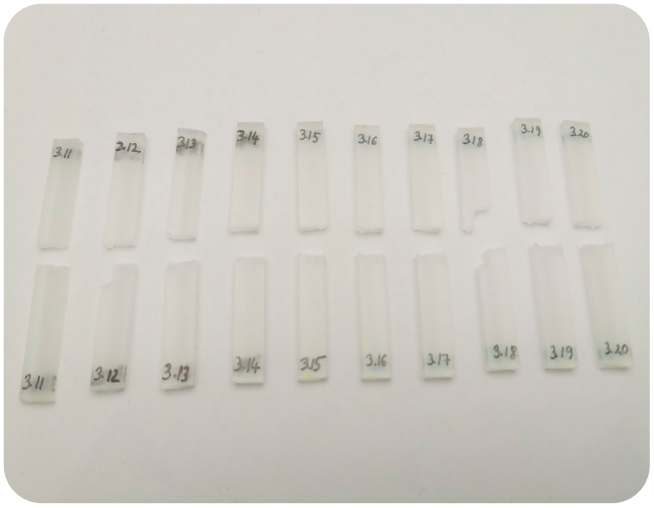

Sample E - Specimens without notch

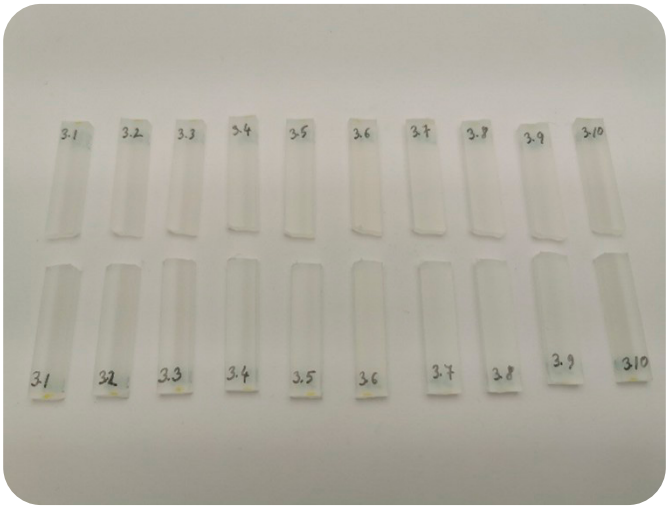

Sample E - Speciemens with notch

Figure 10: Charpy impact strength at 23 °C for unnotched and notched specimens of Samples A-E.

The Charpy impact strength results for unnotched specimens tested at 23□ are summarized in Table 20. The detailed raw data for the impact tests are provided in Appendix I. For each material variant (Samples A–E), 10 specimens were tested and the results are reported as average impact strength with standard deviation and 95% confidence interval. In addition to absorbed energy, the failure type was recorded for each specimen to support interpretation of differences in impact behaviour between the investigated materials.

Table 20: The results of Charpy impact strength at 23°C for unnotched specimens of Samples A-E.

Samples	Repetition	Impatch strength (kJ/m²)	Std. deviation (kJ/m²)	95% confidence interval (%)	Failure type
A without notch	10	73.7	12.4	[66.0, 81.4]	C - 8 speciments N - 2 speciments
B without notch	10	54.6	14.5	[45.6, 63.6]	C
C without notch	10	61.0	12.3	[53.4, 68.7]	C
D without notch	10	64.1	2.4	[62.6, 65.6]	C
E without notch	10	64.3	7.0	[59.9, 68.7]	C

Sample A exhibits the highest average unnotched impact strength (73.7 kJ/m²) and does not show reduced average impact performance compared with the blended or virgin reference materials under unnotched conditions. However, Sample A also shows a different failure response: 8 specimens resulted in complete break (C) while 2 specimens did not break (N), indicating greater scatter and mixed failure behaviour compared with the other samples, which predominantly showed complete break. This increased variability may reflect heterogeneity in the recycled Aarhus River material, for example due to variations in degradation level, impurities, or micro-defects introduced during environmental exposure and recovery/processing.

Among the remaining materials, the blended samples (B and C) show lower impact strengths (54.6–61.0 kJ/m²) than the virgin references (D and E, 64.1–64.3 kJ/m²), suggesting that adding 50% recycled material can reduce impact resistance compared with fully virgin PP. Overall, the unnotched impact test indicates that Sample A does not show reduced average impact performance, but the observed scatter and mixed failure types suggest that the recycled material may be less uniform; therefore, the notched impact results are expected to be particularly important for evaluating degradation-related notch sensitivity.

Table 21 presents the corresponding Charpy impact strength results for the notched specimens (23 ^{O}C, n = 10), including the failure type classification.

Table 21: The results of Charpy impact strength at 23 °C for notched specimens of Samples A-E.

Samples	Repetition	Impatch strength (kJ/m²)	Std. deviation (kJ/m²)	95% confidence interval (%)	Failure type
A with notch	10	2.6	0.1	[2.5, 2.7]	C
B with notch	10	2.2	0.6	[1.8, 2.6]	C
C with notch	10	2.2	0.3	[2.0, 2.4]	C
D with notch	10	1.8	0.1	[1.8, 1.9]	C
E with notch	10	2.1	0.4	[1.9, 2.3]	C

The notched impact results show substantially lower impact strengths compared with the unnotched condition, as expected due to the stress concentration introduced by the notch. All samples exhibited complete break (C). Among the investigated materials, Sample A shows the highest notched impact strength (2.6 kJ/m²), followed by Samples B, C, and E (2.1–2.2 kJ/m²), while Sample D shows the lowest value (1.8 kJ/m²). The relatively high impact observed for Sample A may reflect differences in polymer grade/type and morphology (e.g., crystallinity) compared with the selected virgin reference materials, rather than indicating superior intrinsic performance of the recycled fraction.

Summary Impact Test

From the perspective of evaluating degradation of the recycled Aarhus River PP, the notched results indicate that Sample A is not weaker than the blended or virgin reference materials under notch-sensitive loading; instead, it performs at least as well as the other materials in this dataset.

The relatively small differences between samples and the partially overlapping confidence intervals suggest that notch impact strength at 23 ^{O}C is influenced not only by recycled content but also by the specific virgin grade and specimen-to-specimen variability. Nevertheless, the combination of notched and unnotched results is useful for assessing notch sensitivity: while Sample A shows high average values in both conditions, the larger scatter and mixed failure behaviour observed in the unnotched tests may still indicate greater material heterogeneity in the recycled fraction.

This is particularly important because tensile strain values are interpreted with caution due to differing gauge length; therefore, impact behaviour and OIT provide key support when assessing embrittlement and ageing.

16. Discussion

The combined mechanical, thermal, and chemical results provide an overall picture of the condition of polypropylene recovered from the Aarhus River (Sample A) and how blending with virgin polypropylene (Samples B and C) influences performance and stability.

From an ageing perspective, the clearest degradation-related signal is observed in the oxidation induction time (OIT). This is also consistent with the stiffness results, as oxidation in PP can initially increase modulus (stiffer material) while OIT decreases, before later-stage degradation becomes dominated by embrittlement. Sample A shows the lowest oxidative stability, while the blends are intermediate and the virgin references show the highest values. This supports that the recovered PP has reduced resistance to oxidation, consistent with antioxidant depletion and/or oxidative ageing during environmental exposure and reprocessing, and that blending partially restores oxidative stability but does not fully recover virgin-level stability. The observed difference between the two virgin grades (Samples D and E) is most likely explained by normal grade-to-grade variation in stabilization/additive package rather than ageing.

In contrast, the polymer “fingerprint” results indicate that the recovered material remains PP-dominated. FTIR confirms PP as the dominant polymer and does not show strong additional contamination bands. DSC shows PP-typical melting behaviour for all samples and does not indicate additional melting transitions that would suggest contamination by other common polymer types. TGA likewise shows PP-like decomposition behaviour and very low ash/residual mass for all variants (<1%), indicating no strong evidence of elevated inorganic residue after cleaning and processing. Together, these findings suggest that major inorganic contamination is not the primary driver of performance differences, and that differences are more likely linked to additive state, molecular-weight distribution, morphology/crystallinity, and heterogeneity of the recovered stream rather than gross contamination.

For TGA, small differences in degradation onset are visible in the overlay, where Samples A and C show a slightly earlier onset of mass loss than the other materials. Given that Sample A (and consequently the blends) can represent a heterogeneous stream of PP items with different grades and additive packages (and potentially minor low-level secondary components), such small shifts should be interpreted cautiously and not used alone to rank “thermal stability” between materials. The key outcome from TGA is that all samples have low non-volatile residue and PP-typical decomposition behaviour.

From a mechanical perspective, the results do not follow a simple “recycled = weaker” trend. Several stiffness/strength-related values for Sample A are comparable to (or higher than) the virgin references. However, this must be interpreted carefully because Sample A may originate from a different PP grade/type than the selected EP400/EP500 references. This is supported by the melt flow behaviour: Sample A exhibits markedly lower MFI than the injection-grade references, suggesting that the recovered stream may behave more like a lower-flow PP (potentially closer to extrusion-type material) and/or a mixture of PP grades. Therefore, differences in stiffness/strength cannot be attributed to degradation alone and should be interpreted in the context of grade effects and heterogeneity.

Tensile strain-based parameters require additional caution because the specimen type and strain measurement basis differ between Sample A (ISO 527-1B; gauge length 50 mm) and Samples B–E (ISO 527-1A; gauge length 75 mm). A shorter gauge length can influence reported strain values if strain is derived from crosshead displacement and affected by system compliance. Therefore, the higher strain values reported for Sample A cannot be used alone to conclude higher ductility or lower degradation; instead, tensile failure behaviour should be assessed using stress-at-break together with notch-sensitive impact behaviour and OIT.

Impact testing provides an important fracture-sensitivity indicator. Sample A does not appear systematically weaker in average impact strength, but it shows higher scatter and mixed failure response in unnotched testing (including non-breaks), which may reflect heterogeneity in the recovered stream (variation in ageing state, minor defects, or composition differences between recovered items). Blends can also show scatter, potentially influenced by mixing quality and local recycled/virgin distribution. Overall, the results indicate that environmental exposure is most clearly reflected as reduced oxidative stability, while many mechanical properties remain within a usable range, provided that variability and long-term durability risks are considered.

17. Conclusion

Conclusion

This study evaluated whether polypropylene recovered from the Aarhus River shows signs of degradation and reduced performance compared with virgin polypropylene using a combination of mechanical testing, melt-flow characterization, and chemical/thermal analyses. Three material scenarios were assessed: (i) 100% recycled Aarhus River PP (Sample A), (ii) 50/50 recycled–virgin blends (Samples B and C), and (iii) 100% virgin PP references (Samples D and E).

FTIR, DSC, and TGA confirm that all investigated materials remain PP-dominated and show PP-typical thermal behaviour. No additional DSC melting transitions characteristic of other common polymers were observed, and TGA residual mass values are low for all samples (<1%), indicating no strong evidence of elevated inorganic residue after processing. Small differences in TGA onset behaviour (slightly earlier onset for Samples A and C) are observed but should be interpreted cautiously given the heterogeneous nature of the recovered stream; the main conclusion from TGA is that all materials show PP-like decomposition and low ash content.

The clearest evidence of ageing-related effects is provided by OIT. Sample A exhibits the lowest oxidative stability compared with the virgin references, and the blends show intermediate values. This supports that the recovered Aarhus River PP is more oxidation-prone, consistent with antioxidant depletion and/or oxidative ageing during environmental exposure, and that blending provides partial but not full restoration of oxidative stability. Differences between the two virgin grades (Samples D and E) are expected and likely reflect normal grade-to-grade variation in stabilization/additive package.

Mechanically, the recovered material does not show consistent weakening across all properties, and several stiffness/strength values are comparable to the virgin references. However, interpretation is influenced by important limitations: (1) the recovered Aarhus River PP may represent a different PP grade/type (or a mix of grades) than the EP400/EP500 injection-grade references, and (2) tensile strain values must be interpreted cautiously because the specimen type and gauge length differed (Sample A: ISO 527-1B, 50 mm; Samples B–E: ISO 527-1A, 75 mm). Therefore, degradation assessment should rely more strongly on oxidative stability (OIT), fracture-related tensile stress-at-break behaviour, and notch-sensitive impact performance than on yield/strength values alone.

Overall, polypropylene recovered from the Aarhus River can be processed and remains mechanically usable in this study, but it shows reduced oxidative stability relative to virgin PP and may exhibit greater variability consistent with heterogeneity in recovered material streams.

Blending with virgin PP improves stability and provides intermediate performance but does not fully restore virgin-level oxidative resistance. The reuse suitability of the recovered material therefore depends on the intended application and processing route: the melt flow behaviour suggests that reuse may be more appropriately evaluated relative to lower-flow PP applications (e.g., extrusion-type processing) rather than assuming direct equivalence with injection-grade references. For long service-life or high-demand products, additional stabilization and quality control are recommended, while for less demanding applications the results support Aarhus River PP as a viable recycled material stream within circular plastics strategies.

Appendix

APPENDIX A – FTIR SPECTRA OF SAMPLES

Sample A – 1

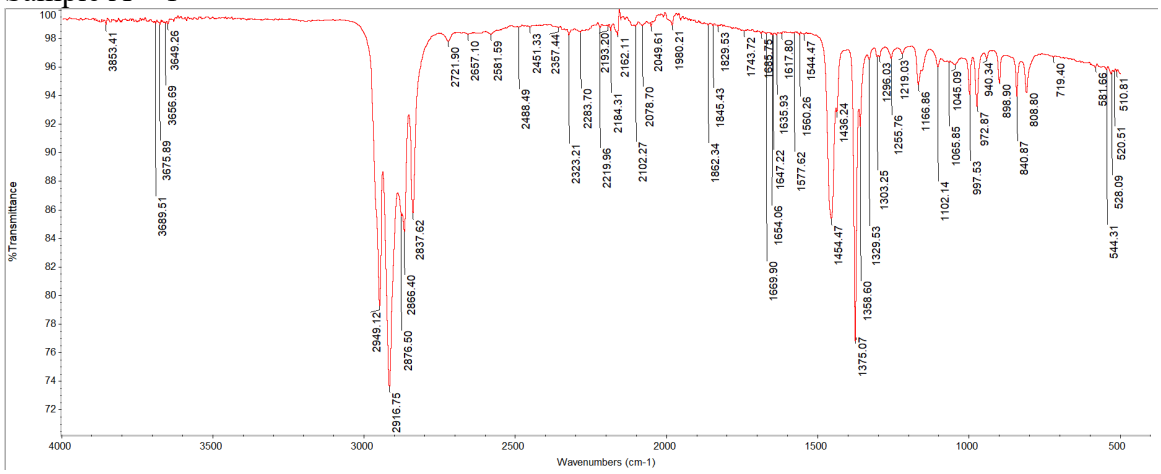

Figure 11: FTIR spectrum of Sample A – 1.

Sample A – 2

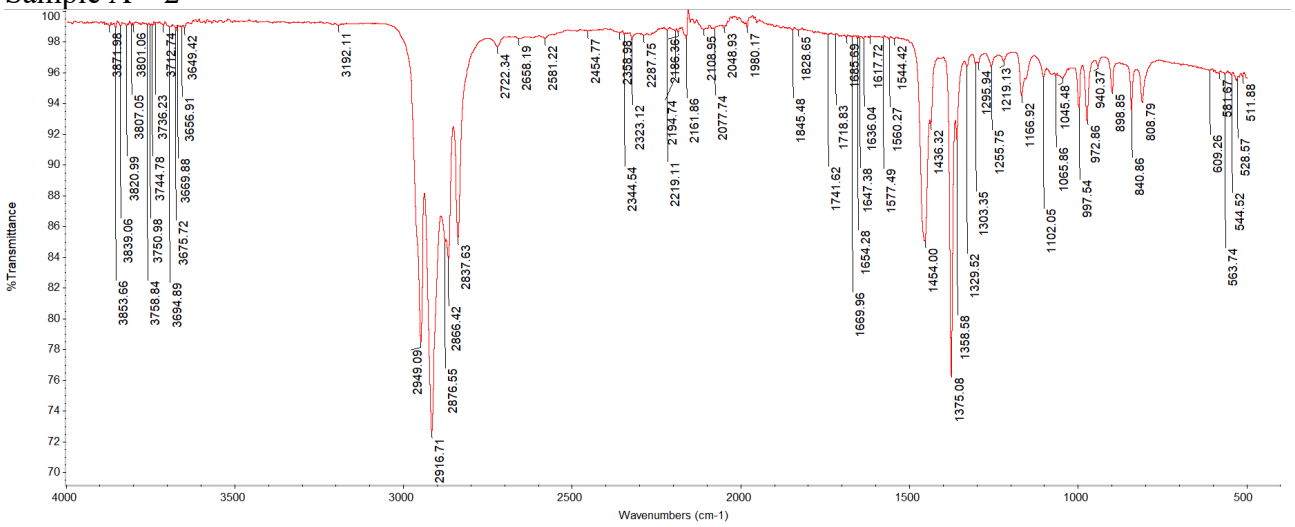

Figure 12: FTIR spectrum of Sample A – 2.

Sample B – 1

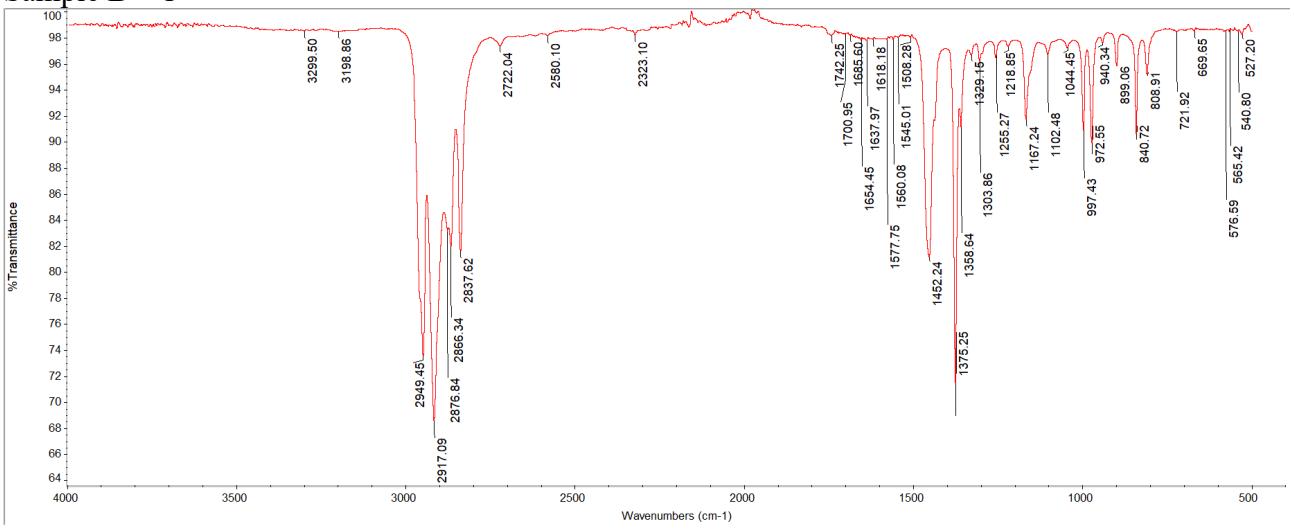

Figure 13: FTIR spectrum of Sample B – 1.

Sample B – 2

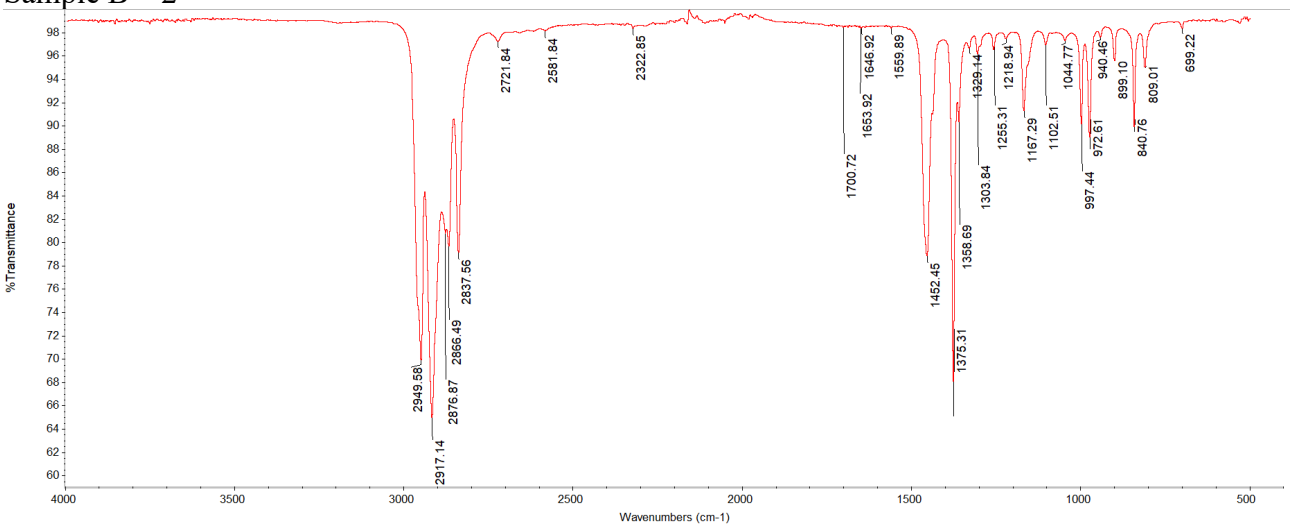

Figure 14: FTIR spectrum of Sample B – 2.

Sample C – 1

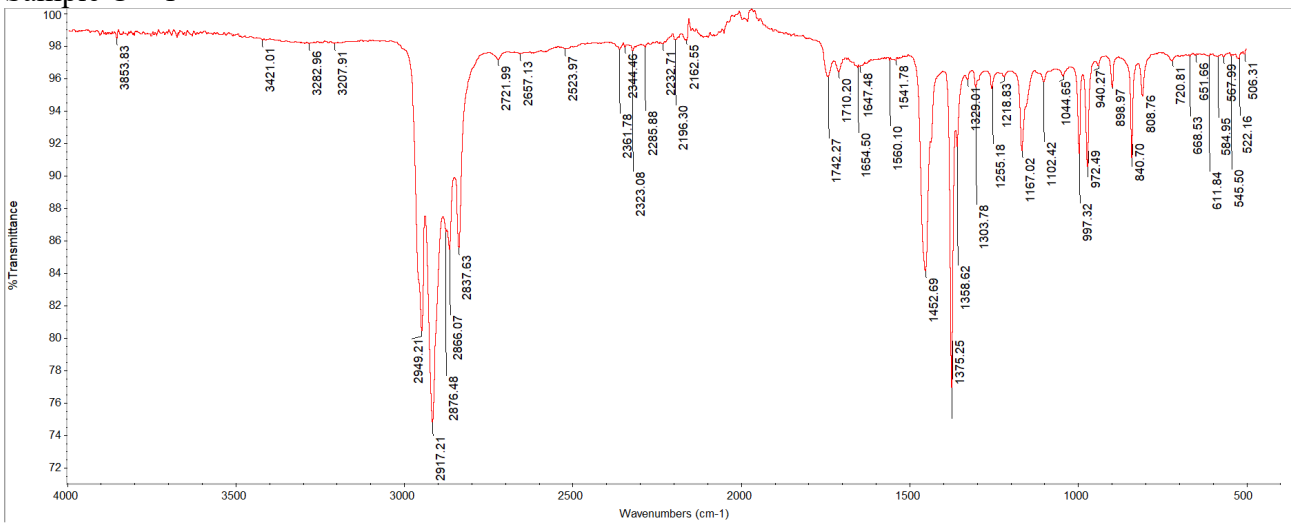

Figure 15: FTIR spectrum of Sample C – 1.

Sample C – 2

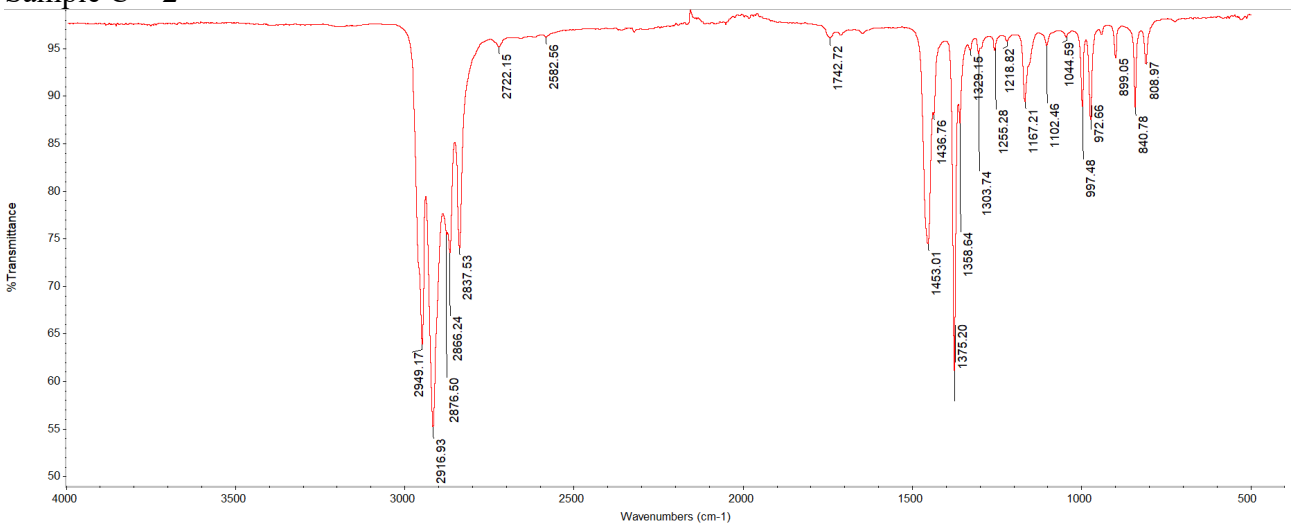

Figure 16: FTIR spectrum of Sample C – 2.

Sample D – 1

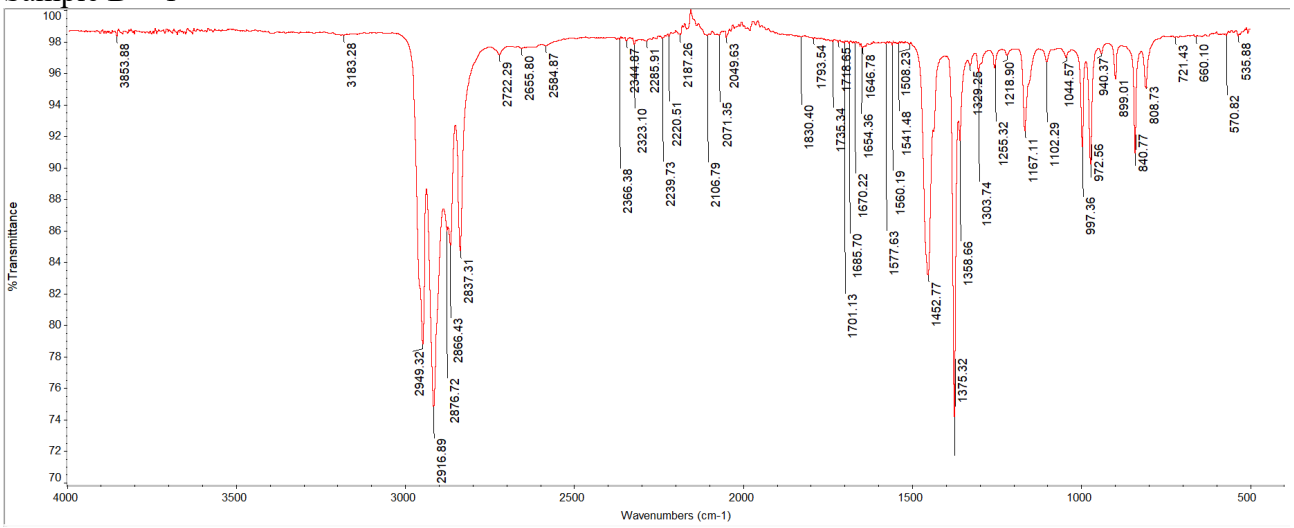

Figure 17: FTIR spectrum of Sample D – 1.

Sample D – 2

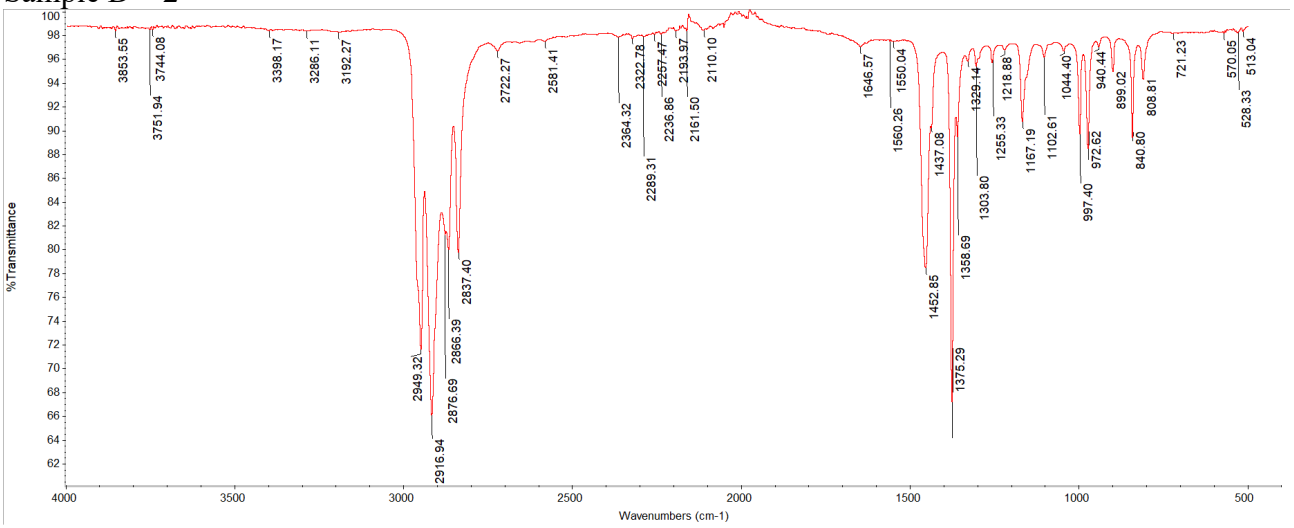

Figure 18: FTIR spectrum of Sample D – 2.

Sample E – 1

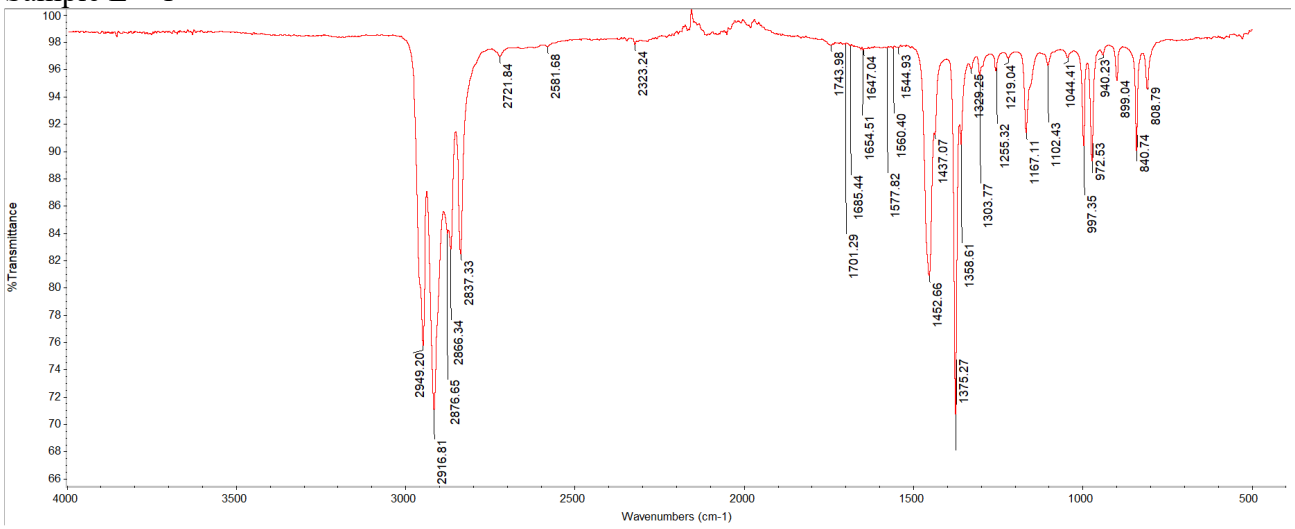

Figure 19: FTIR spectrum of Sample E – 1.

Sample E - 2

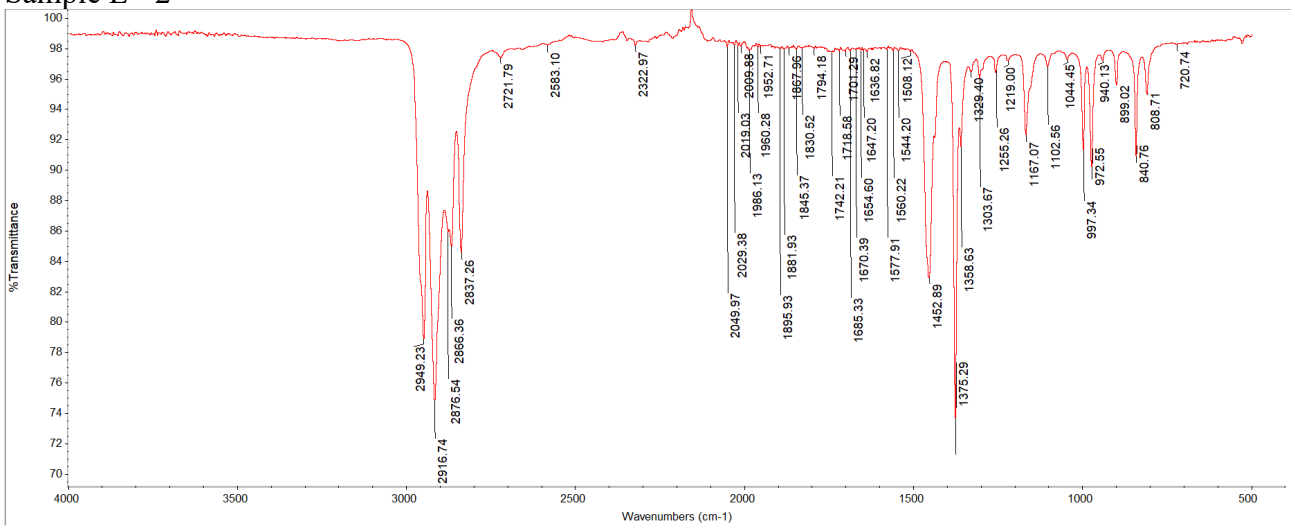

Figure 20: FTIR spectrum of Sample E – 2.

APPENDIX B – DSC THERMOGRAMS OF SAMPLES

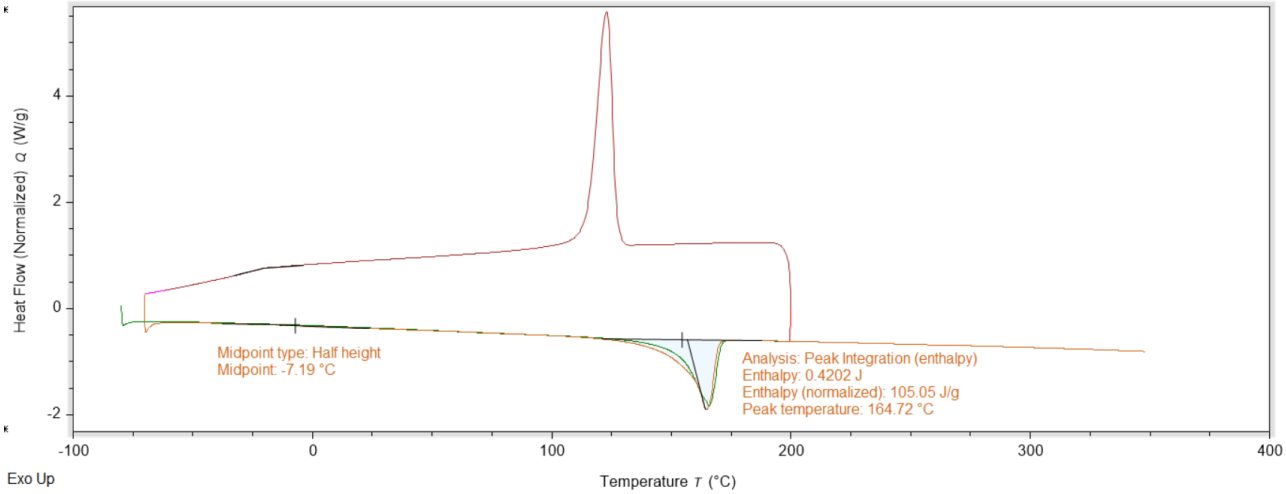

Figure 21: DSC thermogram for Sample A.

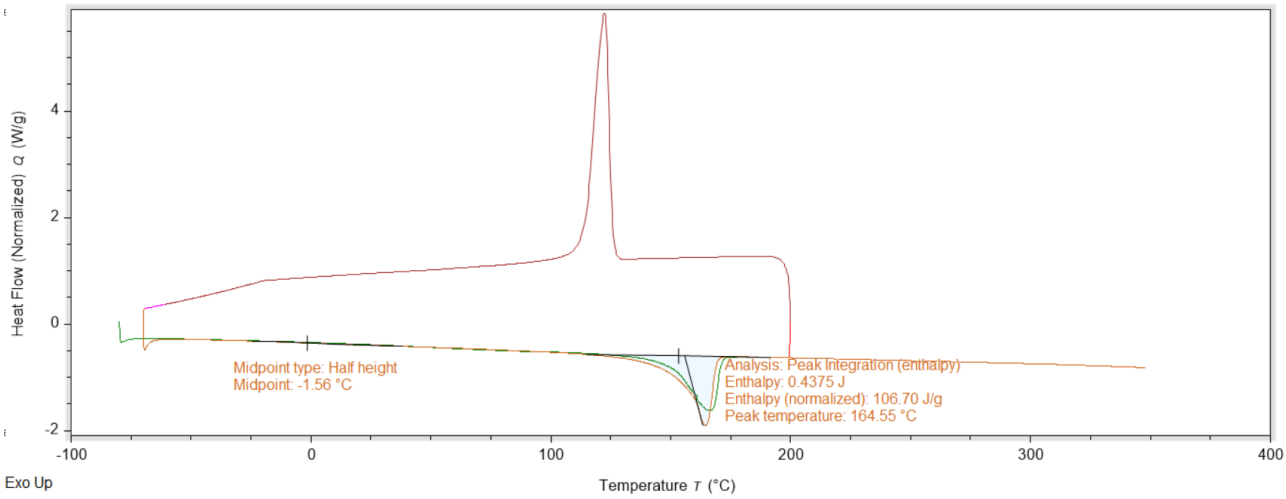

Figure 22: DSC thermogram for Sample B.

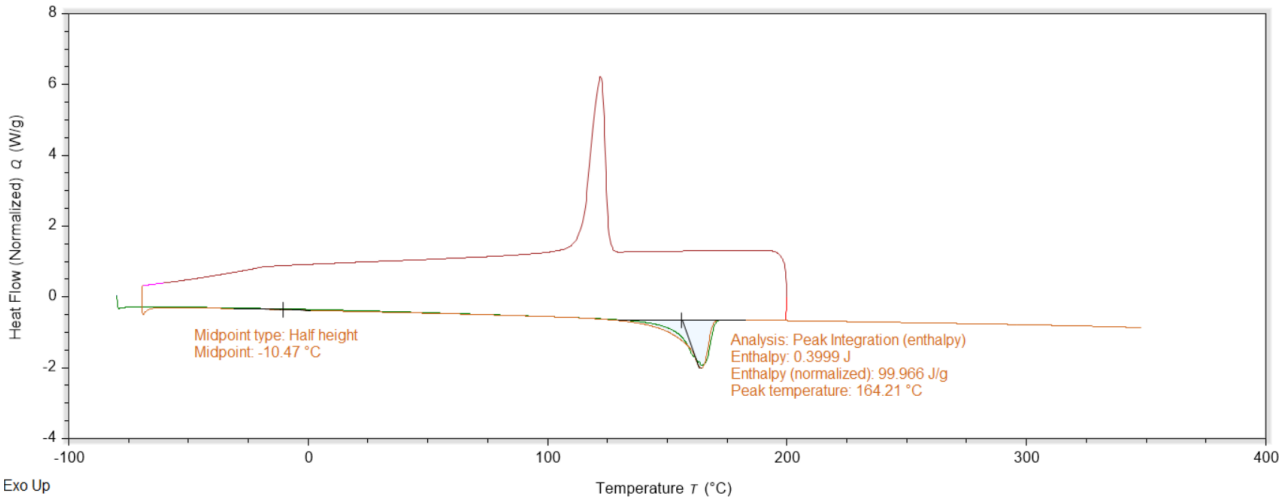

Figure 23: DSC thermogram for Sample C.

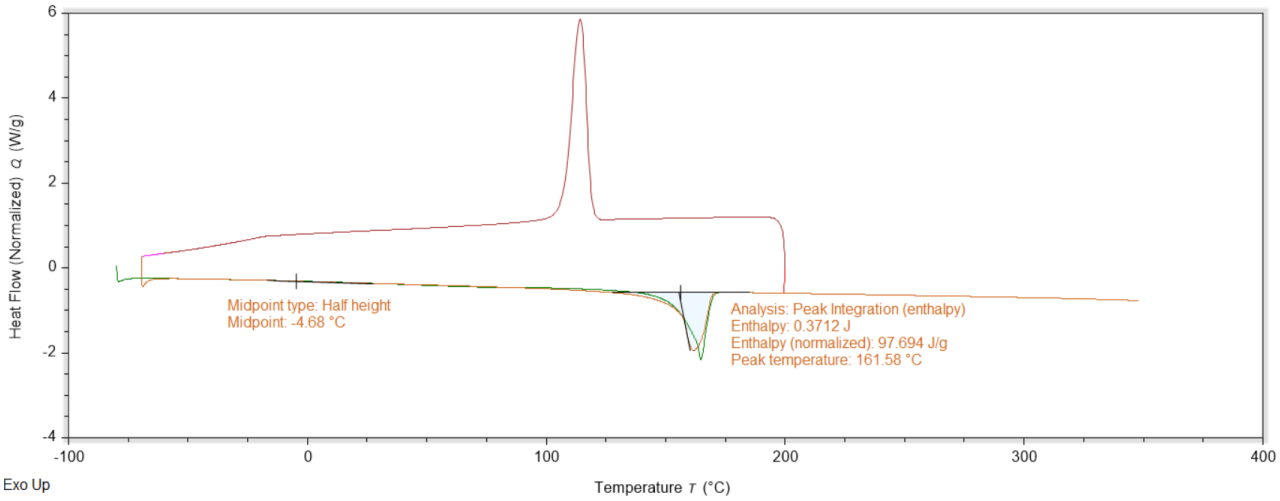

Figure 24: DSC thermogram for Sample D.

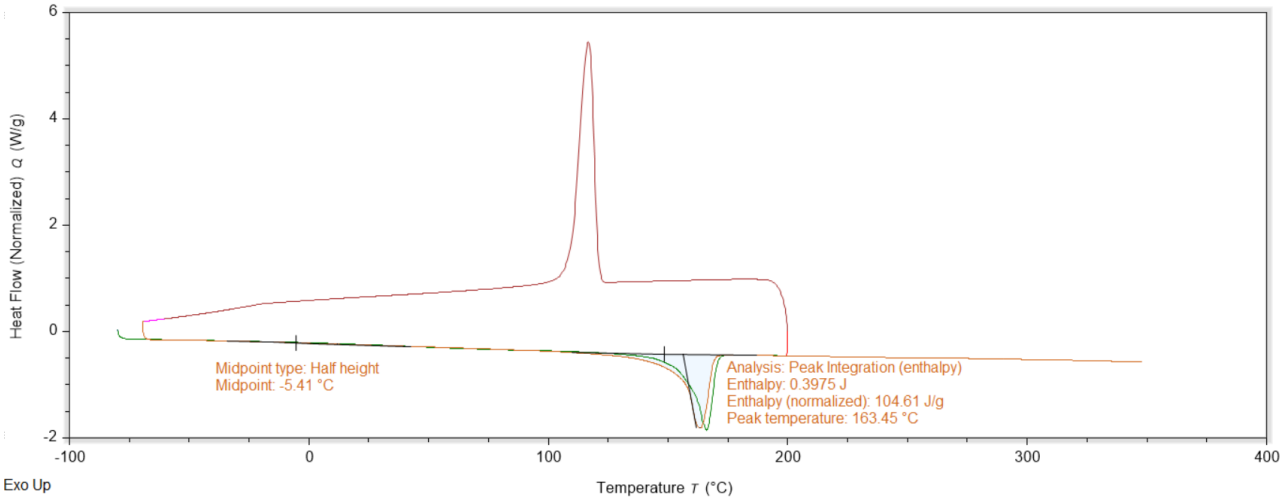

Figure 25: DSC thermogram for Sample E.

APPENDIX C – OIT THERMOGRAMS OF SAMPLES

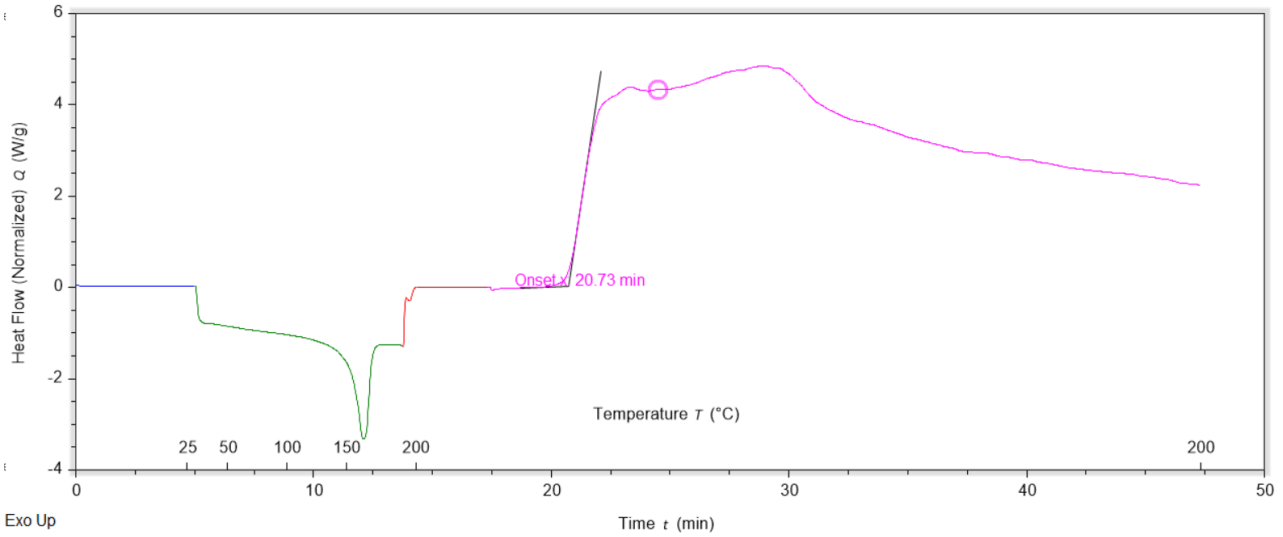

Figure 26: OIT thermogram for Sample A.

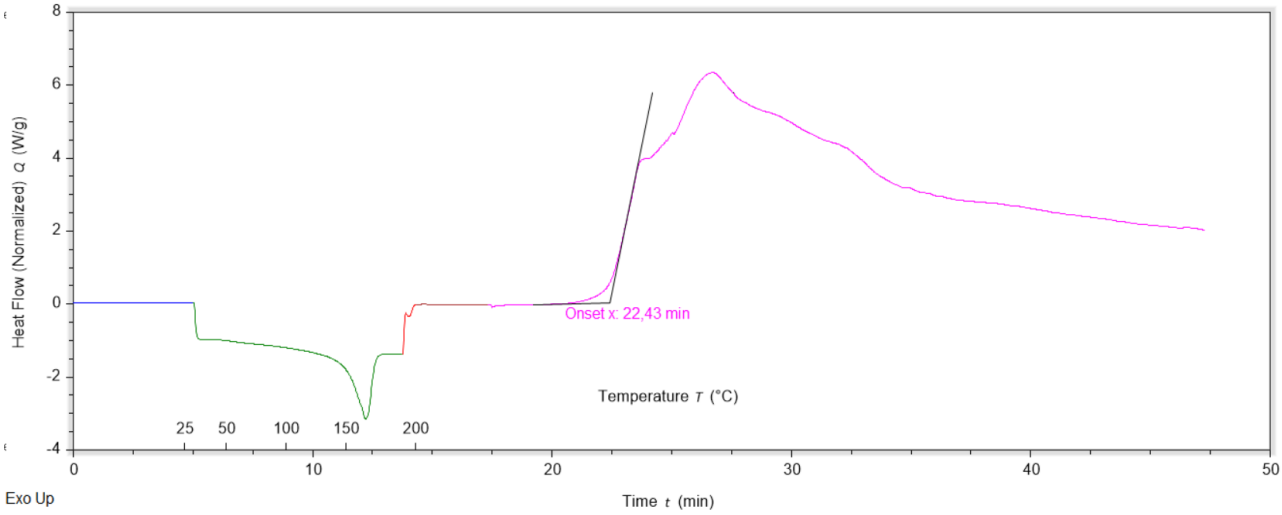

Figure 27: OIT thermogram for Sample B.

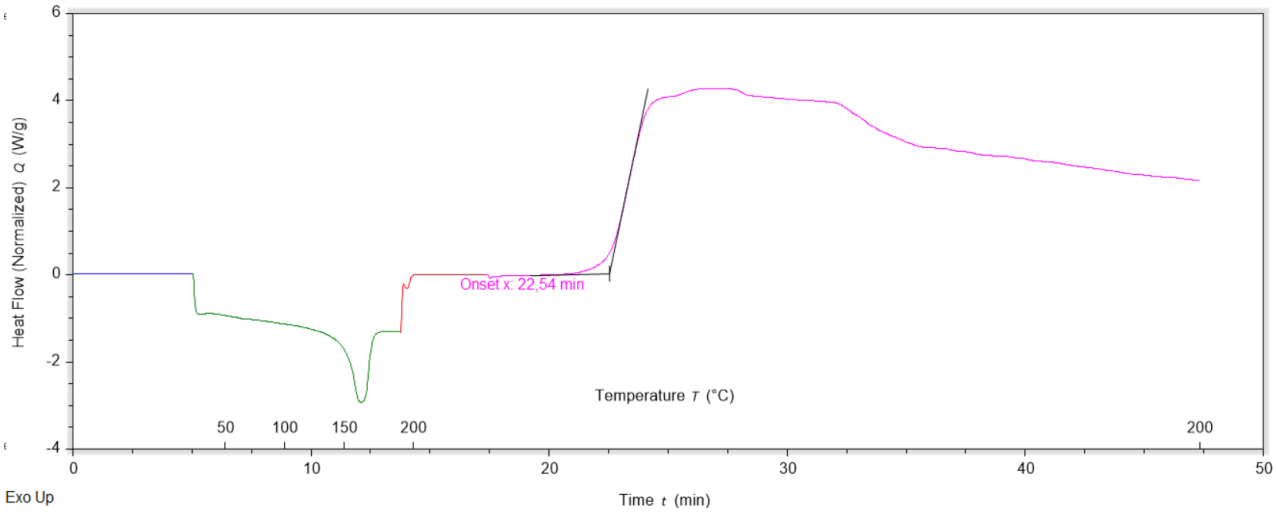

Figure 28: OIT thermogram for Sample C.

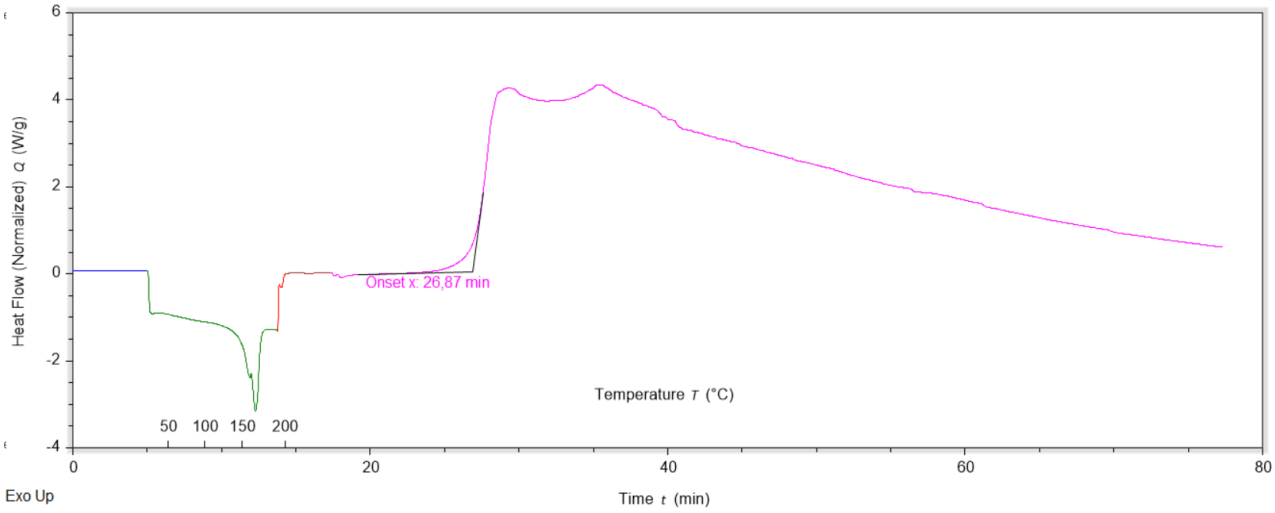

Figure 29: OIT thermogram for Sample D.

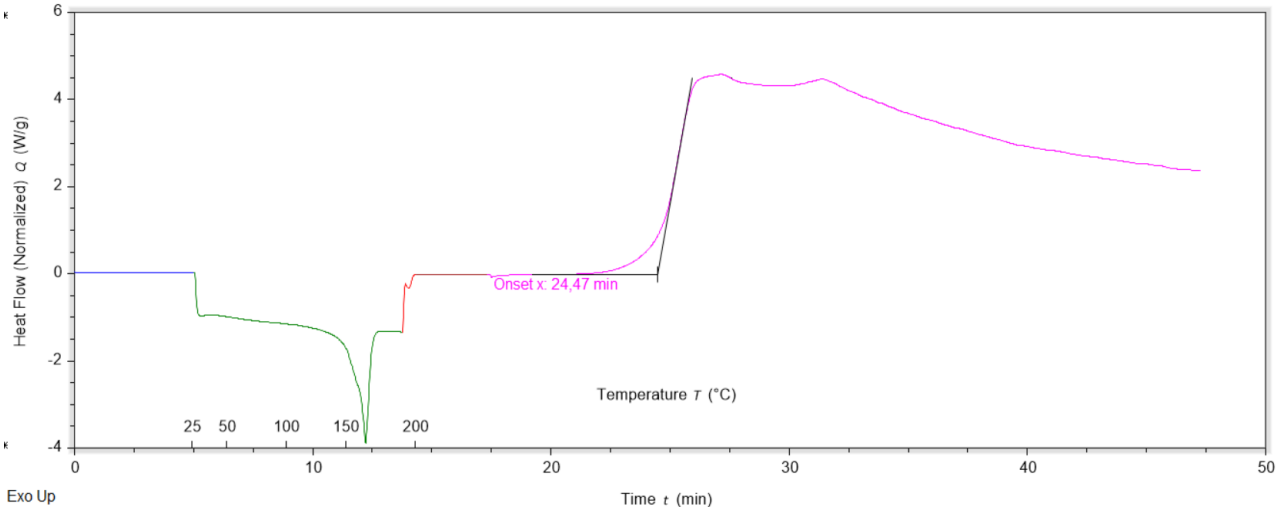

Figure 30: OIT thermogram for Sample E.

APPENDIX D – TGA THERMOGRAMS OF SAMPLES

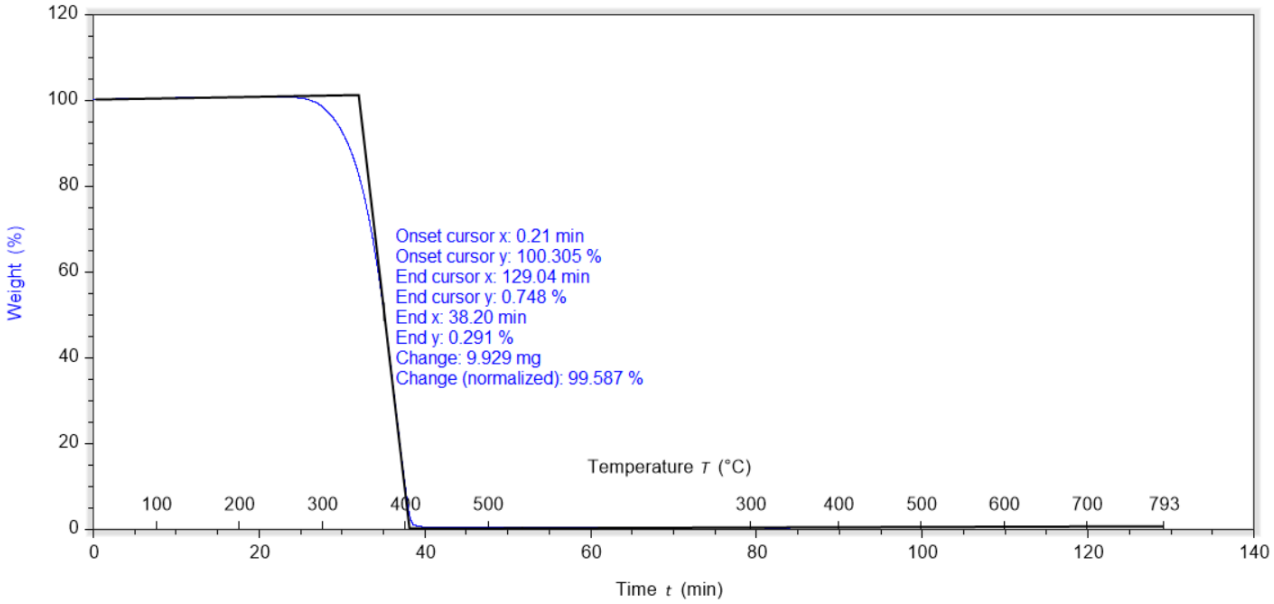

Figure 31: TGA thermogram of Sample A.

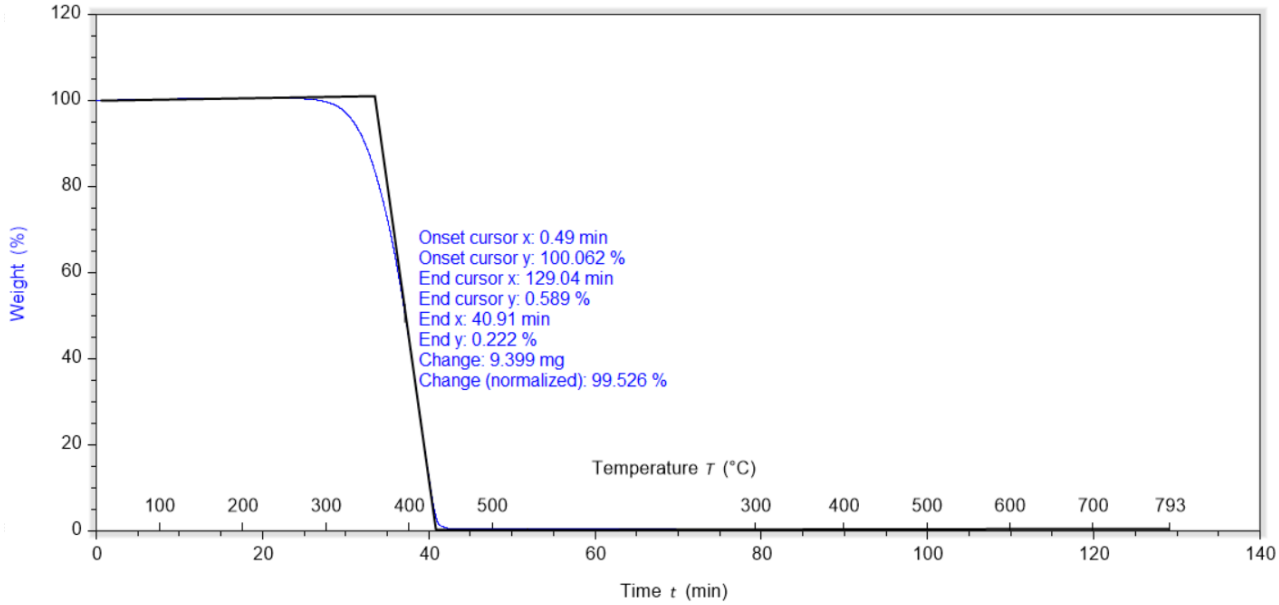

Figure 32: TGA thermogram of Sample B.

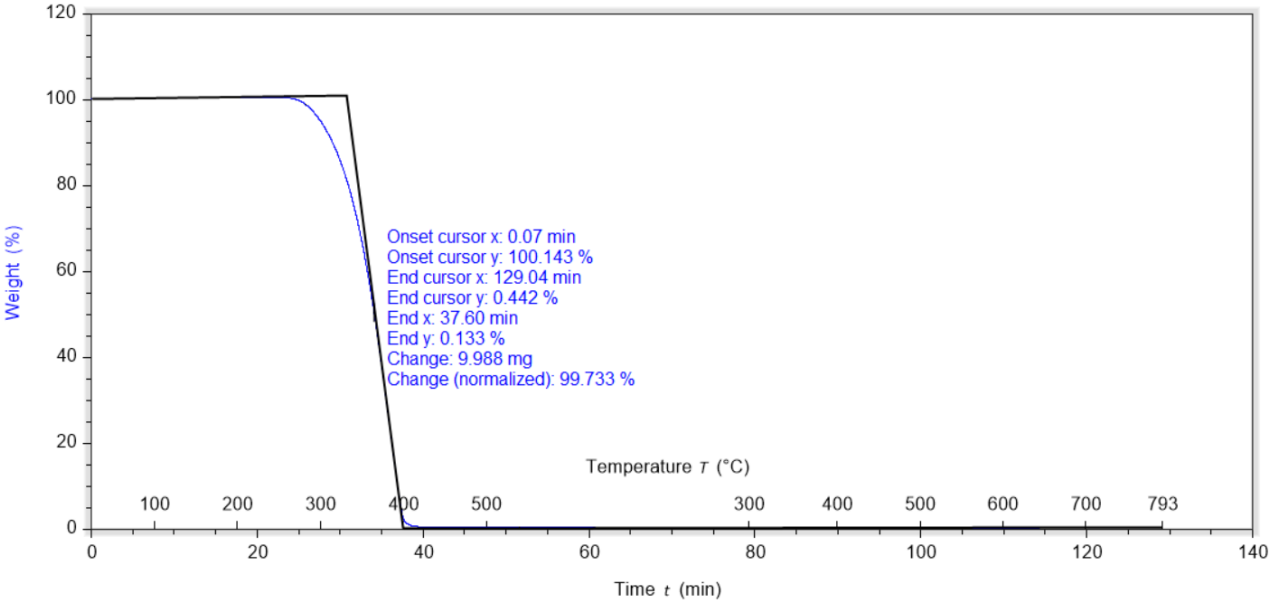

Figure 33: TGA thermogram of Sample C.

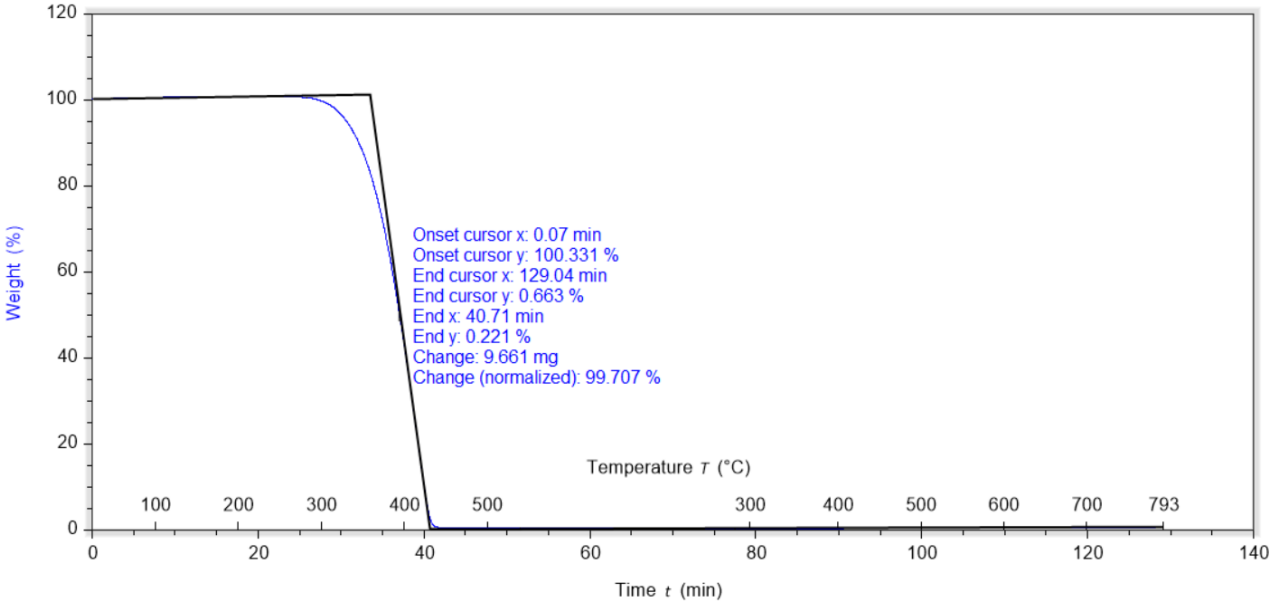

Figure 34: TGA thermogram of Sample D.

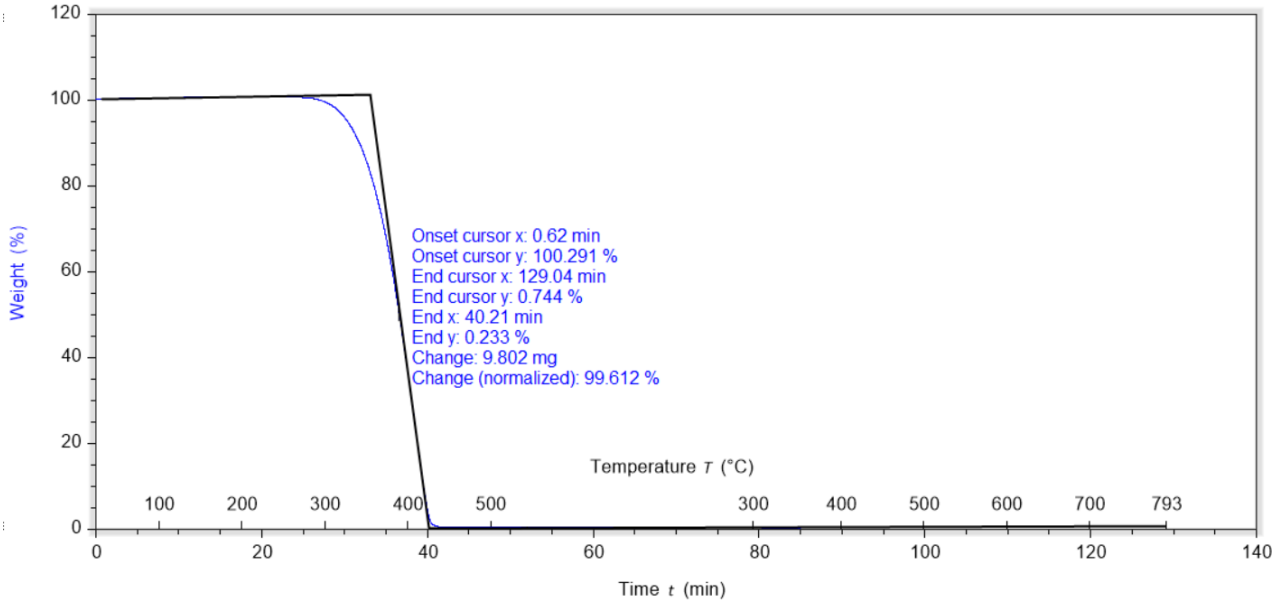

Figure 35: TGA thermogram of Sample E.

APPENDIX E – DATA FROM DENSITY

Table 22: The weighing of the samples in air ($m_{S,A}$) and the samples immersed in liquid ($m_{S,IL}$) of the porous specimens.

Sample	Repetition	$m_{S,A}$(g)	$m_{S,IL}$(g)	Density g/cm^3	Average Density g/cm^3	Standard Deviation	95% confidence interval
A	1	1.8838	0.2492	0.91	0.91	0.00	[0.91, 0.91]
	2	1.8513	0.2449	0.91			
	3	1.8725	0.2480	0.91			
	4	1.8613	0.2470	0.91			
	5	1.8715	0.2482	0.91			
B	1	1.8147	0.2425	0.91	0.91	0.00	[0.91, 0.91]
	2	1.8293	0.2443	0.91			
	3	1.8107	0.2427	0.91			
	4	1.7665	0.2363	0.91			
	5	1.8240	0.2477	0.91			
C	1	1.8695	0.2488	0.91	0.91	0.00	[0.91, 0.91]
	2	1.8440	0.2451	0.91			
	3	1.8497	0.2451	0.91			
	4	1.8534	0.2460	0.91			
	5	1.8373	0.2449	0.91			
D	1	1.7030	0.2220	0.91	0.91	0.00	[0.91, 0.91]
	2	1.7977	0.2354	0.91			
	3	1.7774	0.2322	0.91			
	4	1.8323	0.2384	0.91			
	5	1.7903	0.2340	0.91			

E	1	1.8137	0.2359	0.91	0.91	0.00	[0.91, 0.91]
	2	1.8092	0.2346	0.91			
	3	1.8247	0.2380	0.91			
	4	1.8051	0.2348	0.91			
	5	1.8225	0.2371	0.91			

APPENDIX F – DATA FROM SHORE HARDNESS TEST

Table 23: The measurements and the statistical results on the five samples by Shore D.

Sample	Repetition	Hardness	Average hardness	Standard deviation	95% confidence interval
A	1.1	73.0	73.0	0.8	[72.5, 73.5]
	1.2	73.0			
	1.3	74.0			
	1.4	73.0			
	1.5	74.0			
	1.6	73.0			
	1.7	74.0			
	1.8	72.0			
	1.9	72.0			
	1.10	72.0			
B	2.1	73.0	73.35	1.6	[72.4, 74.3]
	2.2	71.5			
	2.3	73.0			
	2.4	71.0			
	2.5	73.5			
	2.6	74.5			
	2.7	73.5			
	2.8	76.0			
	2.9	75.5			
	2.10	72.0			
C	2.11	71.0	73.0	1.8	[71.9, 74.1]
	2.12	69.0			
	2.13	72.0			
	2.14	74.0			
	2.15	73.0			
	2.16	74.0			
	2.17	73.5			
	2.18	74.5			
	2.19	74.0			
	2.20	75.0			
D	3.1	71.0	70.2	1.3	[69.4, 71.0]
	3.2	69.5			
	3.3	68.5			

	3.4	68.0			
	3.5	70.5			
	3.6	69.5			
	3.7	70.5			
	3.8	72.0			
	3.9	71.0			
	3.10	71.5			
E	3.11	73.0	72.1	0.7	[71.7, 72.5]
	3.12	73.0			
	3.13	71.5			
	3.14	72.5			
	3.15	72.0			
	3.16	72.0			
	3.17	71.0			
	3.18	72.0			
	3.19	72.5			
	3.20	71.5			

APPENDIX G – DATA FROM TENSILE TEST

Table 24: E-modulus results – Sample A.

Specimen no.	Width (mm)	Thickness (mm)	Grip (mm)	Poisson Ratio	E Modulus (MPa)
1	9.84	4.04	115.05	0.41	1786.5
2	9.83	4.06	114.82	0.42	1756.5
3	9.83	4.06	115.06	0.40	1689.5
4	9.83	4.07	114.97	0.40	1727.6
5	9.87	4.08	115.2	0.40	1779.8
6	9.86	4.1	115.12	0.40	1713.5
7	9.87	4.09	115.18	0.41	1718.0
8	9.87	4.11	115.46	0.41	1730.9
9	9.86	4.09	114.96	0.43	1784.6
10	9.86	4.1	114.94	0.41	1766.5
Average	**9.85**	**4.08**	**115.08**	**0.41**	**1745.3**
Std. dev.	**0.02**	**0.02**	**0.18**	**0.01**	**34.0**
95% confidence interval				**[0.40, 0.4]**	**[1724.3, 1766.4]**

Table 25: E-modulus results – Sample B.

Specimen no.	Width (mm)	Thickness (mm)	Grip (mm)	Poisson Ratio	E Modulus (MPa)
1	9.7	4	115.41	0.49	1809.4
2	9.7	4	114.62	0.44	1806.9
3	9.68	4	114.86	0.45	1728.3
4	9.7	4	115.38	0.42	1717.9
5	9.69	4.4	115.35	0.43	1604.5
6	9.69	4	115.39	0.43	1677.8
7	9.73	4	115.54	0.43	1691.9
8	9.77	4	115.29	0.44	1674.2
9	9.67	4	115.52	0.44	1715.4
10	9.71	4	115.76	0.42	1729.0
Average	**9.70**	**4.04**	**115.31**	**0.44**	**1715.5**
Std. dev.	**0.03**	**0.13**	**0.33**	**0.02**	**61.0**
95% confidence interval				**[0.42, 0.45]**	**[1677.72, 1753.37]**

Table 26: E-modulus results – Sample C.

Specimen no.	Width (mm)	Thickness (mm)	Grip (mm)	Poisson Ratio	E Modulus (MPa)
1	9.74	4.03	115.48	0.43	1621.5
2	9.73	4.01	115.61	0.44	1676.5
3	9.77	4.03	115.69	0.45	1669.0
4	9.74	4.01	115.68	0.45	1622.5
5	9.74	4.01	115.67	0.42	1691.6
6	9.74	4.02	115.46	0.43	1701.0
7	9.75	4.01	115.73	0.45	1634.2
8	9.75	4.01	115.59	0.43	1516.8
9	9.73	4.02	115.17	0.44	1642.5
10	9.77	4.02	114.91	0.44	1655.2
Average	**9.75**	**4.02**	**115.5**	**0.44**	**1643.1**
Std. dev.	**0.01**	**0.01**	**0.26**	**0.01**	**52.2**
95% confidence interval				**[0.43, 0.44]**	**[1610.7, 1675.5]**

Table 27: E-modulus results – Sample D.

Specimen no.	Width (mm)	Thickness (mm)	Grip (mm)	Poisson Ratio	E Modulus (MPa)
1	10	4.09	115.48	0.42	1356.5
2	9.78	4.01	115.67	0.44	1245.2
3	9.77	4.02	115.5	0.40	1308.6
4	9.79	4.02	115.53	0.42	1385.6
5	9.79	4.02	115.46	0.48	1325.0
6	9.79	4.02	115.12	0.51	1450.2
7	9.78	4.03	115.25	0.39	1427.4
8	9.77	4.01	115.17	0.45	1565.6
9	9.82	4.01	115.58	0.44	1406.6
10	9.8	4.01	115.08	0.43	1328.5
Average	**9.8**	**4.02**	**115.38**	**0.44**	**1379.9**
Std. dev.	**0.07**	**0.02**	**0.21**	**0.03**	**89.4**
95% confidence interval				**[0.42, 0.46]**	**[1324.5, 1435.3]**

Table 28: E-modulus results – Sample E.

Specimen no.	Width (mm)	Thickness (mm)	Grip (mm)	Poisson Ratio	E Modulus (MPa)
1	9.8	4.02	115.29	0.48	1334.2
2	9.79	4.02	115.15	0.40	1443.6
3	9.81	4.02	114.93	0.47	1487.8
4	9.82	4.03	115.37	0.44	1496.4
5	9.79	4.02	115.19	0.46	1552.3
6	9.81	4.02	115.21	0.44	1294.1
7	9.82	4.02	115.42	0.52	1317.8
8	9.82	4	114.73	0.47	1402.8
9	9.83	4.03	114.95	0.45	1263.7
10	9.78	4.03	114.87	0.48	1364.9
Average	**9.80**	**4.02**	**115.11**	**0.46**	**1395.7**
Std. dev.	**0.02**	**0.01**	**0.23**	**0.03**	**96.6**
95% confidence interval				**[0.44, 0.48]**	**[1335.9, 1455.6]**

Table 29: Specimen A – Tensile Test results.

Specimen no.	Width (mm)	Thickness (mm)	Grip (mm)	Stress at maximum load (MPa)	Strain at maximum load (%)	Strength at break (MPa)	Strain at break (%)
1	9.82	3.95	115.01	36.5	195,5	21.3	35.1
2	9.81	3.93	114.99	37.1	175,6	25.2	29.5
3	9.82	3.92	115.01	37.1	282,1	23.2	37.2
4	9.86	3.94	115.03	37.2	295,8	27.7	29.7
5	9.85	3.95	115.02	36.9	303,5	24.9	33.5
6	9.85	3.95	114.94	37.1	297,0	25.1	32.2
7	9.85	3.95	115.07	37.2	235,0	29.9	31.2
8	9.84	3.95	115.08	37.3	250,4	26.5	35.0
9	9.86	3.95	115.05	36.9	249,7	30.5	29.6
10	9.85	3.95	114.91	37.1	199,2	24.5	36.6
Average	**9.84**	**3.94**	**115.01**	**37.0**	**248,4**	**25.9**	**33.0**
Std. dev.	**0.018**	**0.011**	**114.99**	**0.2**	**46,5**	**2.9**	**2.9**
95% confidence interval				**[36.9, 37.2]**	**[13.5, 14.0]**	**[24.1, 27.6]**	**[31.1, 34.8]**

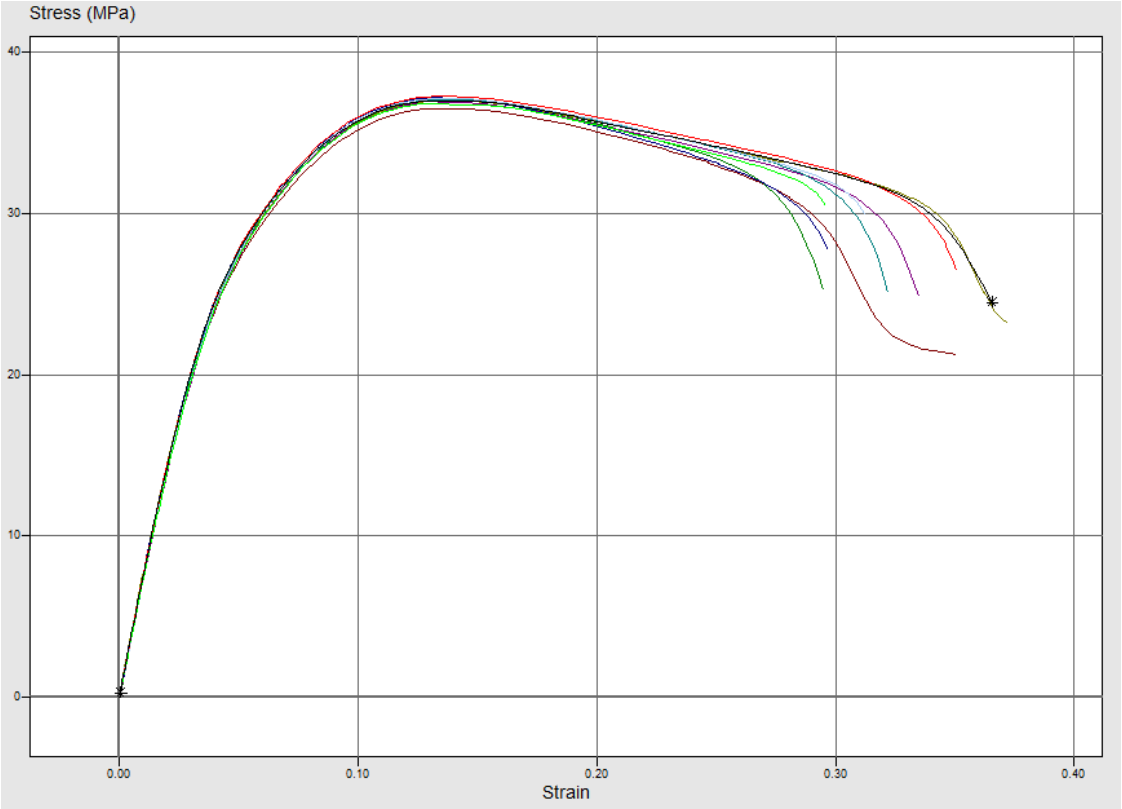

Figure 36: The Stress/Strain curves of Sample A are gathered. Dark red: 1.1, Green: 1.2, Yellow: 1.3, Blue: 1.4, Purple: 1.5, Turquoise: 1.6, Light blue: 1.7, Red: 1.8, Lime green: 1.9 and Black: 1.10.

Table 30: Specimen B – Tensile Test results.

Specimen no.	Width (mm)	Thickness (mm)	Grip (mm)	Stress at maximum load (MPa)	Strain at maximum load (%)	Strength at break (MPa)	Strain at break (%)
1	9.74	3.98	115.35	32.5	8.4	32.3	8.8
2	9.69	3.97	114.86	33.1	9.8	29.6	18.4
3	9.72	3.98	115.06	33.2	10.0	28.2	22.3
4	9.72	3.96	115.01	33.6	9.6	29.1	19.1
5	9.72	3.98	114.99	33.7	9.6	30.2	19.0
6	9.72	3.98	115.04	32.9	9.8	29.0	20.0
7	9.73	3.98	115.02	33.4	10.1	26.9	23.8
8	9.7	3.98	115.03	33.4	9.9	29.5	19.9
9	9.75	3.98	115.02	32.9	9.6	29.5	18.4
10	9.71	3.98	115.02	33.3	9.8	30.0	19.3
Average	**9.72**	**3.98**	**115.04**	**33.2**	**9.7**	**29.4**	**18.9**
Std. dev.	**0.018**	**0.01**	**0.12**	**0.4**	**0.5**	**1.4**	**4.0**
95% confidence interval				**[33.0, 33.4]**	**[9.4, 9.9]**	**[28.6, 30.3]**	**[16.4, 21.4]**

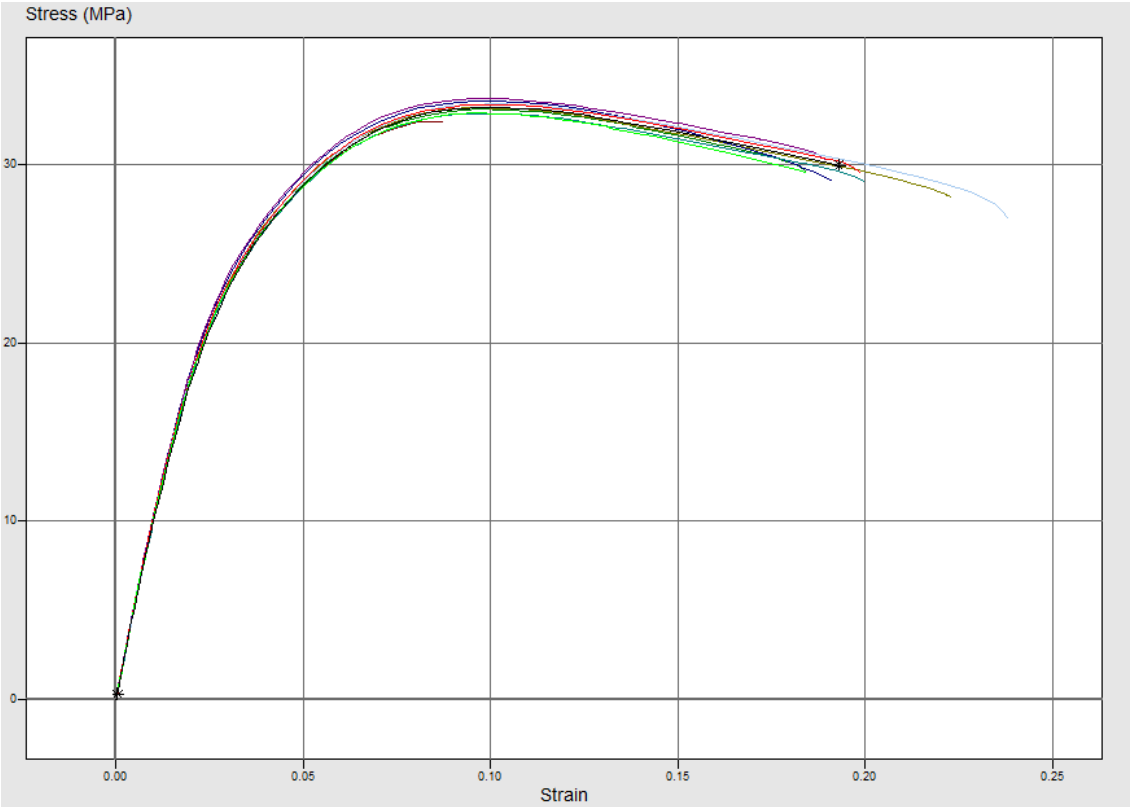

Figure 37: The Stress/Strain curves of Sample B are gathered. Dark red: 2.1, Green: 2.2, Yellow: 2.3, Blue: 2.4, Purple: 2.5, Turquoise: 2.6, Light blue: 2.7, Red: 2.8, Lime green: 2.9 and Black: 2.10.

Table 31: Specimen C – Tensile Test results.

Specimen no.	Width (mm)	Thickness (mm)	Grip (mm)	Stress at maximum load (MPa)	Strain at maximum load (%)	Strength at break (MPa)	Strain at break (%)
1	9.77	3.99	115.00	34.0	10.6	29.4	21.9
2	9.76	4.02	115.07	34.2	10.4	30.2	19.6
3	9.8	3.99	114.99	34.0	10.5	27.5	20.3
4	9.81	3.99	115.02	34.1	10.1	29.0	21.6
5	9.85	4	114.97	33.7	10.0	31.4	16.3
6	9.82	3.99	115.1	34.2	10.2	29.3	20.8
7	9.81	4	115.01	34.1	10.4	30.6	20.1
8	9.8	4	114.92	33.7	10.3	26.6	28.1
9	9.81	4	114.9	33.8	10.1	27.9	24.3
10	9.81	4	114.93	33.6	10.4	25.1	22.2
Average	**9.80**	**4.00**	**114.99**	**34.0**	**10.3**	**28.7**	**21.5**
Std. dev.	**0.03**	**0.01**	**0.07**	**0.2**	**0.2**	**1.9**	**3.1**
95% confidence interval				**[33.8, 34.1]**	**[10.2, 10.4]**	**[27.5, 29.9]**	**[19.6, 23.5]**

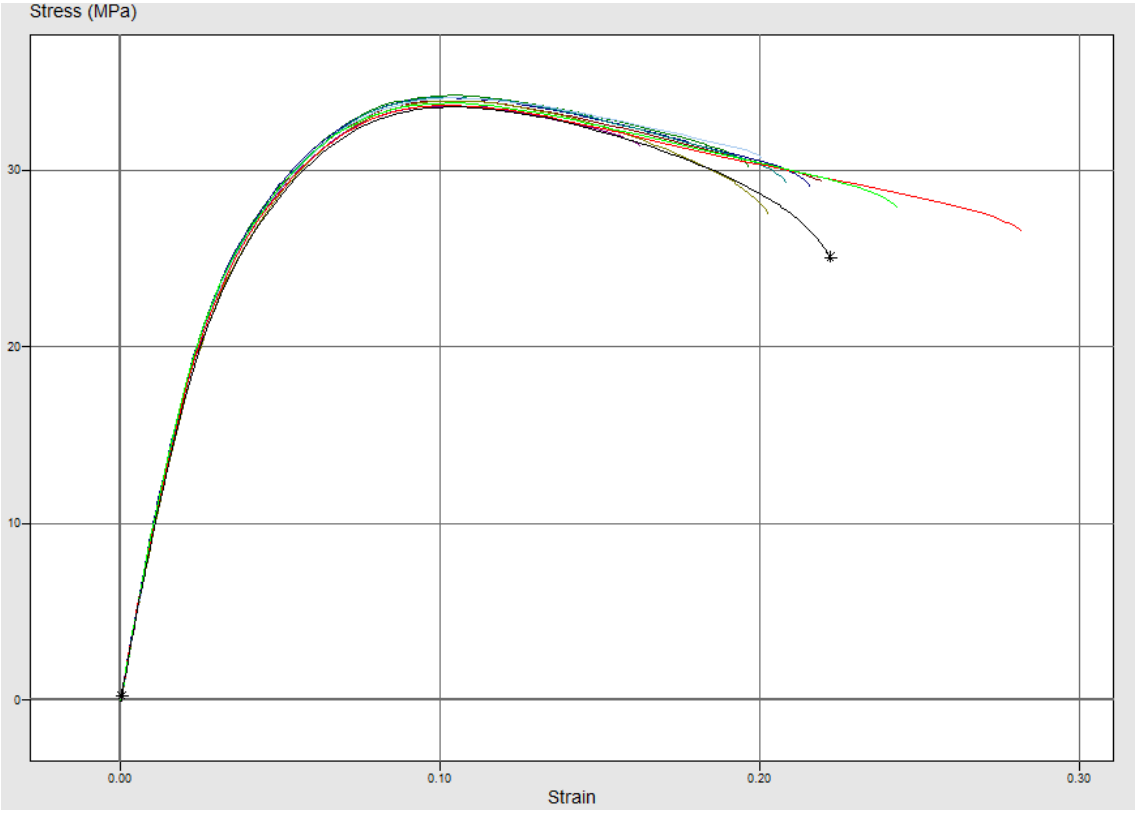

Figure 38: The Stress/Strain curves of Sample C are gathered.1 Dark red: 2.12, Green: 2.12, Yellow: 2.13, Blue: 2.14, Purple: 2.15, Turquoise: 2.16, Light blue: 2.17, Red: 2.18, Lime green: 2.19 and Black: 2.20.

Table 32: Specimen D – Tensile Test results.

Specimen no.	Width (mm)	Thickness (mm)	Grip (mm)	Stress at maximum load (MPa)	Strain at maximum load (%)	Strength at break (MPa)	Strain at break (%)
1	9.8	4	115.16	31.1	11.1	27.5	18.6
2	9.84	4	115.13	31.8	11.4	28.9	19.3
3	9.84	4	115.1	31.7	11.7	28.4	19.6
4	9.84	4	115.12	31.7	11.5	28.4	20.2
5	9.81	4	114.95	31.9	11.4	29.3	17.5
6	9.82	4	114.91	31.8	11.2	28.9	18.2
7	9.82	3.98	114.75	31.3	11.6	27.6	22.7
8	9.81	3.99	115.24	31.7	11.6	28.3	21.3
9	9.84	3.99	115.21	31.4	12.0	28.1	21.0
10	9.81	3.97	115.2	32.1	11.6	28.5	22.7
Average	**9.82**	**3.99**	**115.08**	**31.7**	**11.5**	**28.4**	**20.1**
Std. dev.	**0.02**	**0.01**	**0.16**	**0.3**	**0.3**	**0.6**	**1.8**
95% confidence interval				**[31.5, 31.9]**	**[11.4, 11.7]**	**[28.0, 28.7]**	**[19.0, 21.2]**

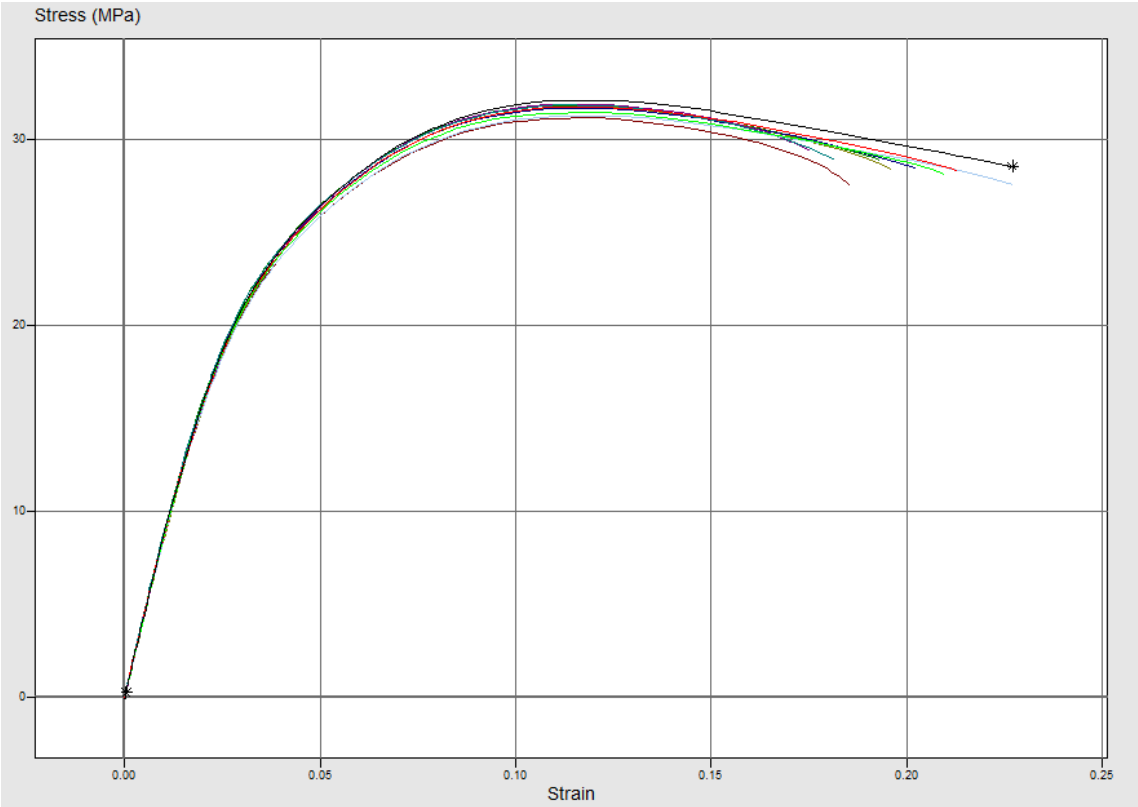

Figure 39: The Stress/Strain curves of Sample D are gathered. Dark red: 3.3, Green: 3.2, Yellow: 3.3, Blue: 3.4, Purple: 3.5, Turquoise: 3.6, Light blue: 3.7, Red: 3.8, Lime green: 3.9 and Black: 3.10.

Table 33: Specimen E – Tensile Test results.

Specimen no.	Width (mm)	Thickness (mm)	Grip (mm)	Stress at maximum load (MPa)	Strain at maximum load (%)	Strength at break (MPa)	Strain at break (%)
1	9.82	4	114.99	32.2	11.7	29.0	20.2
2	9.83	3.99	114.9	32.5	11.7	31.4	15.2
3	9.82	3.98	114.89	32.4	12.2	28.9	21.0
4	9.84	4	114.97	32.8	11.1	29.3	17.6
5	9.87	3.99	114.93	32.0	11.3	28.7	18.9
6	9.85	4	114.8	32.0	11.6	30.5	15.9
7	9.86	4	114.91	31.8	11.9	27.7	20.0
8	9.9	4	115.23	31.5	11.9	29.5	17.5
9	9.89	4	115.31	32.0	11.7	29.4	17.7
10	9.87	3.98	115.34	32.0	11.6	28.2	20.5
Average	**9.86**	**3.99**	**115.03**	**32.1**	**11.7**	**29.3**	**18.4**
Std. dev.	**0.03**	**0.01**	**0.2**	**0.4**	**0.3**	**1.1**	**2.0**
95% confidence interval				**[31.9, 32.3]**	**[11.5, 11.9]**	**[28.6, 29.9]**	**[17.2, 19.7]**

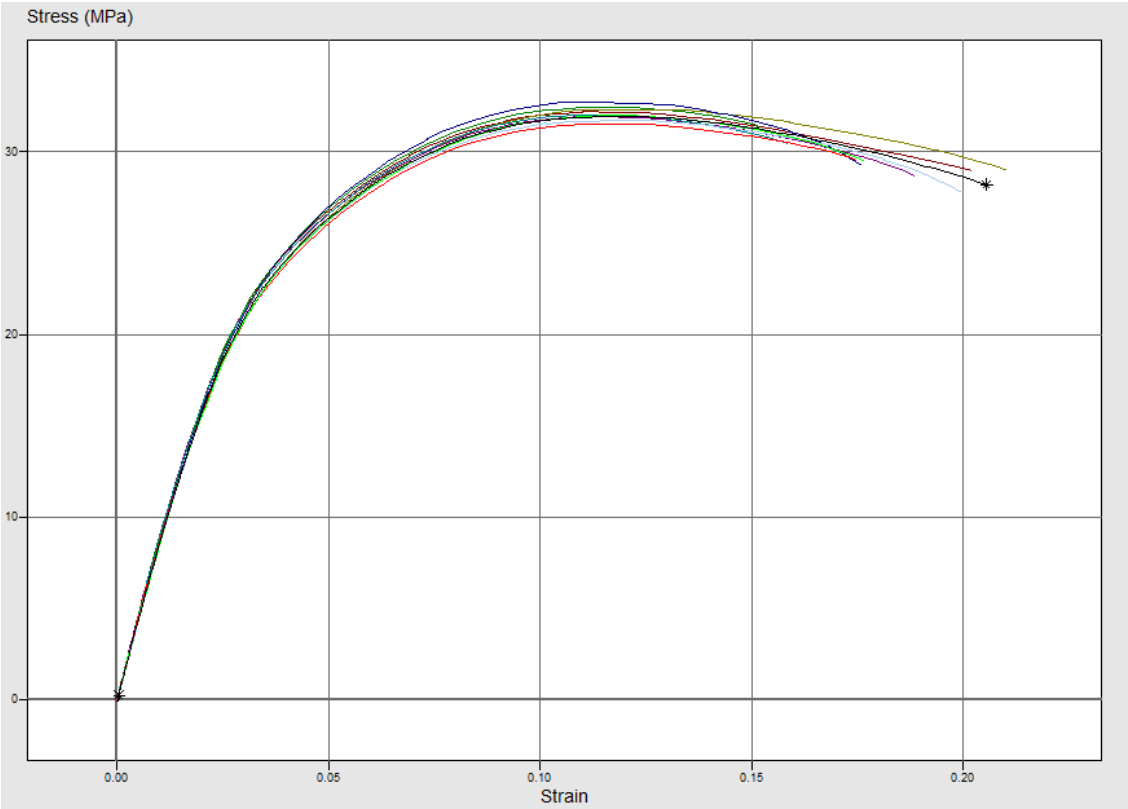

Figure 40: The Stress/Strain curves of Sample E are gathered.1 Dark red: 3.11, Green: 3.12, Yellow: 3.13, Blue: 3.14, Purple: 3.15, Turquoise: 3.16, Light blue: 3.17, Red: 3.18, Lime green: 3.19 and Black: 3.20.

APPENDIX H – DATA FROM THREE-POINT BENDING TEST

Table 34: Results from the three-point bending test on Sample A.

Sample A	Flexural modulus (MPa)	Flexural Stress (MPa)	Flexural Strain (%)
1.1	1397.8	44.4	7.3
1.2	1238.9	44.5	7.4
1.3	1295.4	44.9	7.4
1.4	1316.3	44.8	7.0
1.5	1327.1	46.8	7.6
1.6	1352.8	46.4	7.5
1.7	1347.5	46.3	7.5
1.8	1370.2	46.9	7.3
1.9	1402.2	46.7	8.6
1.10	1325.7	46.9	8.8
Average	**1337.4**	**45.9**	**7.6**
Std. dev.	**48.8**	**1.0**	**0.6**
95% confidence interval	**[1307.152, 1367.631]**	**[45.200, 46.524]**	**[7.303, 7.9939]**

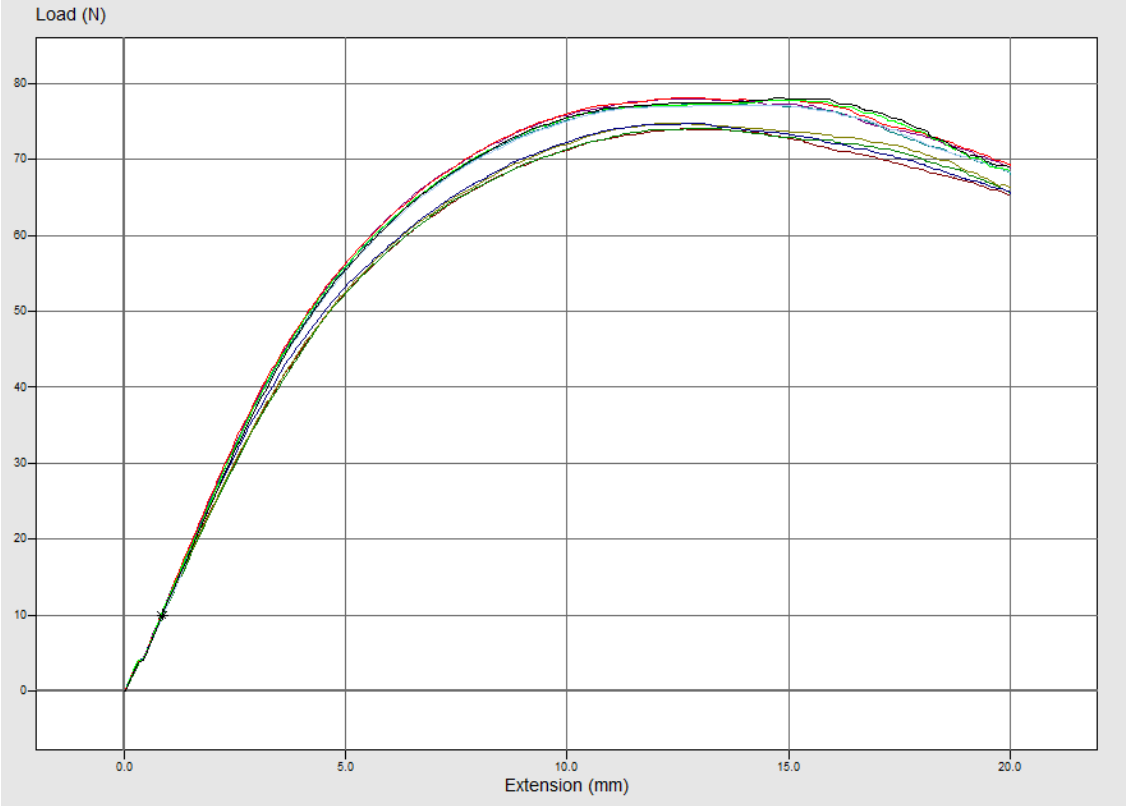

Figure 41:The Load/Extension curves of Sample A are gathered. Dark red: 1.1, Green: 1.2, Yellow: 1.3, Blue: 1.4, Purple: 1.5, Turquoise: 1.6, Light blue: 1.7, Red: 1.8, Lime green: 1.9 and Black: 1.10.

Table 35: Results from the three-point bending test on Sample B.

Sample B	Flexural modulus (MPa)	Flexural Stress (MPa)	Flexural Strain (%)
2.1	1149.5	40.5	7.7
2.2	1137.0	40.8	7.6
2.3	1115.4	41.8	7.9
2.4	1086.2	40.2	7.5
2.5	1108.7	40.4	7.9
2.6	1140.4	40.4	7.6
2.7	1153.0	40.4	7.4
2.8	1149.3	41.4	7.6
2.9	1156.2	41.1	7.9
2.10	1176.1	41.8	8.0
Average	**1137.2**	**40.9**	**7.7**
Std. dev.	**26.5**	**0.6**	**0.2**
95% confidence interval	**[1120.8, 1153.6]**	**[40.5, 41.2]**	**[7.6, 7.8]**

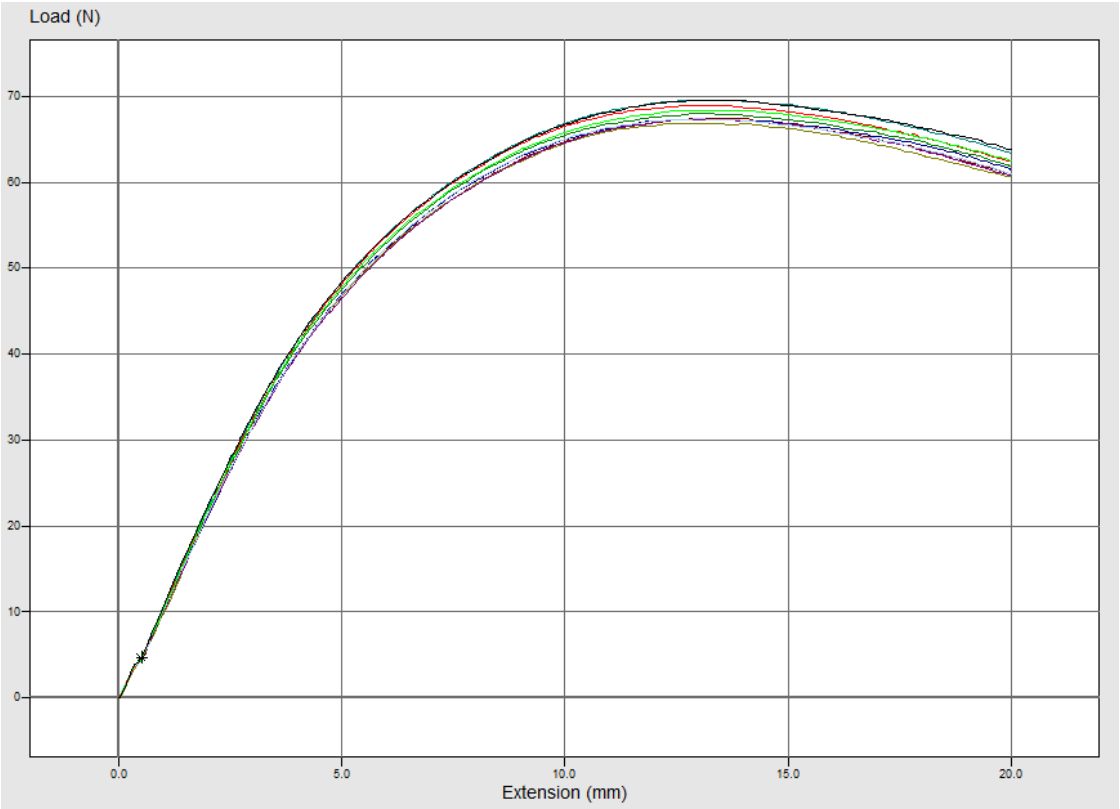

Figure 42: The Load/Extension curves of Sample B are gathered. Dark red: 2.1, Green: 2.2, Turquoise: 2.3, Yellow: 2.4, Blue: 2.5, Purple: 2.6, Light blue: 2.7, Red: 2.8, Lime green: 2.9 and Black: 2.10.

Table 36: Results from the three-point bending test on Sample C.

Sample C	Flexural modulus (MPa)	Flexural Stress (MPa)	Flexural Strain (%)
2.11	1182.2	42.0	7.5
2.12	1170.5	41.6	7.5
2.13	1223.2	42.5	7.5
2.14	1248.9	42.4	7.7
2.15	1214.7	41.9	7.6
2.16	1211.8	42.6	7.4
2.17	1182.9	42.2	7.7
2.18	1167.7	41.6	7.8
2.19	1194.4	42.4	7.6
2.20	1119.4	41.8	7.8
Average	**1191.6**	**42.1**	**7.6**
Std. dev.	**35.9**	**0.4**	**0.1**
95% confidence interval	**[1169.3, 1213.8]**	**[41.863, 42.3]**	**[7.5, 7.7]**

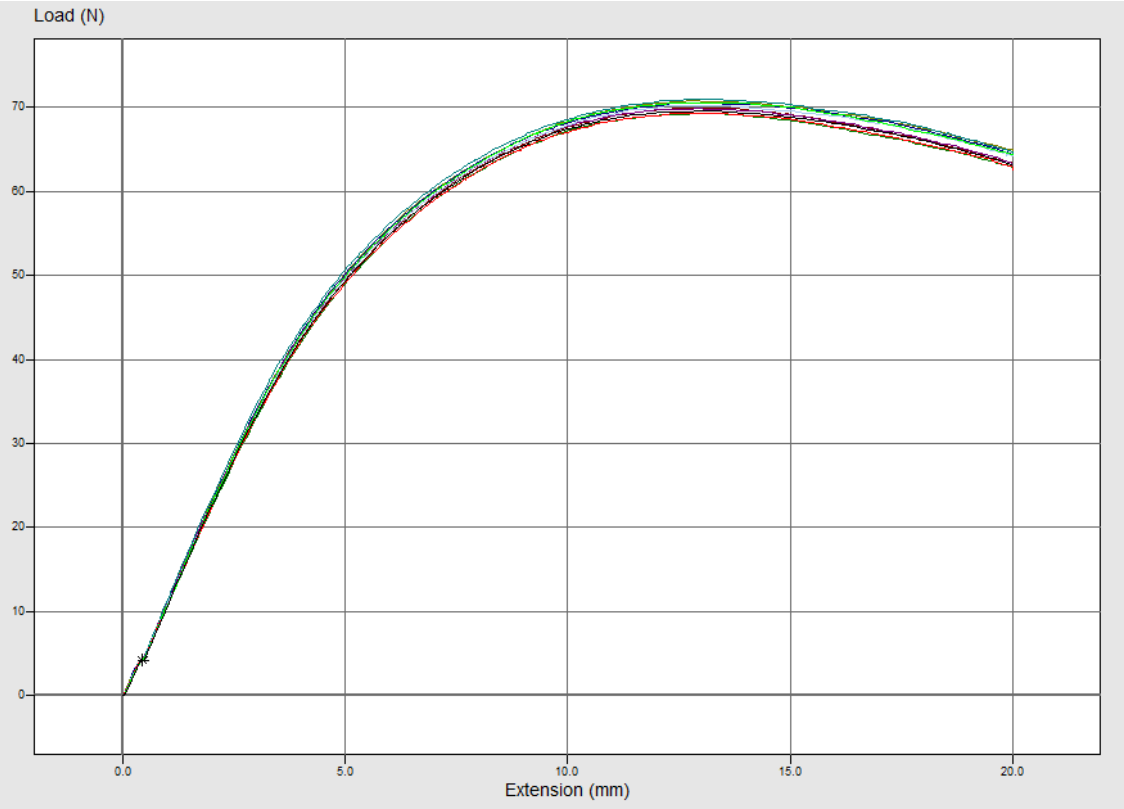

Figure 43: The Load/Extension curves of Sample C are gathered. Dark red: 2.11, Green: 2.12, Yellow: 2.13, Blue: 2.14, Purple: 2.15, Turquoise: 2.16, Light blue: 2.17, Red: 2.18, Lime green: 2.19 and Black: 2.20.

Table 37: Results from the three-point bending test on Sample D.

Sample D	Flexural modulus (MPa)	Flexural Stress (MPa)	Flexural Strain (%)
3.1	930.9	36.4	8.2
3.2	1095.4	36.4	7.6
3.3	996.7	35.8	8.1
3.4	973.2	36.9	8.0
3.5	980.5	36.2	7.8
3.6	881.0	36.4	7.7
3.7	1009.9	36.9	7.8
3.8	985.8	36.3	7.9
3.9	953.1	36.3	7.9
3.10	937.3	35.9	8.1
Average	**974.4**	**36.4**	**7.9**
Std. dev.	**56.8**	**0.4**	**0.2**
95% confidence interval	**[939.2, 1009.6]**	**[36.1, 36.6]**	**[7.8, 8.0]**

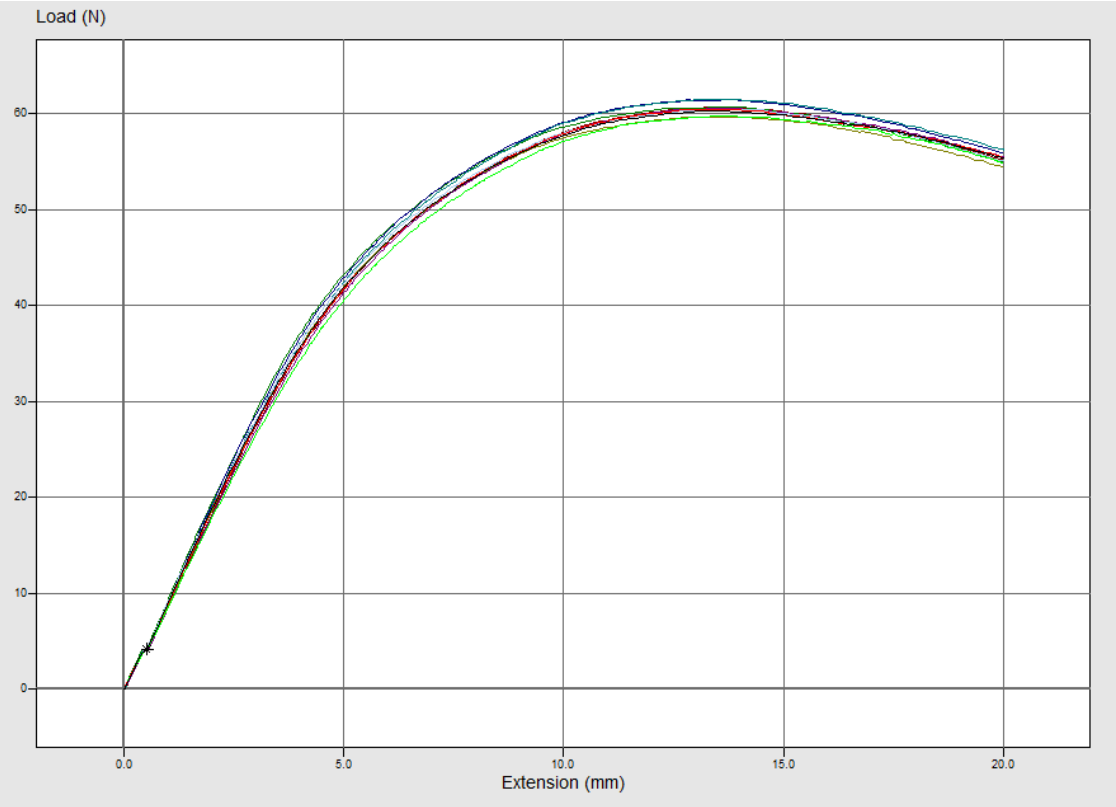

Figure 44: The Load/Extension curves of Sample D are gathered. Dark red: 3.1, Green: 3.2, Yellow: 3.3, Blue: 3.4, Black: 3.5, Purple: 3.6, Turquoise: 3.7, Light blue: 3.8, Red: 3.9, and Lime green: 3.10.

Table 38: Results from the three-point bending test on Sample E.

Sample E	Flexural modulus (MPa)	Flexural Stress (MPa)	Flexural Strain (%)
3.11	1027.8	37.4	7.9
3.12	986.0	37.4	7.8
3.13	1065.7	37.4	8.1
3.14	979.6	37.5	8.1
3.15	1043.4	37.6	8.0
3.16	1065.2	37.9	7.9
3.17	972.1	37.1	8.0
3.18	1006.3	36.8	8.0
3.19	1044.8	36.9	7.7
3.20	1005.3	37.0	8.0
Average	**1019.6**	**37.3**	**7.9**
Std. dev.	**34.7**	**0.3**	**0.1**
95% confidence interval	**[998.1, 1041.1]**	**[37.1, 37.5]**	**[7.8, 8.0]**

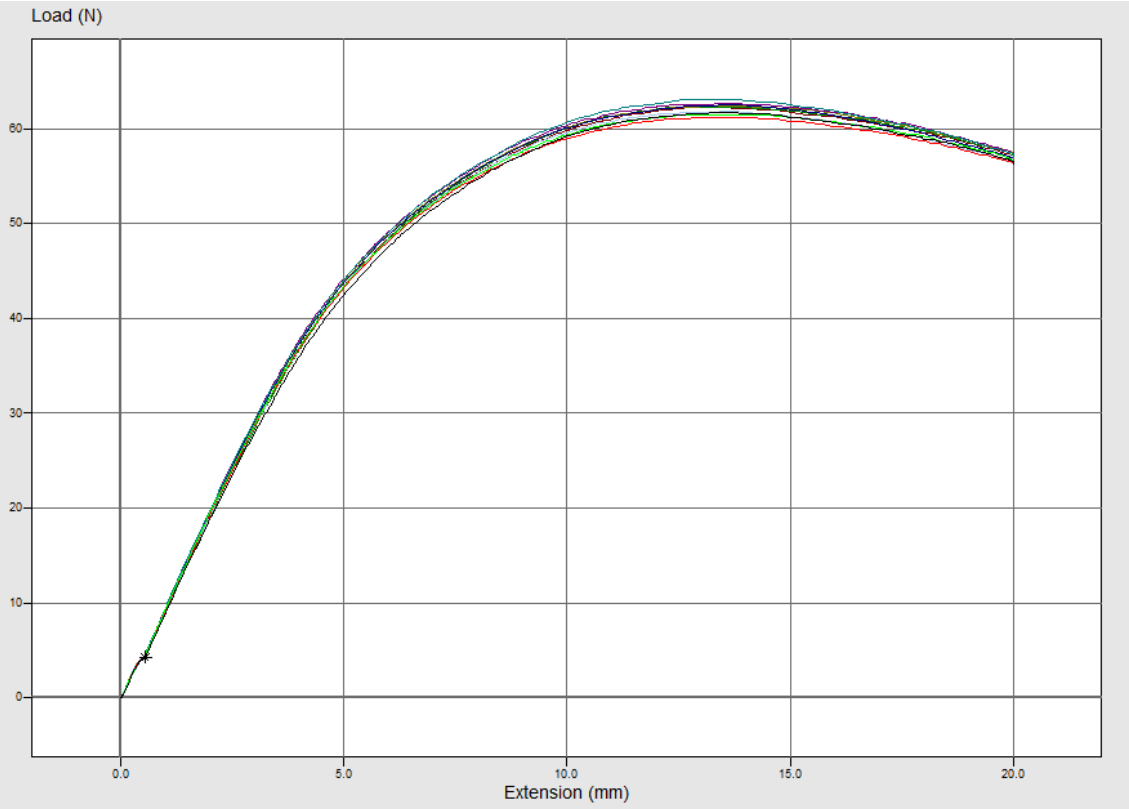

Figure 45: The Load/Extension curves of Sample E are gathered. Dark red: 3.11, Green: 3.12, Yellow: 3.13, Blue: 3.14, Purple: 3.15, Turquoise: 3.16, Light blue: 3.17, Red: 3.18, Lime green: 3.19 and Black: 3.20.

APPENDIX I – DATA FROM IMPACT TEST

Table 39: Data and results obtained from impact test on Sample A with notch at 23℃.

Specimen no.	Width (mm)	Thickness (mm)	Impact energy (J)	Impact strength (kJ/m^2)
1.1	8.82	4.07	0.10	2.8
1.2	8.11	4.08	0.08	2.4
1.3	8.19	4.08	0.08	2.4
1.4	8.31	4.06	0.09	2.7
1.5	8.33	4.11	0.09	2.6
1.6	8.38	4.11	0.09	2.6
1.7	8.62	4.11	0.10	2.8
1.8	8.38	4.11	0.09	2.6
1.9	8.70	4.13	0.10	2.8
1.10	8.33	4.11	0.09	2.6
Average	**8.42**	**4.06**	**0.09**	**2.6**
Std. deviation	**0.23**	**0.01**	**0.01**	**0.1**
95% confidence interval				**[2.5, 2.7]**

Table 40: Data and results obtained from impact test on Sample A without notch at 23℃.

Specimen no.	Width (mm)	Thickness (mm)	Impact energy (J)	Impact strength (kJ/m^2)
1.11	9.84	4.06	3.05	76.3
1.12	9.85	4.08	2.46	61.2
1.13	9.84	4.08	2.94	73.2
1.14	9.84	4.07	1.94	48.4
1.15	9.89	4.11	3.41	83.9
1.16	9.88	4.11	3.82	94.1
1.17	9.89	4.11	2.79	68.6
1.18	9.88	4.11	3.21	79.1
1.19	9.88	4.10	3.11	76.8
1.20	9.89	4.11	3.05	75.0
Average	**9.87**	**4.09**	**2.98**	**73.7**
Std. deviation	**0.02**	**0.02**	**0.51**	**12.4**
95% confidence interval				**[66.0, 81.4]**

Table 41: Data and results obtained from impact test on Sample B with notch at 23℃.

Specimen no.	Width at notch (mm)	Thickness (mm)	Impact energy (J)	Impact strength (kJ/m^2)
2.1	8.09	4.00	0.07	2.2
2.2	8.13	4.01	0.09	2.8
2.3	7.95	4.01	0.06	1.9
2.4	7.73	4.01	0.06	1.9
2.5	7.98	4.01	0.07	2.2
2.6	8.08	4.01	0.03	0.9
2.7	8.13	4.01	0.07	2.2
2.8	8.58	4.01	0.10	2.9
2.9	8.11	4.01	0.06	1.8
2.10	7.97	4.01	0.10	3.1
Average	**8.08**	**4.01**	**0.07**	**2.2**
Std. deviation	**0.22**	**0.00**	**0.02**	**0.6**
95% confidence interval				**[1.8, 2.6]**

Table 42: Data and results obtained from impact test on Sample B without notch at 23℃.

Specimen no.	Width at notch (mm)	Thickness (mm)	Impact energy (J)	Impact strength (kJ/m^2)
2.11	9.72	4.02	1.77	45.6
2.12	9.69	4.01	2.47	63.6
2.13	9.70	4.01	2.33	59.9
2.14	9.70	4.01	2.81	72.2
2.15	9.72	4.01	2.69	69.0
2.16	9.72	4.01	2.71	69.5
2.17	9.71	4.01	1.43	36.7
2.18	9.75	4.01	2.19	56.0
2.19	9.74	4.01	1.43	36.6
2.20	9.72	4.01	1.43	36.7
Average	**9.72**	**4.01**	**2.13**	**54.6**
Std. deviation	**0.02**	**0.00**	**0.56**	**14.5**
95% confidence interval				**[45.6, 63.6]**

Table 43: Data and results obtained from impact test on Sample C with notch at 23℃.

Specimen no.	Width at notch (mm)	Thickness (mm)	Impact energy (J)	Impact strength (kJ/m^2)
3.1	8.06	4.02	0.08	2.5
3.2	7.51	4.02	0.06	2.0
3.3	7.99	4.02	0.08	2.5
3.4	8.13	4.02	0.07	2.1
3.5	8.09	4.03	0.06	1.8
3.6	7.85	4.03	0.07	2.2
3.7	8.07	4.03	0.08	2.5
3.8	8.15	4.03	0.07	2.1
3.9	8.15	4.02	0.08	2.4
3.10	8.06	4.03	0.06	1.9
Average	8.01	4.03	0.07	2.2
Std. deviation	0.20	0.01	0.01	0.3
95% confidence interval				**[2.0, 2.4]**

Table 44: Data and results obtained from impact test on Sample C without notch at 23℃.

Specimen no.	Width at notch (mm)	Thickness (mm)	Impact energy (J)	Impact strength (kJ/m^2)
3.11	9.75	4.02	3.39	86.8
3.12	9.73	4.03	1.81	46.2
3.13	9.78	4.02	2.67	67.9
3.14	9.75	4.03	2.65	67.4
3.15	9.79	4.03	2.61	66.2
3.16	9.80	4.03	1.81	45.8
3.17	9.78	4.03	2.17	55.1
3.18	9.77	4.02	2.21	56.3
3.19	9.80	4.03	2.11	53.4
3.20	9.79	4.02	2.57	65.3
Average	9.77	4.03	2.40	61.0
Std. deviation	0.02	0.01	0.48	12.3
95% confidence interval				**[53.4, 68.7]**

Table 45: Data and results obtained from impact test on Sample D with notch at 23℃.

Specimen no.	Width at notch (mm)	Thickness (mm)	Impact energy (J)	Impact strength (kJ/m^2)
4.1	8.10	4.02	0.06	1.8
4.2	8.27	4.00	0.06	1.8
4.3	8.00	4.02	0.06	1.9
4.4	8.08	4.02	0.06	1.9
4.5	8.08	4.02	0.06	1.9
4.6	7.97	4.02	0.06	1.9
4.7	8.02	4.02	0.05	1.6
4.8	8.04	4.02	0.06	1.9
4.9	8.05	4.03	0.06	1.9
4.10	7.66	4.02	0.06	2.0
Average	8.03	4.02	0.06	1.9
Std. deviation	0.15	0.01	0.00	0.1
95% confidence interval				**[1.8, 1.9]**

Table 46: Data and results obtained from impact test on Sample D without notch at 23℃.

Specimen no.	Width at notch (mm)	Thickness (mm)	Impact energy (J)	Impact strength (kJ/m^2)
4.11	9.82	4.03	2.62	66.2
4.12	9.85	4.03	2.62	66.0
4.13	9.83	4.02	2.29	58.0
4.14	9.91	4.02	2.58	64.8
4.15	9.88	4.02	2.55	64.2
4.16	9.85	4.02	2.57	64.9
4.17	9.84	4.02	2.47	62.4
4.18	9.87	4.02	2.61	65.8
4.19	9.82	4.03	2.55	64.4
4.20	9.81	4.02	2.55	64.7
Average	9.85	4.02	2.54	64.1
Std. deviation	0.03	0.00	0.10	2.4
95% confidence interval				**[62.6, 65.6]**

Table 47: Data and results obtained from impact test on Sample E with notch at 23℃.

Specimen no.	Width at notch (mm)	Thickness (mm)	Impact energy (J)	Impact strength (kJ/m^2)
5.1	8.25	4.04	0.06	1.8
5.2	8.12	4.03	0.08	2.4
5.3	8.06	4.03	0.06	1.9
5.4	8.29	4.03	0.06	1.8
5.5	8.23	4.05	0.10	3.0
5.6	7.28	4.03	0.06	2.0
5.7	7.90	4.03	0.06	1.9
5.8	7.87	4.03	0.07	2.2
5.9	8.04	4.03	0.07	2.2
5.10	8.24	4.04	0.06	1.8
Average	8.03	4.03	0.07	2.1
Std. deviation	0.30	0.01	0.01	0.4
95% confidence interval				**[1.9, 2.3]**

Table 48: Data and results obtained from impact test on Sample E without notch at 23℃.

Specimen no.	Width at notch (mm)	Thickness (mm)	Impact energy (J)	Impact strength (kJ/m^2)
5.11	9.83	4.02	2.25	56.9
5.12	9.85	4.03	2.67	67.3
5.13	9.86	4.03	2.66	66.9
5.14	9.84	4.03	2.79	70.4
5.15	9.85	4.03	2.70	68.0
5.16	9.82	4.03	2.63	66.5
5.17	9.87	4.03	2.61	65.6
5.18	9.85	4.03	1.87	47.1
5.19	9.84	4.03	2.74	69.1
5.20	9.88	4.03	2.60	65.3
Average	9.85	4.03	2.55	64.3
Std. deviation	0.02	0.00	0.28	7.0
95% confidence interval				**[59.9, 68.7]**

Circular Ocean-bound Platic

Breaking the waves of ocean plastic pollution
- From source to solution

www.circularoceanplastic.eu

The report is co-funded by:

Co-funded by the European Union

Interreg South Baltic
Circular Ocean-Bound Plastic
www.circularoceanplastic.eu